

A Novel Protective Role for p130 in Neuron Oxidative Stress

NINOSCHKA CAROLYN D'SOUZA

A THESIS SUBMITTED TO
THE FACULTY OF GRADUATE STUDIES
IN PARTIAL FULFILMENT OF THE REQUIREMENTS
FOR THE DEGREE OF
MASTER OF SCIENCE

GRADUATE PROGRAM IN KINESIOLOGY AND HEALTH SCIENCE
YORK UNIVERSITY
TORONTO, ONTARIO

SEPTEMBER 2017

© NINOSCHKA CAROLYN D'SOUZA, 2017

ABSTRACT

The human brain is the most energy-consuming and highly oxidative organ in the body. It generates high levels of mitochondrial reactive oxygen species (ROS), damaging proteins and DNA. This is evident in neurodegenerative diseases and aging where the brain's defence mechanisms prove insufficient. We provide insight into a novel mechanism of ROS defence in the brain, mediated via p130 that limits oxidative phosphorylation. Conditions of increased metabolic stress or treatment of neurons with ROS inducing agent resulted in mitochondrial localization of p130 in neurons. In the mitochondria, p130 bound to mitochondrial DNA and was associated with decreased mitochondrial gene expression. This resulted in decreased ATP production, thus limiting ROS generation. Our results highlight a new understanding of transcriptional regulation of the mitochondrial genome by the nuclear transcriptional co-repressor p130. This might serve as a potential mechanism to control ROS production of neurons in response to increased metabolic stress.

DEDICATION

I would like to dedicate the research done in my thesis to my grandmother who is currently battling Alzheimer's Disease. Nana, you are one of the most independent people I have known and have given me a first-hand experience into much Alzheimer's has changed your life. Even though there wasn't much I could do to help you, I hope that my research can contribute at least in a small way towards helping other people in the future. Thank you for everything you have done for us.

ACKNOWLEDGEMENTS

I would like to thank God for giving me the opportunity to complete my Master's at York University and for all the divine help throughout.

I am extremely grateful to my supervisor Dr. Anthony Scimè for his patience, encouragement, help, guidance and support through every aspect of my Master's thesis. I am also so thankful to have been blessed with amazing lab mates. Thank you guys for being my support and friends I could always count on. Debasmita Bhattacharaya and Maryam Abbaszadeh thank you for teaching me everything I know and patiently helping me through every hurdle. Nareh Edjiu you are more than a lab mate and lab twin and I am so grateful I had the opportunity to share every high and low of this journey through our Master's with you.

A big thank you to our lab volunteers Chetna, Mirna, Ben, Hanad, Aneeshka and Divya for making my lab life a lot easier. I would also like to thank the Haas, Zoidl, Perry, Benchimol and Pearlman lab members for being my family outside of the lab and always lending a helping hand when needed.

Very importantly I would like to thank my committee members Dr. Haas and Dr. Zoidl for taking the time to personally guide me through several aspects of my project.

Finally, I would like to thank my parents, brothers and my extended family and friends for their prayers, love and encouragement through every phase of my Master's. Thank you for believing in me.

TABLE OF CONTENTS

Abstract	ii
Dedication	iii
Acknowledgements	iv
Table of contents	iv
List of Tables	vii
List of Figures	viii
List of abbreviations	x
Statement of contribution	xi
1. Literature Review	1
1.1. Introduction.....	1
1.2. Glucose metabolism.....	3
1.3.Lactate metabolism.....	4
1.4. Metabolic homeostasis in the brain.....	5
1.5. ATP production in the mitochondria	7
1.6. Mitochondrial DNA	8
1.7. Mitochondrial ROS generation.....	10
1.8. Mitochondrial ROS defence mechanisms.....	12
1.9. Mitochondria and neurodegenerative diseases.....	13
1.10. Rb family and the brain.....	15
1.11. p130 and neurons.....	17
2. Rationale and Hypothesis	19
3. Materials and Methods	20

4. Results	28
5. Figures	35
6. Discussion	49
7. Illustrations	58
8. References	64

LIST OF TABLES

Table 1. List of Primers in qPCR analysis.....	26
---	-----------

LIST OF FIGURES

Figure 1.1 A schematic diagram illustrating nutrient shuttling in neurons.....	3
Figure 1.2 The mammalian mitochondrial genome containing genes encoding subunits of ETC complexes involved in OxPhos and rRNAs	7
Figure 1. 3 Mitochondrial oxidative phosphorylation.....	9
Figure 1.4 Mitochondrial ROS defence mechanisms.....	11
Figure 1.5 Role of p130 as a nuclear transcriptional co-repressor.....	16
Figure 5.1 p130 expression during differentiation of Neuro2A cells.....	35
Figure 5.2 p130 is localized in the mitochondria of differentiated neurons.....	36
Figure 5.3. p130 cytoplasmic and mitochondrial localization in various brain regions.....	37
Figure 5.4. p130 is localized in the mitochondria of all brain regions.....	38
Figure 5.5 p130 levels increase in mitochondria with high and low glucose stress.....	39
Figure 5.6 Increase in mitochondrial p130 levels with lactate stress.....	40
Figure 5.7 Increased p130 mitochondrial localization with increase in ROS production....	41
Figure 5.8 Increase in mitochondrial p130 levels with rotenone stress.....	42
Figure 5.9 p130 mitochondrial localization decreases with Nac treatment.....	43
Figure 5.10 p130 binding to mitochondrial D-Loop promoter in vitro and in vivo.....	44
Figure 5.11 Increased p130 interaction with mitochondrial DNA with oxidative stress....	44
Figure 5.12 Reduced mitochondrial encoded gene expression with lactate induced stress..	45
Figure 5.13 p130 protein levels remain unchanged in the nucleus of lactate stressed neurons.....	46
Figure 5.14 Rescue of oxidative stress increases expression of mitochondrial encoded OxPhos genes.....	47

Figure 5.15 Increased ATP production with decreased mitochondrial p130 localization...48

ABBREVIATIONS

AD	Alzheimer's disease
ATP	Adenosine triphosphate
ADP	Adenosine diphosphate
ChIP	Chromatin Immunoprecipitation
cDNA	Complimentary DNA
cdk	Cyclin dependent kinase
Cu/ZnSOD	Copper/Zinc superoxide dismutase
Cyt c	Cytochrome c
Cyt b	Cytochrome b
DMEM	Dulbecco's modified eagle medium
DTT	Dithiothreitol
ETC	Electron transport chain
EDTA	Ethylenediaminetetraacetic acid
FBS	Fetal bovine serum
FADH ₂	Flavin adenine dinuceotide (reduced)
FMN	Flavin mononucleotide
G1 phase	Gap1 phase
G2 phase	Gap 2 phase
G0 phase	Quiescent phase
G6P	Glucose-6-phosphate
GLUT	Glucose transporter
Glu	Glucose

GPx	Glutathione peroxidase
GSH	Glutathione
GSSG	Oxidized glutathione
HDAC	Histone deacetylase
H strand	Heavy strand
HSP	Heavy strand promoter
Ldh	Lactate dehydrogenase
L strand	Light strand
LSP	Light strand promoter
MCT	Monocarboxylate transporter
mRNA	Messenger RNA
MTERF	Mitochondrial transcription termination factor
mtDNA	Mitochondrial DNA
MnSOD	Manganese superoxide dismutase
NP40	Nonidet P- 40
NADH	Nicotinamide adenine dinucleotide (reduced)
Nd1	NADH dehydrogenase 1
Nd2	NADH dehydrogenase 2
Nd3	NADH dehydrogenase 3
Nd4	NADH dehydrogenase 4
Nd4L	NADH dehydrogenase 4L
Nd5	NADH dehydrogenase 5
Nd6	NADH dehydrogenase 6

NOX	NADPH oxidase
OxPhos	Oxidative phosphorylation
PPP	Pentose phosphate pathway
PBS	Phosphate buffered saline
PD	Parkinson's disease
Pdk	Pyruvate dehydrogenase kinase
PDH	Pyruvate dehydrogenase
PFK	Phosphofructokinase
POLRMT	Mitochondrial specific polymerase γ
Pyr	Pyruvate
qPCR	Quantitative polymerase chain reaction
Rb	Retinoblastoma susceptibility gene
ROS	Reactive oxygen species
SD	Standard deviation
SOD	Superoxide dismutase
TCA	Tricarboxylic acid cycle
TBS	Tris buffered saline
TFAM	Mitochondrial transcription factor A
TFB1M/TFB2M	Mitochondrial transcription factor B paralogues

STATEMENT OF CONTRIBUTION

I independently performed all experiments presented in this thesis.

1. LITERATURE REVIEW

1.1. Introduction

The brain is made up primarily of two main types of cells-neurons and glia. Neurons are the post-mitotic cells responsible for sensory and motor coordination. They are not capable of self-renewal and the pool of neural progenitors that replenishes neurons decreases with age. Hence, once damaged or destroyed, neurons cannot be sufficiently replaced, subsequently resulting in a decline in brain function. Neurons are made up of a cell body with axons and dendrites. Dendrites are short, spiny processes that receive impulses and transmit them to the cell body. Axons are long thread-like projections that conduct impulses from the cell body to dendrites of other neurons. Glial cells are cells that support the neurons in a functional and metabolic manner, of which the most prevalent are astrocytes (Aubert et al., 2007; Escartin et al., 2006; Hertz et al., 2007; Sokoloff et al., 1999).

Although the human brain occupies only about 2% of the total body mass, it's high rate of consumption of oxygen and glucose, make it the most energy-consuming and highly oxidative organ in the body. Most of the energy consumed by the brain is utilized by the neurons with about 80% of the energy being consumed for excitatory neurotransmission in grey matter due to which neurons are the most energy consuming cells in the brain (Lebon et al., 2002; Itoh et al., 2003; Bouzier-Sore et al., 2006; Boumezbeur et al., 2010a; Sibson et al., 1998; Hyder et al., 2006; Shulman et al., 2004; Attwell and Laughlin, 2001). On account of this, the brain generates high levels of reactive oxygen species (ROS) that damages proteins and DNA. This is particularly evident in neurodegenerative diseases such as Parkinson's and Alzheimer's as well as during aging. To maintain metabolic homeostasis, the brain has devised several surveillance

mechanisms against ROS, however, they are barely sufficient (Efeyan et al., 2015; Lam et al., 2010; Kirchner et al., 2009).

In this study, we provide insight into a novel mechanism of ROS defence in the brain, mediated via the retinoblastoma susceptibility protein (Rb) family member p130. Our unexpected finding highlights a role for how p130 functions against ROS generation by reducing oxidative phosphorylation (Oxphos). In neurons, during conditions of increased metabolic stress with lactate or glucose or treatment with inducers of ROS such as rotenone, p130 was found to localize in the mitochondria. But its nuclear levels remained constant. Interestingly, within the mitochondria, p130 bound to mitochondrial DNA (mtDNA), serving as a transcriptional repressor similar to its established nuclear function. Indeed, p130, bound to mtDNA was associated with decreased expression of mitochondrial encoded genes across all complexes in the electron transport chain (ETC) that resulted in reduced ATP generation. Thus, the repressive function of p130 could serve as a potential mechanism to control ROS levels to protect the cell in response to increased oxidative stress by reducing OxPhos. Though its function as a nuclear transcriptional co-repressor has been documented, we are the first to discover and characterize a role for p130 in the mitochondria. Moreover, we have uncovered another mechanism of transcriptional regulation of the poorly studied mitochondrial genome.

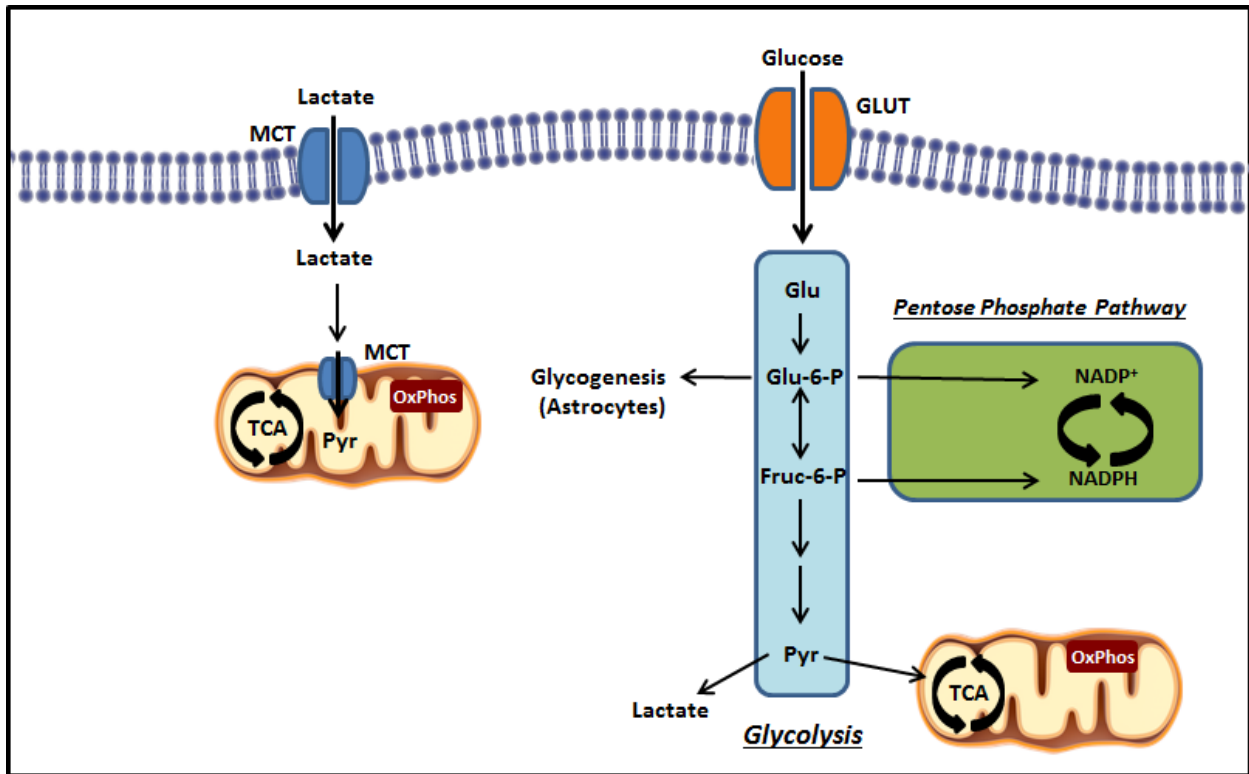


Figure 1.1 A schematic diagram illustrating nutrient shuttling in neurons. Neurons can utilize pyruvate from glucose via glycolysis or from lactate. Alternatively, under conditions of high oxidative stress, the pentose phosphate pathway (PPP) is activated to produce reducing equivalents such as NADPH. Excess glucose can also be converted to glycogen in astrocytes from Glu-6-P. (Glu, glucose; Pyr, pyruvate; GLUT, glucose transporter; MCT, monocarboxylate transporter; OxPhos, Oxidative Phosphorylation; TCA, tricarboxylic acid; Glu-6-P, Glucose-6-phosphate; Fruc-6-P, Fructose-6-phosphate) (Adapted from Mergenthaler et al., 2013).

1.2. Glucose metabolism

The brain utilizes various nutrients to meet its energy needs among which glucose is regarded as the primary substrate (Nehlig, 2004; Magistretti, 2008). Blood glucose enters brain cells via glucose transporters following which it is phosphorylated to glucose-6-phosphate (G6P) by the enzyme hexokinase. G6P is then processed by one of three main pathways (**Fig 1.1**): (1) glycolysis, (2) the pentose phosphate pathway (PPP) or (3) glycogenesis, which occurs only in astrocytes (Hertz and Chen, 2017). Glycolysis gives rise to two molecules of pyruvate and the production of 2 ATP and 2 NADH molecules. Pyruvate is subsequently shuttled into the

mitochondria and converted to acetyl CoA by pyruvate dehydrogenase (Pdh) to be utilized in the tricarboxylic acid cycle (TCA). The TCA produces reducing agents, NADH and FADH₂, for OxPhos. In the mitochondria, OxPhos occurs in the electron transport chain (ETC), producing ATP and CO₂ while consuming oxygen. Under non-oxidative conditions the TCA and ETC do not function, as pyruvate does not feed into the TCA but instead is converted to lactate rather than acetyl CoA by lactate dehydrogenase (LDH). This process can take place in the presence of oxygen (aerobic glycolysis) or its absence (anaerobic glycolysis) (Mergenthaler et al., 2013).

G6P shuttles into the PPP especially during oxidative stress, which takes place when free radicals and/or ROS are generated beyond the cell's capacity to scavenge it (Betteridge, 2000). Here it gives rise to NADPH, which is required to produce reduced glutathione (GSH) a primary antioxidant that acts as a ROS scavenger. Glyceraldehyde-3-phosphate and fructose-6-phosphate can also feed into the PPP (**Fig 1.1**). Glycogenesis on the other hand occurs only in astrocytes and allows storage of glucose into glycogen chains (Belanger et al, 2011).

1.3. Lactate metabolism

Lactate is formed from pyruvate as the end product of glycolysis, but it can function as an energy substrate, as well as influence intracellular pH and redox balance (Schurr and Payne, 2007). It is important in formation of long term memory (Suzuki et al., 2011) as well as plasticity (Yang et al., 2014) and ventilation control (Erllichman et al., 2008). As an energy source, lactate can be utilized by both neurons and astrocytes (Zielke et al., 2009). Lactate usage is thought to be a mechanism for reserving glucose for other vital functions such as generating reducing equivalents NADPH via the PPP (Mergenthaler et al., 2014) (**Fig 1.1**). Its entry into the cell is facilitated via monocarboxylate transporter (MCT) 1 and 2 (Hashimoto et al, 2008). Once

transported into the cell via MCTs, LDH oxidizes the lactate into pyruvate (Hung et al., 2011). The pyruvate then enters the TCA cycle for mitochondrial energy generation. Both astrocytes and neurons can utilize lactate (Bolanos et al., 2010). Intense physical activity or increased brain activity can stimulate lactate production from astrocytes as an energy substrate for neurons (van Hall et al, 2009). The production of lactate occurs at a faster rate than it is consumed especially under conditions of high brain activity (Barros et al., 2013; Pritchard et al, 1991; Newman et al, 2011). Moreover, under varying conditions such as conditions of development or starvation, other substrates such as ketone bodies, glutamate, pyruvate and acetate can also be utilized by the brain. (Nehlig, 2004; Magistretti, 2008; Zielke et al., 2009).

1.4. Metabolic homeostasis in the brain

Neurons have high amounts of mitochondria to sustain the high levels of energy production (Lovatt et al, 2007). For example, at the pre-synaptic and post-synaptic junctions they provide energy for transmission of excitatory signals that occur within extremely quick time frames. Thus, without a high level of available energy, neuron function would not occur at a rate fast enough to sustain synaptic activity (Lovatt et al, 2007). Neurons are incapable of sustaining a high glycolytic rate. They have low levels of the glycolytic activator phosphofructokinase (PFK) due to reduced levels of the enzyme fructose-2,6-bisphosphate/6-phosphofructose-2-kinase, which is responsible for making PFK (Almeida et al, 2004; Herrero-Mendez et al, 2009). The glucose unable to be used up by glycolysis is shunted towards the PPP to produce NADPH. When both glucose and lactate are available under high energy demand, the glucose needed as a defence against oxidative stress is shunted to the PPP. (Bolanos et al, 2010).

An Astrocyte-neuron lactate shuttle hypothesis has been proposed by Pellerin and Magistretti that holds (i) an increase in neural activity, results in increased production and uptake of extracellular glutamate via Na^+ dependent mechanisms in glial cells (ii) activation of Na^+/K^+ ATPase due to increased Na^+ , results in increased consumption of ATP (iii) this causes an increase in lactate production through glycolysis and release into the extracellular space and (iv) the lactate produced can serve as a nutrient for production of ATP via OxPhos by neurons (**Fig. 1.1.**) (Pellerin et al, 2007; Magistretti et al, 2009; Magistretti and Chatton, 2005).

1.5. ATP production in the mitochondria

The ETC in the mitochondria are essential for proper functioning of the brain by producing energy in the form of ATP. The ETC is located within the mitochondrial inner membrane comprising of five complexes that contain multiple subunits. During the process of OxPhos, NADH and FADH_2 produced from the TCA cycle and/or glycolysis are oxidized at Complex I and Complex II, respectively. The electrons obtained from NADH and FADH_2 oxidation are then transferred to Complex III through its electron carrier-ubiquinone. From there, electrons are then passed on to Complex IV by cytochrome c located in Complex III (Al-Kafaji et al., 2016). In the final step, the electrons transferred are accepted by molecular oxygen and results in the formation of water (Boyer, 1997) (**Fig 1.3**). At Complex I, III and IV, this transfer of electrons pumps protons from the matrix into the intermembrane space. At the last complex, ATP synthase, the protons are pumped back into the matrix using the electrochemical gradient that is generated. (Grzybowska-Szatkowska et al., 2014). This results in a simultaneous synthesis of ATP from ADP and inorganic phosphate (Boyer, 1997). (**Fig. 1.3**)

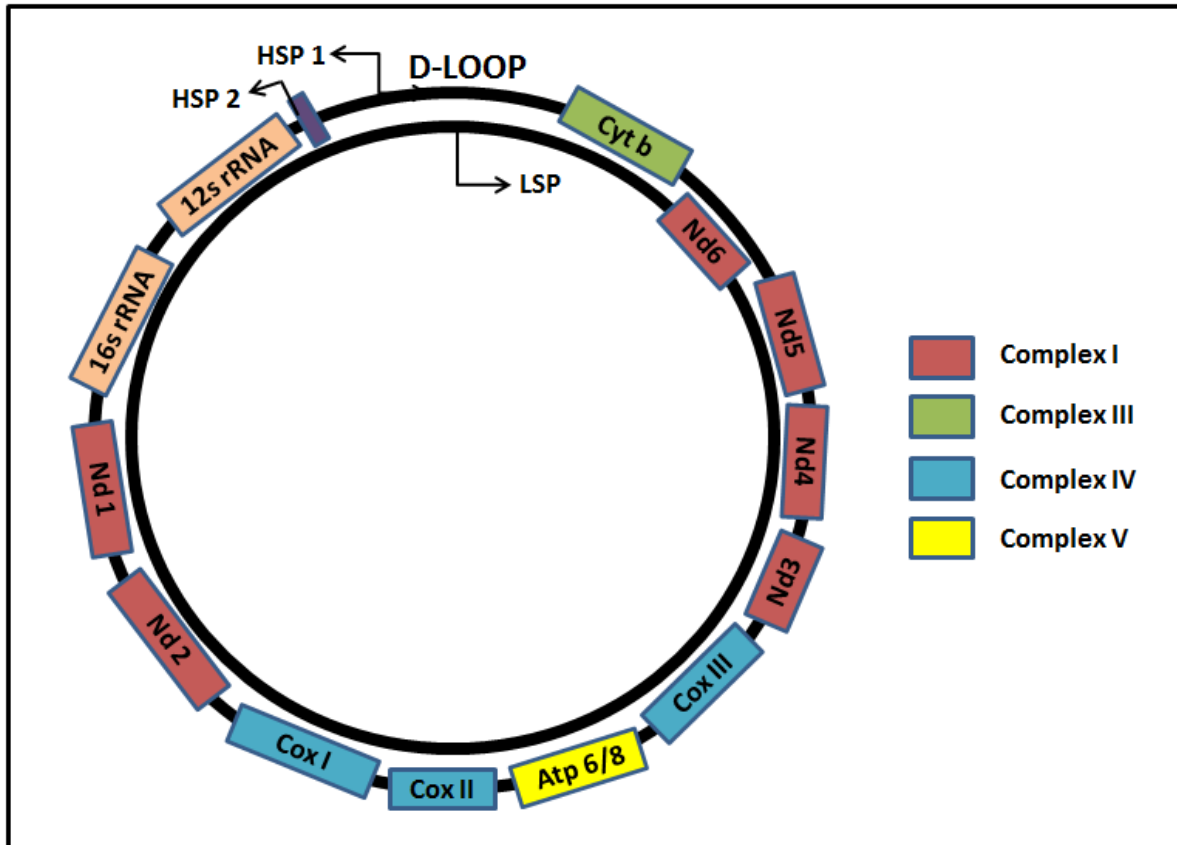


Figure 1.2 The mammalian mitochondrial genome. The double stranded mitochondrial DNA showing the 13 genes encoding subunits of ETC complexes involved in OxPhos and rRNAs. (Adapted from Uhler and Falkenberg, 2015)

1.6. Mitochondrial DNA

The subunits of the ETC are encoded from genes present on both nuclear and mtDNA. mtDNA is circular and approximately 16.5kb, encoding a total of 37 genes (**Fig. 1.2.**). Thirteen of these transcribe essential subunits for four out of the five complexes in the ETC that carries out OxPhos (Bonawitz et al., 2006). The other subunits of these complexes and the entire complex II are nuclear encoded (Scarpulla, 2008). mtDNA encodes 7 subunits of complex I (NADH dehydrogenase-Nd1, Nd2, Nd3, Nd4, Nd4L, Nd5, Nd6), 1 subunit in Complex III (Cytochrome b (Cyt b)), 3 subunits in complex IV (Cytochrome c oxidase (Cox I, Cox II, Cox III) and 2 subunits in Complex V (Atp6, Atp8) (Anderson et al., 1981, Al-Kafaji et al., 2016).

Complexes I, III and IV are responsible for electron transfer and pump protons into the intermembrane space. mtDNA also encodes 2 rRNAs that are mitochondrial ribosomal subunits and 22 tRNAs that are instrumental in the translation of the ETC subunits (Shadel, 2008).

Mitochondrial gene expression is required for the proper assembly and functioning of the ETC complexes (Bonawitz et al., 2006). mtDNA is made up of a heavy (H) and light (L) strand, both of which contain genes (**Fig. 1.2**). Mitochondrial gene promoters heavy strand promoter 1 and 2 (HSP1 and HSP2) are located on the H strand while light strand promoter (LSP) is on the L strand. HSP1 and LSP are both located in the displacement loop (D-Loop), which is the only noncoding region in the mtDNA, while HSP2 is located downstream of the HSP1 promoter. HSP2 produces a polycistronic near full genome length transcript LSP transcribes ND6, while transcription from HSP1 is specialized for the production of the 12s and 16s RNAs (Scarpulla, 2008; Shadel, 2008). High copy numbers of mtDNA are usually maintained in mammals.

Studies show that maintenance and transcription of mtDNA are mediated by the transcription factor Tfam (Dairaghi et al., 1995; Ramachandran et al., 2016), which binds the D-loop region of the LSP and the HSP promoters (Parisi et al., 1991; Fisher et al., 1992; Ramachandran et al., 2016). Tfam contains 2 HMG motifs and a COOH terminal tail through which it exerts its transcriptional activation functions, which is carried out by binding to the promoter recognition site and advancing bidirectional transcription (Topper et al., 1989, Scarpulla, 2008). Additionally, in order to stabilize mtDNA, it can also bind to random non-promoter sites (Fisher et al., 1992; Fisher et al., 1989; Ramachandran et al., 2016). A second protein, mTERF has also been found to possess the ability to both initiate and terminate transcription at the HSP1 site (Asin Cayuela et al., 2004).

The amount of ATP generation is dependent on ETC complex formation; hence the complexes are limiting for ATP production. Within Complex V for example the mitochondrial encoded subunits, Atp6 and Atp8 are crucial for ATP formation. They form the F₀ structural domain that is used to generate ATP by pumping protons into the matrix from the intermembrane space (Grzybowska-Szatkowska et al., 2014). Moreover, the subunits Nd4 and Nd6 are crucial for Complex I formation (Sharma et al., 2009). Dysregulation of Complex I leads to decreased intracellular ATP levels and increased ROS production.

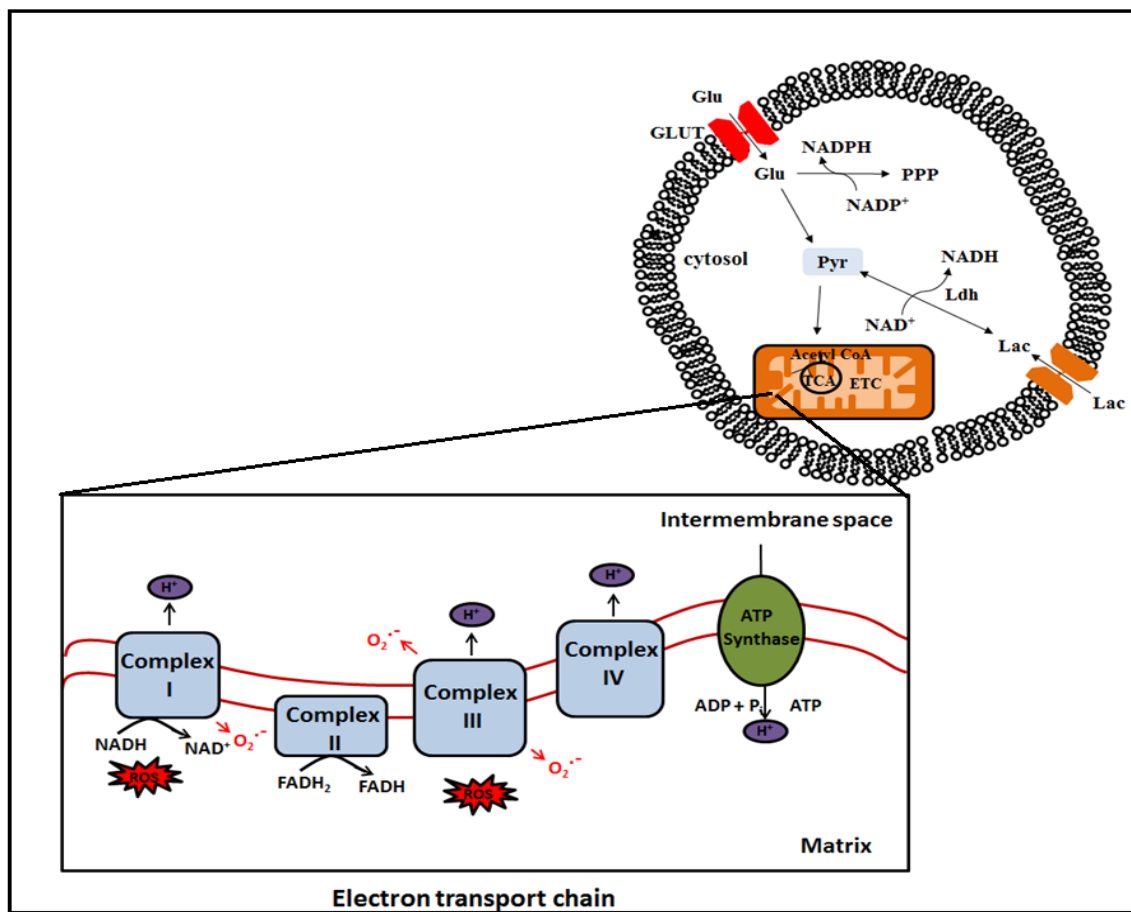


Figure 1.3 Mitochondrial oxidative phosphorylation. Pyruvate from glycolysis or lactate is ultimately used to produce reducing agents NADH and FADH₂ that transfer their electrons along the ETC complexes during the process of OxPhos to produce ATP. As electrons move across complexes protons are pumped into the inter membrane space generating a proton gradient that is used by Complex V to form ATP. ROS is produced at Complex I and Complex III as a by-product of ATP formation. (Glu, glucose; Pyr, pyruvate; GLUT, glucose transporter; Ldh, lactate dehydrogenase; Lac, lactate; ETC, electron transport chain; TCA, tricarboxylic acid; ROS, reactive oxygen species). (Adapted from Mergenthaler et al., 2013).

1.7 Mitochondrial ROS generation

Neurons are responsible for producing high levels of ROS through electron leakage from Complex I or Complex III that can form oxygen radicals that are harmful to the cell (Takeshige and Minakami, 1979; Beyer, 1992). ROS can also occur when there is a blockage of electron movement from one molecule to the next acceptor molecule in the ETC. This causes electrons to be backed up and leak out of the complexes. The electrons that leak out can then react with oxygen to form oxygen radicals in the form of hydroxyl ions, superoxide or hydrogen peroxide (Chouchani et al., 2014; Takeshige and Minakami, 1979; Beyer, 1992). ROS can be generated on account of metabolic stress due to increased nutrient concentrations, such as glucose or lactate that drives the ETC (Liemburg-Apers et al., 2015; Russell et al., 2002; Shi and Liu, 2006; Sepehr & Mohseni, 2010; Yates et al., 1990), as well chemicals such as rotenone and antimycin A, which inhibit Complex I and Complex III, respectively (Li e al., 2003; Zhou et al., 2014).

The main site of ROS production is Complex I where it can be generated in two ways (Liu et al., 2002). Complex I acts as a point of entry for the electrons accepted by its flavin mononucleotide (FMN) cofactor from NADH. Under conditions of high NADH/NAD⁺, electrons are backed up at FMN, unable to be passed along through a chain of seven FeS centres. Oxygen can react with the reduced form of FMN and cause superoxide production. (**Fig. 1.3**). Another method for ROS generation at Complex I, is through reverse electron transport that forces the electron flow back into Complex I resulting in an increase in electrons (Chance and Hollunger, 1961a, b; Hinkle et al., 1967; Chouchani et al., 2014).

Apart from the ETC, ROS can also be produced in the mitochondria from monoamine oxidases. These flavoenzymes exist in two main forms- monoamine oxidase A and monoamine oxidase B. They are located on the outer membrane of the mitochondria and utilize FAD to

metabolize monoamines in neurotransmitters such as dopamine, serotonin, and epinephrine (Kalgutkar et al., 2001). Aldehydes are formed as a product of this reaction, which might generate ROS with the reduction of FAD to FADH₂ (Edmondson et al., 2009).

ROS can also be produced in the cytoplasm by a family of enzymes known as NADPH oxidases (NOX). Although there are seven known NOX family members, NOX2 is the most highly expressed in the brain although expression of NOX1 and NOX3 has also been documented in neurodegenerative diseases (Shimohama et al., 2000; de la Monte and Wands, 2006).

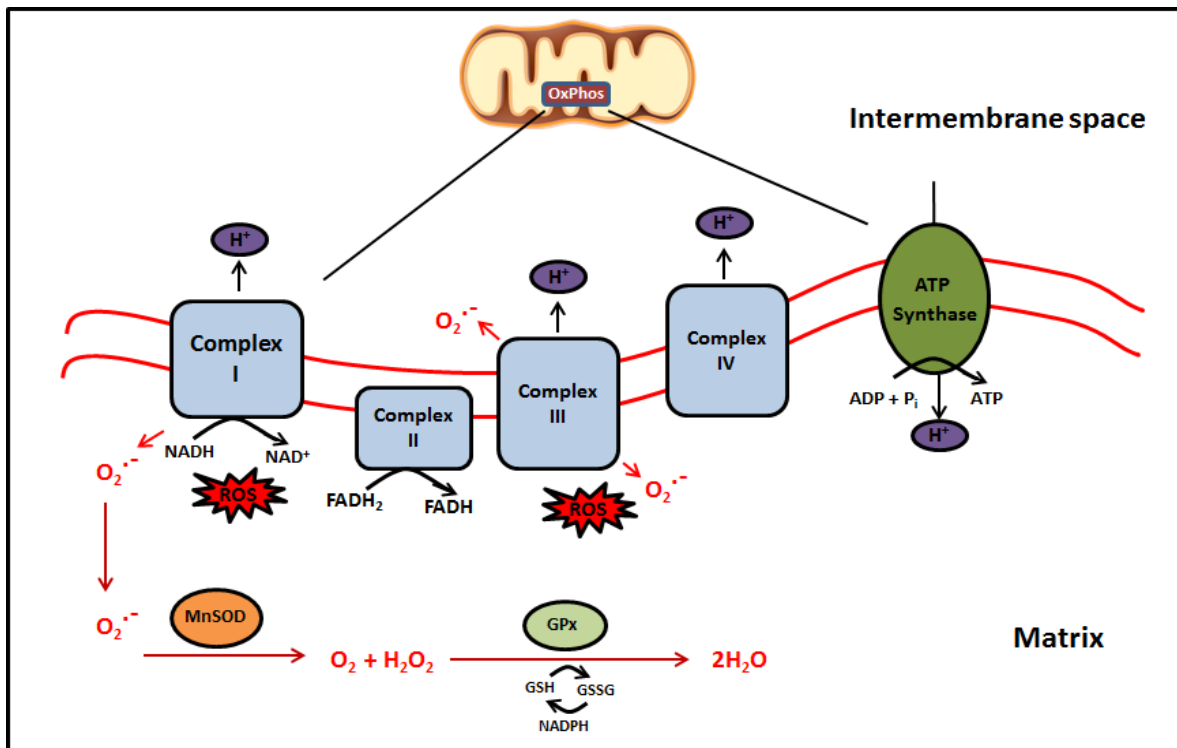


Figure 1.4 Mitochondrial ROS defence mechanisms. ROS generated from Complex I or Complex III can be neutralized through antioxidant defence mechanisms mediated by SOD and GSH. MnSOD converts superoxide radicals to hydrogen peroxide. GSH then converts this hydrogen peroxide to water in a reaction catalyzed by GPx. ROS generated from Complex III can also be released into the intermembrane space. (SOD, superoxide dismutases; MnSOD, manganese containing superoxide dismutase; ROS, reactive oxygen species; GPx, glutathione peroxidase). (Adapted from Mergenthaler et al., 2013)

1.8 Mitochondrial ROS defence mechanisms

mtDNA lacks protective histones and possesses a poor capacity for DNA repair, thus minimizing ROS is a high priority for neurons (Moreira et al., 2008). In addition, as they are unable to divide once differentiated and have a limited pool of progenitors, it becomes extremely important to maintain the neurons formed during development throughout an individual's lifetime. Mitochondrial antioxidant mechanisms are thus mainly mediated by manganese superoxide dismutase (MnSOD) and glutathione (GSH), which are sufficient for removal of superoxide generated by the ETC (Kudin et al., 2008; Cadenas et al., 2000).

The antioxidant enzymes, of superoxide dismutases (SODs), are thought to be the first line of defense in scavenging superoxide radicals. There are three main types of SOD enzymes that exist in different compartments of the cell. Two are present in the mitochondria, copper/zinc and manganese containing SODs, Cu/ZnSOD and MnSOD respectively (Candas et al., 2014; Okado-Matsumoto and Fridovich, 2001; Weisiger and Fridovich, 1973; Borgstahl et al, 1992; Duttaroy et al, 2003; Ravindranath and Fridovich, 1975) (**Fig. 1.4**). MnSOD is extremely important for cell survival and is known to cause lethality in mice when genetically deleted (Lee et al., 2012). The MnSOD enzyme converts superoxide radicals into hydrogen peroxide and oxygen (Fridovich, 1995; Candas et al., 2014). The hydrogen peroxide produced can further be neutralized to water by GSH also present in the mitochondria.

GSH is formed from glutamate and cysteine with ATP as a co-substrate by the enzyme γ GluCys synthase (Meister, 1974; Lash, 2006). GSH can then be used in an enzymatic or non-enzymatic reactions to neutralize existing ROS radicals. Although GSH is synthesized in the cytosol, it can localize to other organelles such as the mitochondria (Lash, 2006). Under the non-enzymatic reactions, reduced GSH reacts directly with ROS radicals for their removal by

forming adducts with them or causing their reduction. Alternatively, reduced GSH can act as part of an enzymatic reaction by scavenging hydrogen peroxides produced by SOD (Ruszkiewicz and Albrecht, 2015). In this reaction, GSH is converted by glutathione peroxidase to an oxidized form (GSSG) while bringing about conversion of hydrogen peroxides to water (**Fig 1.4**). GSSG can then be recycled back to GSH by glutathione reductase using reducing equivalent NADPH generated from the PPP. A consistent supply of available GSH is dependent on the availability of NADPH. Under oxidative stress conditions, neurons revert to the PPP to generate more NADPH reducing equivalents to help recycle GSH to keep up with its rapid rate of consumption with superoxide and peroxide removal (Ruszkiewicz and Albrecht, 2015).

1.9 Mitochondria and neurodegenerative diseases

Neurodegeneration is a broad term that is used to describe the condition in which there is progressive death of neurons and brain tissue, which gradually leads to a decline in mental capacity and function (Stocchi and Olanow, 2003; Cicero et al., 2017). Mutations in mtDNA tend to accumulate over time and manifest themselves in pathologies such as diabetes, aging and neurodegenerative diseases such as amyotrophic lateral sclerosis, Huntington's Disease, Parkinson's Disease (PD) and Alzheimer's Disease (AD) (Liu et al., 2013; Trifunovic, 2006). There is substantial evidence pointing toward mutations in mtDNA being the outcome of high oxidative stress caused by ROS (Kudin et al., 2005). Moreover, increasing ROS levels could potentially bring about the impairment in ETC function, hypometabolism and OxPhos decline that is observed (Manczak et al., 2006; Halliwell et al., 2006, Islam, 2017).

Defects in mitochondrial metabolism play a role in the impairment of neuro-plasticity and neurodegeneration (Alves et al., 2015; Lee et al., 2012). In high concentrations, lactate causes a

condition known as metabolic acidosis, a phenomenon often observed in neurodegeneration that can lead to ROS generation (Horowitz et al., 2010). Additionally, the metabolic shift from OxPhos to aerobic glycolysis that furthers production of lactate, is characteristic of neuropathophysiology where glycolytic enzymes such as hexokinase are upregulated and mitochondrial oxygen consumption is decreased (Chih and Roberts, 2003; Dienel and Hertz 2001; Kraig et al., 1987; Macauley et al., 2015; Nedergaard et al., 1991; Siesjo et al., 1985; Allen et al., 2014; Yang et al., 2015). This in combination with the decline in OxPhos can cause the impairment of mitochondrial function which contributes to the generation of ROS and the neuropathophysiology.

It is well established that AD, is characterized by dysfunctional mitochondria (Hroudova et al., 2014; Moreira et al., 2006; Moreira et al., 2009; Su et al., 2008; Nunomura et al., 2001). Mitochondrial dysfunction ranges from reduced membrane potential and increased permeability of the mitochondrial membrane and ROS production to altered glucose metabolism leading to general hypometabolism (Foster et al., 1983; Friedland et al., 1983; de Leon et al., 1983). There are lower levels of proteins that localize to the mitochondria such as Pdh and the TCA cycle enzyme α -ketoglutarate dehydrogenase in AD subjects (Gibson et al., 1998). Moreover, in AD, reduced OxPhos is found to take place due to decreased mitochondrial gene expression, leading to dysfunctional mitochondria and hypometabolism. Several findings have determined that mitochondrial gene expression of ETC subunits is downregulated in both early and late AD (Chandrasekaran et al., 1998; Hatanpaa et al., 1996; Parker et al., 1990; Kish et al., 1992; Manczak et al., 2004, Hong et al., 2007). Reduced mitochondrial gene expression of all three subunits of cytochrome oxidase c (Cox) of Complex IV of the ETC are also observed in AD brains (Parker et al., 1990; Kish et al., 1992; Chandrasekaran et al., 1998, Hong et al., 2007).

Complex I subunits Nd1 (Chandrasekaran et al., 1998) and Nd4 were down regulated in some studies (Simonian et al., 1994), whereas in others, all subunits were found to be significantly decreased (Manczak et al., 2004).

Mitochondria also play a major role in contributing to this Parkinson's disease. One mechanism through which this takes place is via inhibition of Complex I in the ETC. There is also a deficiency and misassemble of Complex I as well as decrease in Complex III (Keeney et al., 2006). This in turn could result not only in higher levels of electron leaks leading to ROS production, but also cause severe reductions in function Complex I (Acín-Pérez et al., 2004; Haas et al., 1995; Shinde et al., 2006).

1.10 Rb family and the brain

The Retinoblastoma Susceptibility (Rb) gene family of nuclear transcriptional co-repressors are made up of Rb, Rb11 (p107) and Rb12 (p130). Rb is a known tumor suppressor gene whose loss of function can result in the initiation as well as progression of cancers in numerous tissue types (Dick et al., 2013). The two other members of the Rb family, p107 and p130, which are found in higher organisms, are not known to act as tumor suppressors. p107 and p130 share more regions of homology with each other than with Rb (Harlow et al., 1986; DeCaprio et al., 1988; Ewen et al., 1991).

The Rb family have a role in cell cycle progression by repressing gene expression of cells involved in proliferation. p130 is expressed during cell growth arrest whereas p107 is expressed during proliferation and Rb throughout the cell growth phases of the cell cycle. The Rb family function in their hypophosphorylated forms by binding to E2f transcription factor family members to repress gene expression (**Fig. 1.5**). Rb accomplishes this at the S phase, (Burke et al.,

2010; Chellappan et al., 1991; Hiebert et al., 1992; Bukhart and Sage, 2008; Ajioka et al., 2014), whereas p107 and p130 exert their influence at G1/S and at growth arrest G0 phases, respectively (Cobrinik et al., 1993; Smith et al., 1996; Bukhart and Sage, 2008; Ajioka et al., 2014). Modification of Rb family members by phosphorylation from cyclin dependant kinases (cdks) abrogate E2f interactions that de repress gene promoters.

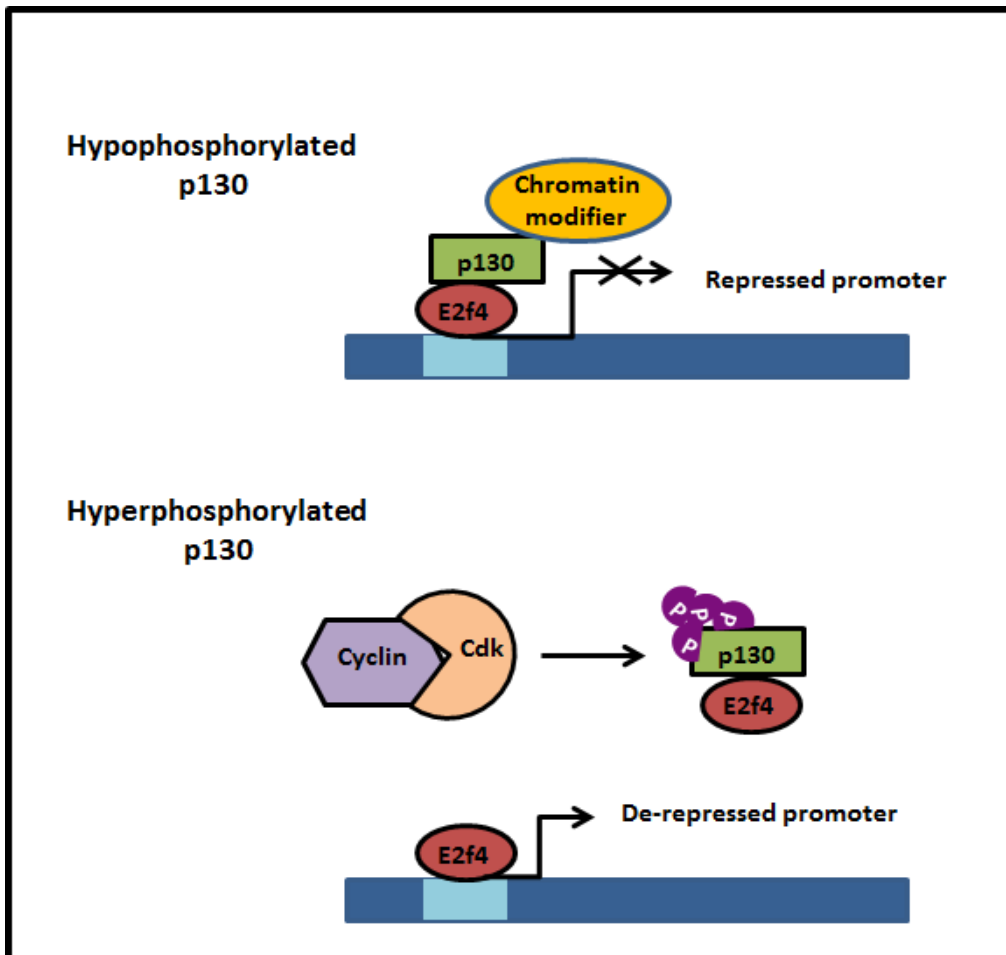


Figure 1.5 Role of p130 as a nuclear transcriptional co-repressor. In its hypophosphorylated state, p130 acts as a co-repressor by binding to E2f4 with the help of chromatin modifiers such as HDAC, thus preventing gene expression. However, when phosphorylated by cyclin/cdks, hyperphosphorylated p130 is unable to bind to E2f4, allowing it to activate gene expression. (Cdk, cyclin dependent kinase). (Adapted from Rayman et al., 2002)

1.11 p130 and neurons

Apart from their role during the cell cycle, the Rb family can also play a role in neural differentiation, and migration. Rb was found to play a role in differentiation and maturation of neural cells such as mouse retinal rod photoreceptor and amacrine cells (Zhang et al., 2004a).

Cell cycle regulation during neural development is tightly regulated by the Rb family due to the disparate timing of progenitor differentiation for the diverse types of brain cells. p130 has a crucial role in cell cycle regulation during differentiation by promoting progenitor exit from the cell cycle (Litovchick et al., 2007; Takahashi et al., 2000; Bukhart and Sage, 2008). p130 functions to maintain a G0 quiescent state of the cell cycle by partnering with E2f4 and HDAC1 reducing histone H3 and H4 acetylation (Takahashi et al., 2000; Rayman et al., 2002).

The total number of neurons in the adult brain is dependent on the timing of progenitor exit from the cell cycle, as the pool of neural progenitors is limited. A timely exit ensures that progenitors have enough time to divide and generate a sufficient quantity of their pool in order to produce enough neurons at later stages in development. If progenitors exit the cell cycle too early, enough progenitors will not be maintained in the stem cell pool to regenerate neurons at later stages. (Dyer et al., 2009; Ajioka et al., 2014).

Another essential function of p130 is with respect to the migration of neurons throughout the brain. Post differentiation, migration of cortical inhibitory neurons to the cerebral cortex is mediated via Rb (Ferguson et al., 2005; McClellan et al., 2007), whereas the migration of excitatory neurons, requires p130 and p107 (Oshikawa et al., 2013; Svoboda et al., 2013).

p130 is the predominant Rb family member expressed in mature brain neurons, where it is responsible for maintaining the differentiated state and promoting cell survival (Liu et al., 2005).

The Balb/c mouse strain, exhibits embryonic lethality with genetically deleted p130 on account of massive neuron death in several regions of the central nervous system (LeCouter et al., 1998b). In neurons, de-repression of nuclear promoters by abrogating p130 binding to E2f4 resulted in apoptosis. This occurred by increasing the transcription of apoptotic inducing genes such as B-myb (Liu et al., 2001; Iyirhiaro et al., 2014).

p130 function has also been found to be perturbed in neurodegenerative diseases where significantly higher levels of p130 were found in the cytoplasm of neurons and glia obtained from AD human brains compared to controls (Previll et al., 2007). Previll et al found that AD neurons not only had higher levels of cytoplasmic p130, but also expressed various proteins that are usually present in dividing cells such as cyclins and cdks. It was postulated that p130 localization from the nucleus to the cytoplasm resulted in de-repression of normally arrested cell cycle gene promoters. The authors further hypothesized that the de-repressed cells could either re-enter the cell cycle depending on their former point of cell cycle exit or die via apoptosis if unable to do so (Previll et al., 2007).

2. RATIONALE AND HYPOTHESIS

1. Rationale:

The retinoblastoma susceptibility (Rb) family member p130 is a nuclear co transcriptional repressor whose potential cytoplasmic role in neurons during neurodegenerative disorders is unknown. Additionally, our knowledge on the transcriptional regulation of the mitochondrial genome and the proteins it encodes are still limited.

2. Hypothesis:

p130 has a mitochondrial role in oxidative defence and ROS control in neurons through regulating oxidative phosphorylation by interacting with mitochondrial DNA to repress gene expression- A mechanism for reducing ROS generation.

3. Objectives:

- 1) To assess ascertain a mitochondrial subcellular localization of for p130 in neurons
- 2) To establish a role for p130 in regulating mitochondrial gene expression.
- 3) To establish the influence of p130 as a defence mechanism of ROS.

3. MATERIALS AND METHODS

Cells

The mouse glioblastoma cell line Neuro2a were grown in Dulbecco's Modified Eagle Medium (DMEM) supplemented with 10% fetal bovine serum (FBS) and 1% penicillin streptomycin. For the purpose of neuron differentiation, the cells were grown in stripped DMEM with 0.5% FBS and supplemented with 5.5mM glucose, 100mM pyruvate and 4mM glutamine for 4 days. Cells were subjected to metabolic stress with 25mM glucose or 10mM lactate. To inhibit metabolic stress cells were pretreated with 2.5mM Nac or pretreated for 12 hours before adding lactate.

Isolation of tissue, primary astrocytes and neurons

Brain, primary astrocytes and neurons were obtained from brains of day 3 neonatal Balb/c mice as approved by York University Animal care committee and performed in accordance with Canadian Council for Animal Care Guidelines. To isolate the cells, brain tissue was homogenized and filtered through a 100 µm cell strainer, followed by drop wise addition of 8ml of 10% DMEM (10% FBS and 1% penicillin streptomycin). The filtrate was centrifuged at 1000g for 5 minutes. The supernatant was discarded and the pellet containing cells was resuspended in 10% DMEM and plated. The culture media was replaced with fresh culture media after 24 hours and cells were allowed to grow.

Immunocytochemistry

Cells were washed twice with phosphate buffered saline (PBS) and fixed for 15 minutes with 4% paraformaldehyde. Cells were permeabilized for 30 minutes at 4°C with blocking buffer (3% BSA and 0.1% saponin in PBS) followed by primary antibody incubation with rabbit polyclonal p130 (C18, Santa Cruz Biotechnology) at a 1:250 dilutions in blocking buffer for

1 hour. After three washes cells were incubated with secondary antibody Alexa Fluor 594 goat anti rabbit IgG (Life Technologies) at a 1:200 dilution. Mitoview Green (Biotium) was then used to stain mitochondria or dihydrorhodamine (Dhr) (Santa Cruz Biotechnology) for mitochondrial ROS for 30 minutes, proceeded by Dapi. For immunocytochemistry of the neural differentiation marker, Map2 a monoclonal antibody (1:250) was used with secondary antibody IgGκ BP-FITC anti-mouse (Santa Cruz Biotechnology) at a 1:200 dilution. Plates were then mounted in mounting medium (Vectasheild) for fluorescence. Images were obtained using the Axio Scope A.1 microscope with 20 x 0.5 Ph2 or 40 x 0,75 Ph2 “EC-Plan-NEOFLUAR” (Carl Zeiss Canada, Toronto, Canada, <https://www.zeiss.ca>). Digital images were captured using AxioCam MRm. The ROS intensity was quantified by measuring the intensity of Dhr fluorescence for each cell using the Image J software.

Immunohistochemistry

Whole mouse brain was rinsed with PBS and immersed in 4% PFA overnight. The brain was then transferred to 30% sucrose solution and stored overnight or until the brain settled to the bottom of the solution. The brain was then prepared for sectioning by freezing with a solution of 2:1 OCT-sucrose. Sections were cut to 10µm using a cryostat set to -20°C. The tissue sections were washed twice with PBS and then permeabilized for 30 minutes at 4°C with blocking buffer followed by primary antibody incubation with p130 (C18, Santa Cruz Biotechnology) at a 1:250 dilution in blocking buffer for 1 hour. After three washes sections were incubated with secondary antibody Alexa Fluor 594 goat anti rabbit IgG (Life Technologies) at a 1:200 dilution. Mitoview Green (Biotium) was then used to stain mitochondria for 30 minutes, proceeded by Dapi. Sections were then mounted in medium for fluorescence (Vectasheild). Images were obtained using the Axio Scope A.1 microscope with

20 x 0.5 Ph2 “EC-Plan-NEOFLUAR” (Carl Zeiss Canada, Toronto, Canada, <https://www.zeiss.ca>). Digital images were captured using AxioCam MRm

Nuclear extraction

Monolayer cells were first washed twice with PBS and then harvested by scraping with ice cold PBS containing protease inhibitors (1mg/ml of each of pepstatin, leupeptine and aprotinin). After centrifuging the cells at 1500 rpm for 5 minutes at room temperature, the supernatant was discarded, and the cell pellet was washed in cold PBS and transferred to a new eppendorf tube. The cell pellet was then dissolved in 500ul of cytoplasmic buffer (10mM Tris pH 7.4, 10mM NaCl, 3mM MgCl₂, 0.5% NP-40 and protease inhibitors) and incubated on ice for 5 minutes followed by rocking at 4°C for 5 minutes. After incubation, a small volume of the solution was removed representing the “whole cell fraction”. The remaining homogenate was then centrifuged at 2500g for 5 minutes at 4°C. The supernatant constituting the cytoplasmic fraction was separated in a pre-chilled tube. The cell pellet comprising the nuclear fraction was then washed 8 times with the cytoplasmic buffer. After several washes the insoluble cell pellet was lysed with nuclear lysis buffer (50mM Tris pH 7.4, 5mM MgCl₂, 0.1mM EDTA, 1mM dithiothreitol (DTT), 40% (wt/vol) glycerol) and 0.15 unit/ul benzonase (SantaCruz Biotechnology) to digest the DNA and RNA in the suspension.

Mitochondrial isolation

Neuro2A cells were washed twice with PBS, scraped with ice cold PBS and pelleted by centrifugation at 1500rpm for 5 minutes. The pellet was dissolved in 5 times the packed volume in isolation buffer (0.25M Sucrose, 0.1% BSA, 0.2mM EDTA, 10mM HEPES with 1mg/ml of each pepstatin, leupeptin and aprotinin protease inhibitors), transferred into a pre-chilled Dounce homogenizer, and homogenized loose (6 times) and tight (6 times) on ice.

The homogenate was transferred into an eppendorf tube and centrifuged at 1000 g at 4°C for 10 minutes. The supernatant was collected and the pellet containing the debris and nucleus were discarded. The supernatant was centrifuged at 14000g for 15 minutes at 4°C and the resulting supernatant was saved as the cytosolic fraction. The pellet comprising the mitochondrial fraction was washed twice and dissolved in 300ul of isolation buffer. The mitochondria were lysed by repeated freeze-thaw cycles (3 times each) on dry ice.

Western blot analysis

For whole cell Western blot analysis, cells, mitochondrial and tissue were lysed in RIPA buffer (0.5% Nonidet P40, 0.1% sodium deoxycholate, 150mM NaCl, 50 mM Tris-Cl pH 7.5, 5mM EDTA with 1mg/ml of each pepstatin, leupeptin and aprotinin protease inhibitors) or by freeze thaw in mitochondrial buffer or in nuclear buffer 1 respectively. (1mg/ml of each of pepstatin, aprotinin and leupeptin). Protein lysates were loaded on gradient (6-15%) or 7.5% polyacrylamide gels. Samples to be loaded were first boiled for 3 minutes in loading buffer containing 4% SDS, 10% 2-mercaptoethanol, 20% glycerol, 0.004% bromophenol blue, 0.125M Tris-HCl and 1mM DTT. Loaded onto gels were placed in running buffer (2.5mM Tris-base, 192mM glycine and 0.1% SDS) and the proteins were separated by electrophoresis for 2 hours at 30 milliamps. Proteins were transferred on a 0.45 a polyvinylidene difluoride (PVDF) membrane (Bio-rad) at 4°C for 80 minutes at 100V, using a wet transfer method (50mM Tris Base, 384mM glycine, 20% methanol). The membranes were blocked for an hour at room temperature in 5% milk in Tris-Buffered Saline (150mM NaCl and 50mM Tris base) containing 0.1% Tween-20 (TBST). The PVDF membranes were probed with antibodies diluted in 5% milk in TBST. Incubation with primary antibodies was done overnight at 4°C with gentle rocking. Primary antibodies used were rabbit polyclonal anti-p130 (C-18, Santa Cruz Biotechnology), rabbit polyclonal anti-Cox4 (Rb anti Cox IV,

Abcam), goat polyclonal anti-Histone H3 (Santa Cruz Biotechnology) and monoclonal anti- α -tubulin (Sigma). After primary antibody incubation, the membranes were washed three times with TBST and secondary antibodies conjugated with horseradish peroxidase were added and incubated for an hour at room temperature with gentle rocking. The secondary antibodies were goat anti-rabbit (Bio-rad), rabbit anti-goat (Bio-rad) and goat anti-mouse (Bio-rad). After secondary antibody incubation, the membranes were washed 3 times with TBST for 5 minutes each followed by a final wash with Tris-Buffered Saline for 10 minutes. The membranes were visualised with chemiluminescence on photographic films (Santa Cruz Biotechnology). Protein levels were then evaluated through densitometry using Image J software.

Quantitative Chromatin immunoprecipitation assay (qChIP)

Isolated mitochondria were resuspended in 200 μ L PBS with 1% formaldehyde and rocked at room temperature (RT) for 15 minutes to enable the crosslinking/fixation reaction. This was quenched by adding 200 μ L of 125mM glycine in PBS and rocked for 5 minutes at RT. 400 μ L of cold PBS (with 1mM NaF and 100mM Na₃VO₄) was added and centrifuged at 14,000g for 5 minutes at 4°C. The supernatant was discarded and the pellet washed in the same buffer. The pellet was re-suspended in 500 μ L of ChIP Dilution Buffer (40mM Tris pH8.0, 1% Triton X-100, 4mM EDTA, 300mM NaCl, 1 μ g/ml aprotinin, leupeptin, pepstatin A, 1mM PMSF, 1mM Na₃VO₄) and kept on ice until sonication. Samples were sonicated at 12 cycles of 15s on, 45s off with amplitude 15%. Post sonication, samples were centrifuged at 13,000 rpm for 10min at 4°C. The supernatant was transferred to a new tube with an equal volume of Dilution Buffer 1 (40mM Tris pH 8.0, 4mM EDTA, 1 μ g/ml aprotinin, leupeptin, pepstatin A, 1mM PMSF, 1mM Na₃VO₄) and the pellet discarded. 20 μ L of the sample was removed, added to 100 μ L Dilution Buffer 2 (40mM Tris pH 8.0, 0.5% Triton X-100, 4mM

EDTA, 150mM NaCl, 1µg/ml aprotinin, leupeptin, pepstatin A, 1mM PMSF, 1Mm Na₃VO₄) and stored as Input DNA at -20°C. The remaining sample was diluted to 750µL with Dilution Buffer 2 and 50µL of Protein A agarose beads (Santa Cruz Biotechnology) were added and rocked at 4°C for 60 minutes to pre clear. The beads were pelleted by centrifugation at 1500rpm for 2 minutes at 4°C and the supernatant transferred into another tube. The sample was incubated overnight on a rocker at 4°C with 5µg of p130 antibody (C-18, Santa Cruz Biotechnology).

50µL of Protein A agarose beads were added to the sample the next day and rocked at 4°C for 90min. The antibody bound beads were pelleted by centrifugation at 1500rpm for 2 minutes at 4°C and the supernatant with unbound protein was removed. The antibody bound beads were washed for 5 minutes on a rocking platform with 1mL of each of various wash buffers and the beads pelleted at 1500rpm for 2 minutes at 4°C in between washes. The wash buffers in order were: Low salt Immune complex wash buffer (0.1% SDS, 1% Triton X-100, 2mM EDTA, 20Mm Tris-HCl-pH 8.1, 150mM NaCl), High salt Immune complex wash buffer (0.1% SDS, 1% Triton X-100, 2mM EDTA, 20Mm Tris-HCl-pH 8.1, 500mM NaCl), LiCl Immune complex wash buffer (0.25M LiCl, 1% IGEPAL-CA630, 1% deoxycholic acid sodium salt, 1mM EDTA, 10Mm Tris pH 8.1). The final wash was done twice with TE buffer (10mM Tris-HCl, 1mM EDTA pH 8.0) at room temperature. After the last wash, the pellet was re-suspended in 250µL in Elution Buffer (1% SDS, 0.1M NaHCO₃), vortexed and placed on a rotator for 15 minutes at RT. The suspension was spun at 1500rpm for 2 minutes and the supernatant transferred to a fresh tube. Another 250µL of Elution Buffer was added and the elution was repeated as before and the eluates combined for a volume of 500µL. 20µL of 5M NaCl was added to the eluates and 4µL to Input DNA to reverse the protein/DNA cross links. by incubating at 65°C for 6 hours. The DNA was purified using the Active Motif Purification

Kit (Active Motif) as per manufacturer's instructions. DNA binding was then detected using qPCR.

qPCR analysis

For RNA isolation from cells, Trizol reagent (Life Technologies) was used according to the manufacturer's instructions and RNA obtained was dissolved in RNAase free water and purity estimated using Nanodrop photospectomter. RNA (1 μ g) was reverse transcribed into cDNA using the GeneAmp Kit (Applied Biosystems) and used for quantitative real time PCR (qPCR). qPCR assays were performed on Light cycler 96 (Roche) using SYBR green Fast qPCR Master mix (Biotool) with primer sets for *Nd4*, *Nd6*, *Cytochrome b*, *Cox II Atp6* and *β -actin*. Relative expression of cDNAs was determined after normalization with *β -actin* using the $\Delta\Delta$ Ct method. For qChIP, relative binding was determined by amplifying isolated DNA fragments using the D-Loop promoter set and analyzed using the $\Delta\Delta$ Ct method and normalized to the control.

Table 1. Primer sets used for qPCR

Gene Name	Sequence accession number	Amplicon length	Forward primer sequence	Reverse primer sequence
β -actin Actb	MGI:87904	34	GCT CTG GCT CCT AGC ACC AT	CCA CCG ATC CAC ACA GAG TAC
Nd4 mt-Nd4	MGI:102498	66	CCT CAC ATC ATC ACT CCT ATT CTG	GGC TAT AAG TGG GGA AGA CCA TTT G
Cox II mt-Co2	MGI:102503	98	AGT TGA TAA CCG AGT CGT TCT G	CTG TTG CTT GAT TTA GTC GGC
Atp 6 mt-Atp6	MGI:99927	55	TCC CAA TCG TTG TAG CCA TC	TGT TGG AAA GAA TGG AGT CGG
Nd6 mt-Nd6	MGI:102495	44	TGT TGC AGT TAT GTT GGA AGG AG	CAA AGA TCA CCC AGC TAC TAC C
D-Loop	MF 133498.1	173	GCG TTA TCG CCT CAT ACG TT	GGT GCG TCT AGA CTG TGT GC

ATP generation assay

Mitochondria were isolated from neurons that were untreated or treated with lactate for 6 hours in the absence (Lac) or presence of 2.5mM Nac (Lac+ Nac). ATP production capacity of isolated mitochondria was measured using the ATP determination kit (Thermo Fisher Scientific) as per manufacturer's instructions. ATP generation was recorded based on luminescence captured. ATP production for each sample was normalized to total mitochondrial protein concentration.

Statistical Analysis

All statistical analysis was performed on GraphPad Prism version 7.0 or Microsoft Excel. Student's unpaired T-tests were used unless stated otherwise. Results were considered to be statistically significant when $p < 0.05$. One way ANOVA was used for a specific data set and regarded as statistically significant when $p < 0.05$. Bonferroni post hoc test was used for analysis of significant differences between groups. For graphs, asterisks denote significance.

* $p < 0.05$, ** $p < 0.01$, *** $p < 0.001$. All data are mean +/- SD.

4. RESULTS

p130 is present in the mitochondria of terminally differentiated neurons in vitro

A recent report from our lab has shown that the Rb family member p107 controls stem cell fates by regulating their metabolism (Porras et al, 2017). We thus wanted to assess if p130, another family member, has a similar role in neurons. We first assessed p130 protein expression during a time course of neural differentiation. Neuro2a (N2A) cells were used to derive terminally differentiated neurons by serum withdrawal over a 4 day period. By Western blot analysis the protein expression of p130 was determined (**Fig. 5.1A**). As expected from previous studies there was no p130 expression in proliferating cells (Litovchick et al, 2007; Takahashi et al, 2000; Bukhart and Sage, 2008; Liu et al., 2005). However it was present in the beginning and at day 4 of terminal differentiation (**Fig. 5.1A**). Immunocytochemistry for p130 confirmed its presence in the terminally differentiated N2A cells with neuron specific marker Map2 (**Fig. 5.1B**).

Our lab also recently showed that p107 has a mitochondrial role in regulating metabolism during proliferation (Bhattacharya et al., 2017). Thus, we investigated if p130 might localize within the mitochondria during differentiation. Western blot analysis of cytoplasmic and mitochondrial fractions during a time course of differentiation showed that the mitochondrial levels of p130 were found to increase on day 1 of differentiation, but reduce to low levels in terminally differentiated neurons (**Fig. 5.2A**). Examination by immunocytochemistry of differentiated N2A cells also confirmed localization of p130 in the cytoplasm, nucleus and in small amounts in the mitochondria (**Fig. 5.2B**).

As mitochondrial proteins are imported via cleavage of target sequences, we evaluated if p130 was possibly cleaved to enable its import. For this we compared p130 protein by Western blot analysis of cytoplasmic and mitochondrial fractions in high resolution electrophoresis. We found no differences in the mobility of the p130 protein within

the gel of both cytoplasmic and mitochondrial fractions. This suggests that there might not have been any cleavage of p130 for mitochondrial import.

p130 is present in the mitochondria of primary neural cells and brain tissue

p130 has been reported to be widely expressed in the brain, as verified by protein expression levels of p130 in whole cell fractions of various brain regions (**Fig. 5.3A**). After confirming a mitochondrial presence for p130 in vitro, we wanted to assess if it was present in the mitochondria of brain tissue in vivo by immunohistochemistry of cerebral cortex sections. Merging images of mitochondrial and nuclear stain with and p130 immunocytochemistry revealed the presence of p130 in both the nucleus and mitochondria (**Fig. 5.3B**). By Western blot analysis, p130 protein was detected in the mitochondrial fractions of all brain regions analyzed, namely the cerebral cortex, hippocampus, midbrain, cerebellum and brain stem (**Fig. 5.4A**). We confirmed the mitochondrial presence of p130 in isolated primary neurons and astrocytes from the whole brain of day 3 neonatal mice by immunocytochemistry (**Fig. 5.4B**).

p130 mitochondria localization increases during oxidative stress with glucose

We next assessed a possible mitochondrial role for p130 by analyzing its behaviour during conditions of increased OxPhos leading to oxidative stress. Both high and low glucose conditions have been known to generate mitochondrial ROS in the brain (Russell et al, 2002; Pirchl et al, 2006; Shi and Liu, 2006). Thus, neurons were treated with high (25mM) and low (1mM) glucose. Western blot analysis of mitochondrial and cytoplasmic fractions revealed a substantial increase in p130 protein expression in the mitochondrial compartments after 24 hours of high or low glucose treatment (**Fig. 5.5A**). This observation was confirmed using immunocytochemistry for p130 at 24h of treatment with high glucose (**Fig. 5.5B**). A clear

increase in mitochondrial p130 was evident from the intense yellow fluorescence obtained from the overlay of p130 (red) and stained mitochondria (green). This suggests a potential mitochondrial role for p130 in conditions for when the cell is stressed by glucose availability.

p130 mitochondria localization increases during oxidative stress with lactate

We next wanted to confirm if oxidative stress caused by other nutrients would also have the same affect. We thus treated neurons with lactate that is known to create an environment of oxidative stress (Horowitz et al, 2010; Macauley et al., 2015; Allen et al., 2014; Yang et al., 2015). As lactate is processed at a faster rate than glucose we performed Western blot analysis for p130 mitochondrial localization at early time points (**Fig. 5.6A**). Our results revealed that from 3h onwards there was an increase in p130 localization to the mitochondria with lactate treatment. Also the increased level of p130 localization to the mitochondria with the 24h treatment was associated with its decrease in the cytoplasm. We also performed immunocytochemistry for p130 localization at 24h of treatment with lactate (**Fig. 5.6**). The intense yellow fluorescence on merge of p130 and mitochondria stain (Mitoview) we observed was indicative of the increased mitochondrial p130 localization (**Fig. 5.6B**). This together with results obtained from glucose treatments, suggest a role for p130 in the mitochondria under conditions of oxidative stress caused by the availability of nutrients.

p130 mitochondrial localization increases with ROS

Based on these results, we considered ROS to be a potential mechanism that directs localization of p130 to the mitochondria. To this end, ROS production levels were assessed using dihydrorhodamine (Dhr) that stains mitochondrial superoxide. We treated neurons with lactate or the ROS inducer- rotenone for a period of 6 hours and then performed immunocytochemistry analysis of mitochondrial ROS production (**Fig 5.7A**). We found

significantly higher ROS levels in lactate treated neurons as well as in cells treated with the ROS inducer rotenone, compared to untreated controls (**Fig. 5.7B**). We confirmed by Western blotting, that p130 mitochondrial levels were upregulated when neurons were stressed by treatment with increasing concentrations of rotenone. (**Fig. 5.8A** and **Fig. 5.8B**).

p130 localization in the mitochondria decreases with ROS inhibitor.

We further established the influence of ROS on p130 mitochondrial localization, by pre-treating cells for 12 hours with ROS inhibitor N-acetyl cysteine (Nac). Nac reduces ROS by increasing GSH levels (Bavarsad et al., 2014), thus providing a gauge for the association of ROS and p130. By Western blot, cells treated with lactate showed increased mitochondrial p130 protein levels, but there was a substantial reversal if the cells were also treated with Nac (**Fig. 5.9**). Together these results convincingly show that the localization of p130 in neurons is based on the degree of mitochondrial ROS.

p130 interacts with mitochondrial DNA in vitro and in vivo

As p130 is a transcriptional co-repressor of nuclear genes, we assessed if it might have the same role in repressing mitochondrial gene expression. To test our hypothesis, we first assessed if p130 interacted at the mtDNA D-Loop promoter region by quantitative chromatin immunoprecipitation (qCHIP) analysis. We tested negative control mitochondria from proliferating cells where p130 is absent and terminally differentiated neurons where it is present within the mitochondria. qPCR analysis of p130 bound DNA revealed that more than 50-fold relative binding was observed from the mtDNA of terminally differentiated neurons compared to the proliferating control (**Fig. 5.10**). We also detected at least a 40-fold binding capacity for p130 at the D-loop of mitochondria isolated from the cerebral and hippocampal cortex tissue of the brain relative to the negative control mitochondria isolated from

proliferating cells (**Fig. 5.10**). These results suggest that p130 in the mitochondria might repress mitochondrial gene expression by interacting at the mtDNA D-Loop promoter.

p130 interaction with mitochondrial DNA increases with oxidative stress

Next we wanted to assess if oxidative stress influenced the binding capacity of p130. By qCHIP analysis p130 interaction with the mitochondrial D-Loop promoter region was found to increase with nutrient stress of either high glucose or lactate treatments for 24 hours when normalized to the proliferating control cells (**Fig. 5.11A**). p130 binding intensity at the D-Loop also increased after 6 hours of ROS generation with lactate and rotenone treatments (**Fig. 5.11B**). Together these results suggest that the mitochondrial function of p130 might be to repress mitochondrial gene expression by interacting at the mtDNA D-Loop promoter under conditions of high ROS generation.

p130 is associated with mitochondrial gene expression

We next evaluated if p130 binding to the D-Loop promoter region of mtDNA might repress gene expression. For this we compared the mitochondrial gene expression using qPCR under normal and nutrient stress conditions with lactate. We evaluated the mitochondrial *Nd4*, *Nd6*, *Cox 2* and *Atp6*. We found that gene expression for *Nd4*, *Cox 2* and *Atp6* were significantly down regulated with lactate treatment, and *Nd6* was almost significant under stress conditions, corresponding to a time point when more p130 is in the mitochondria, binding to mtDNA (**Fig. 5.12**). These results suggest a novel role for p130, as a mitochondrial transcriptional co-repressor. The repression of gene expression under high metabolic stress might be a neuronal defence mechanism against ROS generation.

p130 protein levels remain unchanged in the nucleus of lactate treated neurons

Next we wanted to ensure that the effect on mitochondrial gene expression was a p130 mitochondrial mediated effect and not the result of its nuclear function. For this, protein levels of p130 in the nucleus of lactate treated cells were assessed to determine if its levels remained constant up to 6 hours with lactate treatment (**Fig 5.13A**). Western blotting revealed that there were no significant differences in p130 protein levels in the nucleus after 3 and 6 hours of lactate treatment (**Fig 5.13A** and **Fig. 5.13B**), whereas, mitochondrial p130 levels significantly increased (compare **Fig. 5.13B** with **Fig. 5.6A**). This illustrates a potential lack of p130 nuclear involvement in controlling gene expression based on its protein levels. However, post translational changes of p130 and /or its partners on nuclear promoters are not known.

Increased expression of mitochondrial OxPhos genes with ROS inhibitor

We next verified if ROS influence on p130 localization also affected mitochondrial encoded gene expression. To assess this, lactate stressed neurons were treated with the ROS inhibitor Nac. Gene expression analysis by qPCR of various mitochondrial encoded OxPhos genes, *Nd4*, *Nd6*, *Cox 2* and *Atp6*, showed significantly increased levels of mitochondrial gene expression with the ROS inhibitor Nac (**Fig. 5.14**). This corresponds to the reduced presence of p130 in the mitochondria (**Fig. 5.9A**, **Fig. 5.9B**). Thus, p130 localization corresponds to reduced expression of mitochondrial encoded genes associated with OxPhos (**Fig. 5.14**).

Increased ATP production with decreased mitochondrial p130 localization.

The outcome of decreased OxPhos activity is an attenuation of the ATP producing capacity of the mitochondria (Kioka et al., 2013). Therefore we tested if the decreased gene expression of mitochondrial encoded OxPhos genes corresponding to p130 mitochondrial interaction at

the D-Loop with oxidative stress reduced the capacity for ATP production. For this we assessed ATP generation from mitochondria from neurons stressed with lactate in the absence or presence of Nac, as well as untreated controls. The Nac treatment which results in decreased p130 mitochondrial localization would be expected to have a higher level of ATP production. We found that neurons treated for 6 hours with lactate, which had the highest levels of mitochondrial p130 (**Fig. 5.6A**) and reduced levels of gene expression (**Fig. 5.12**), had the lowest levels of ATP production (**Fig. 5.15**). On the other hand, lactate stressed cells which had been treated with Nac that showed lower levels of mitochondrial p130 presence (**Fig. 5.9A**) and the highest levels of gene expression (**Fig. 5.14**), also displayed the highest levels of ATP production (**Fig. 5.15**). Together this data suggests that mitochondrial p130 levels repress mitochondrial encoded gene expression that reduces the ATP producing capacity of neurons, which results in a lower capacity to generate ROS.

\

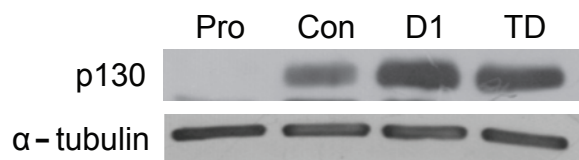
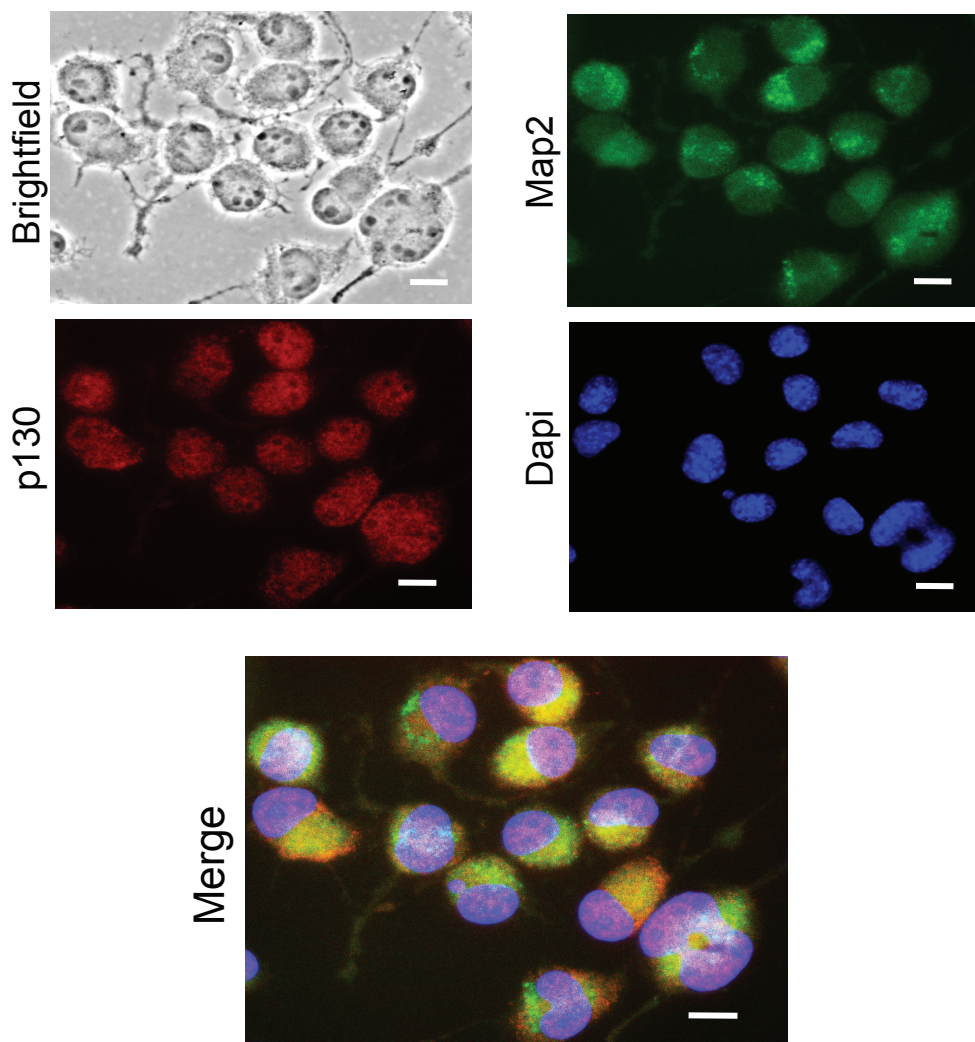
A**B**

Figure 5.1. p130 expression in differentiated Neuro2A cells. (A) Western blot of p130, α -tubulin and Cox IV for a time course of Neuro2A differentiation, proliferation (Pro), contact inhibited (Con), day 1 of differentiation (D1) and day 4 of terminal differentiation (TD). (B) Differentiated Neuro2A cells were visualized for brightfield, Map2 (green), a marker of neuron differentiation, p130 (red) and Dapi nuclear staining (blue) and Merge. Scale bars = 20 μ m.

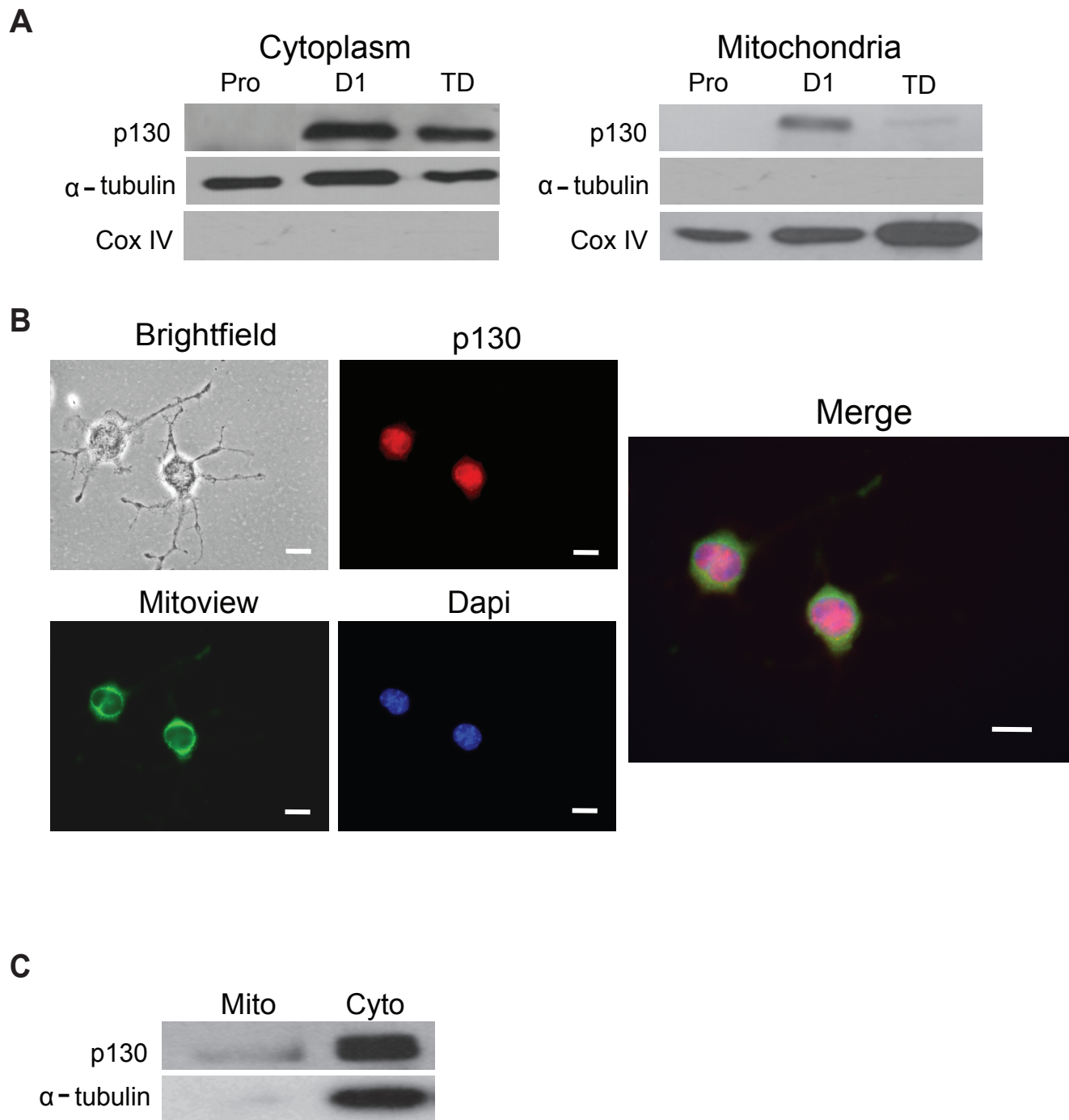


Figure 5.2. p130 is localized in the mitochondria of differentiated neurons. (A) Cytoplasmic and mitochondrial fractions assessed by Western blot for p130, α -tubulin and Cox IV at proliferation (Pro), day 1 (D1) and day 4 of terminal differentiation (TD). (B) Immunocytochemistry of differentiated Neuro2A cells for brightfield, p130 (red), Mitoview (green), Dapi nuclear staining (blue) and Merge. Scale bars = 20 μ m. (C) Representative Western blot for p130 and α -tubulin in mitochondrial (Mito) and cytoplasmic (Cyto) fractions of differentiated Neuro2a neurons resolved on a 7.5% gel.

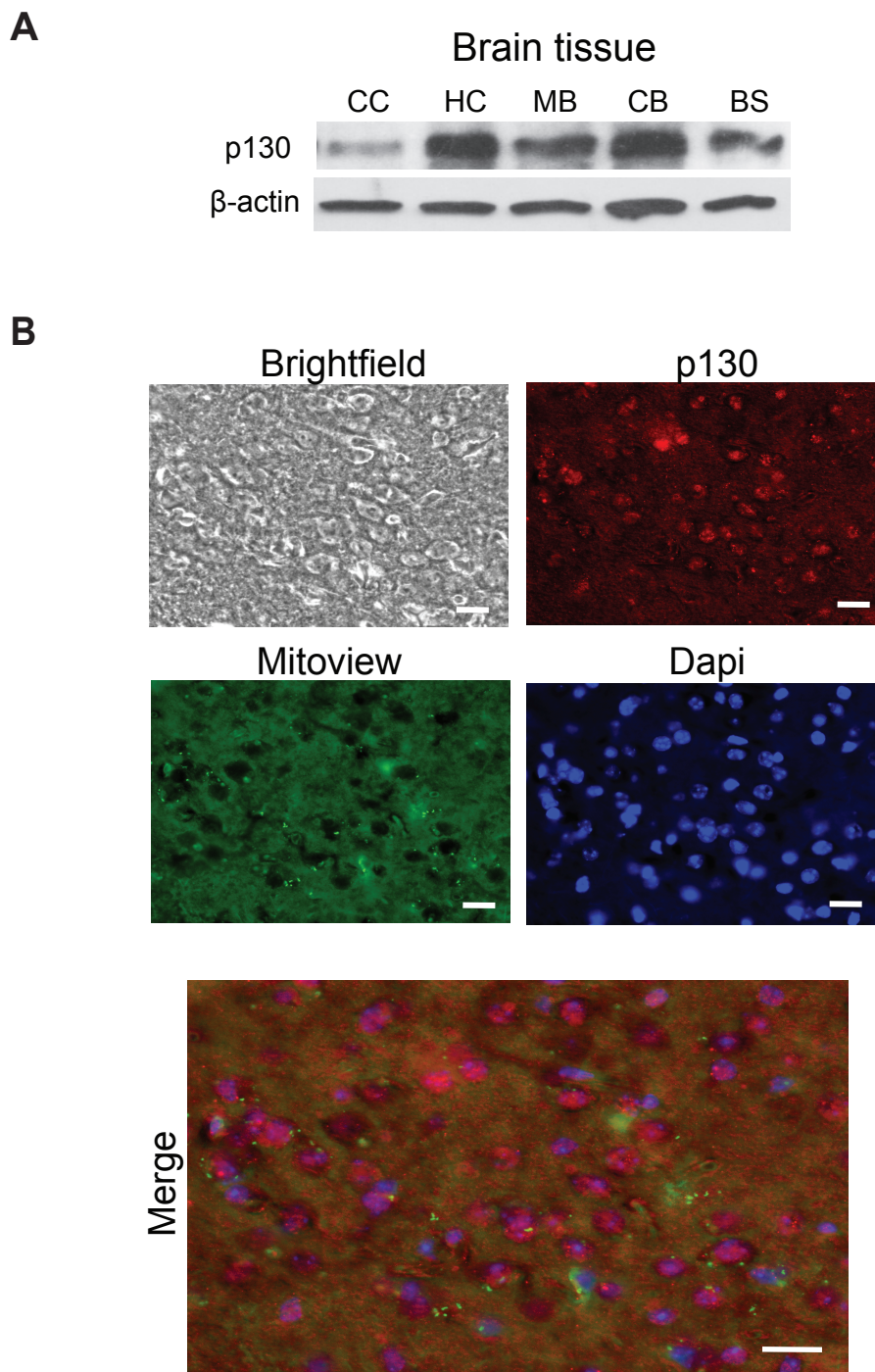


Figure 5.3. p130 localization in various brain regions (A) Representative Western blot of whole tissue fractions for p130, β -actin and Cox IV in different brain regions. Cerebral cortex (CC), hippocampal cortex (HC), mid brain (MB), cerebellum (CB) and brain stem (BS). (B) p130 localization in the cerebral cortex visualized by immunohistochemistry for brightfield, p130 (red), Mitoview (green), Dapi nuclear staining (blue) and merge. Scale bars = 20 μ m.

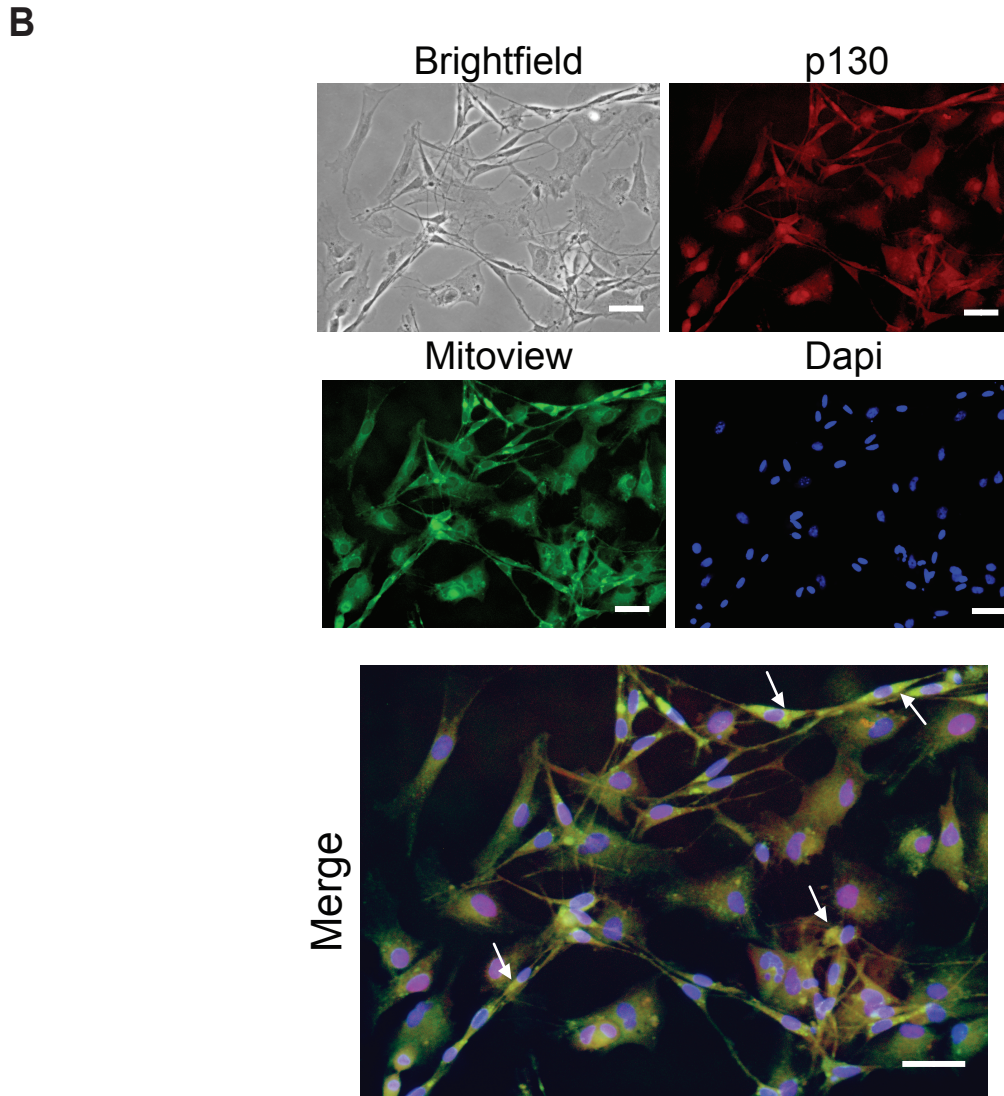
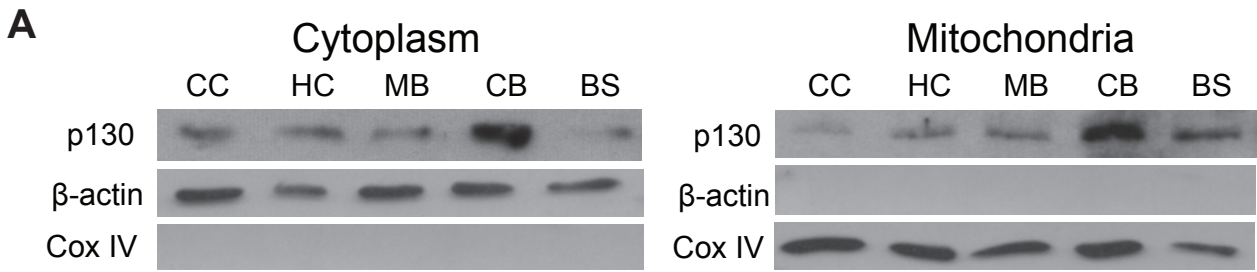


Figure 5.4. p130 is localized in the mitochondria of all brain regions. (A) Representative Western blot for mitochondrial and cytoplasmic fractions for p130, β -actin and Cox IV in different brain regions. Cerebral cortex (CC), hippocampal cortex (HC), mid brain (MB), cerebellum (CB) and brain stem (BS). (B) Immunocytochemistry of mouse primary brain cells for bright-field, p130 (red), Mitoview (green), Dapi nuclear staining (blue) and Merge. Scale bars=1000 μ m. Arrows indicate presence of p130 in the mitochondria (yellow).

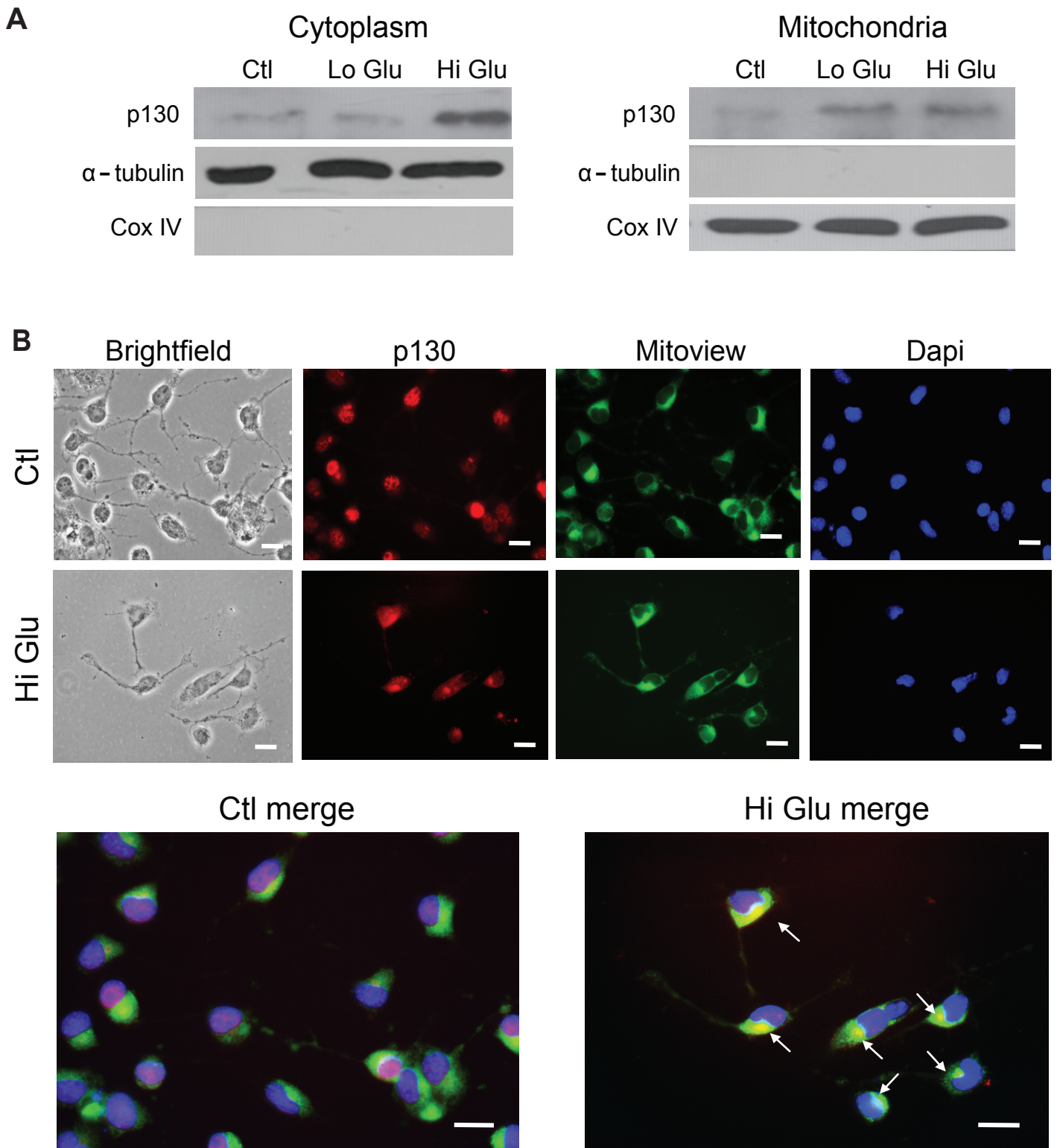


Figure 5.5. p130 levels increase in mitochondria with high and low glucose stress. (A) Representative Western blot for p130, α -tubulin and Cox IV of cytoplasmic and mitochondrial fractions of unstressed (Ctl) or stressed neurons by treatment with high glucose (Hi Glu) and low glucose (Lo Glu) for 24 hours. (B) Immunocytochemistry for brightfield, p130 (red), Mitoview (green), Dapi nuclear staining (blue), and merge in the untreated control (Ctl) and after 24h treatment with Hi Glu. Scale bars = 20 μ m. Arrows indicate presence of p130 in the mitochondria (yellow).

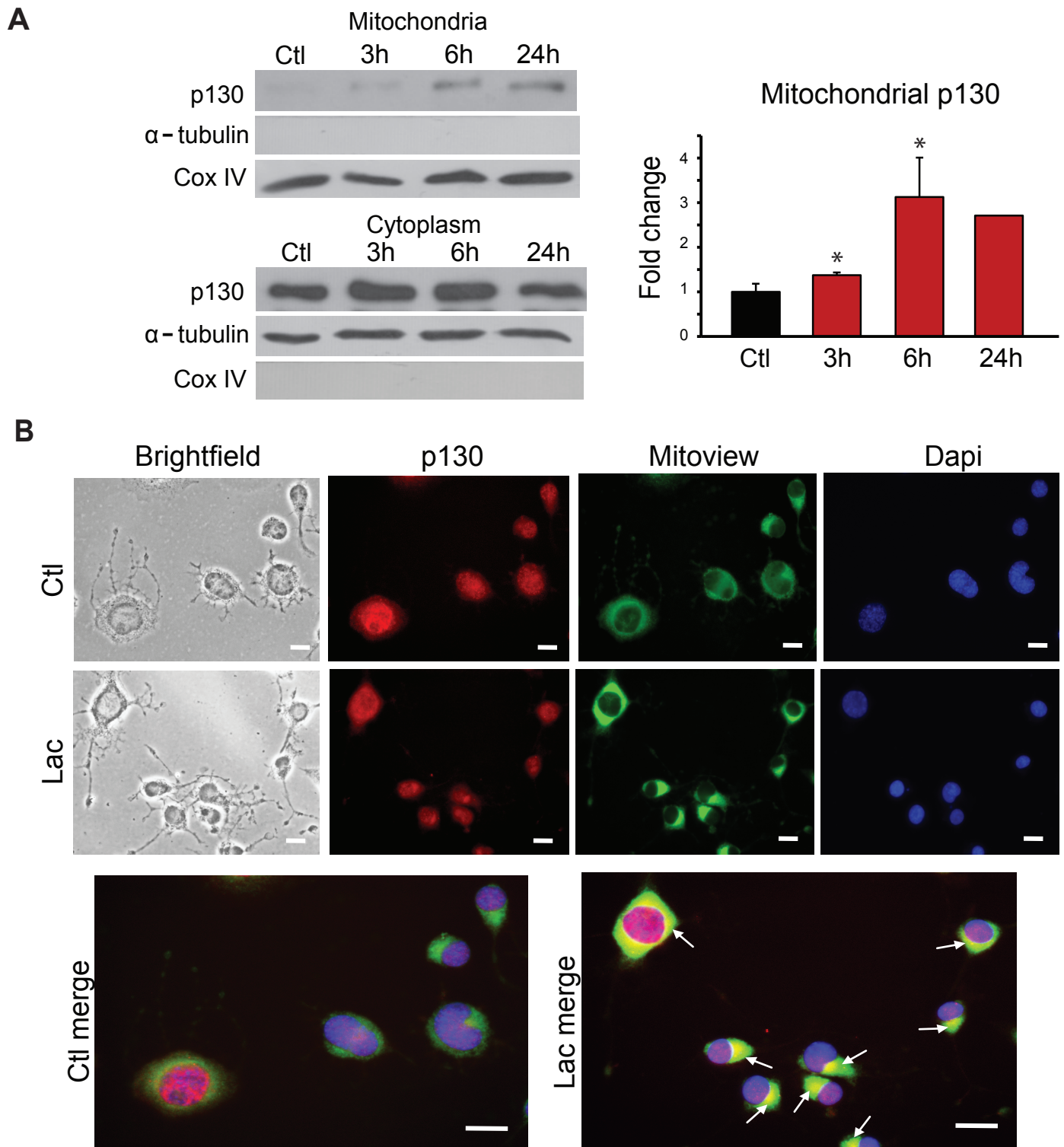


Figure 5.6. Increase in mitochondrial p130 levels with lactate stress. (A) Representative Western blot and enumeration for p130, α - tubulin and Cox IV of cytoplasmic and mitochondrial fractions of neurons treated with lactate for 3, 6 and 24 hours. (n=3 for Ctl, 3h and 6h, n=2 for 24h Student's T test was used for analysis, asterisks denote significance, $*p < 0.05$. All data are mean \pm SD). (B) Sub-cellular localization of p130 visualized by immunocytochemistry in untreated (Ctl) and lactate treated (Lac) for 24h. Brightfield, p130 (red), Mitoview (green), Dapi nuclear staining (blue) and merge. Scale bars = 20 μ m. Arrows indicate presence of p130 in the mitochondria (yellow).

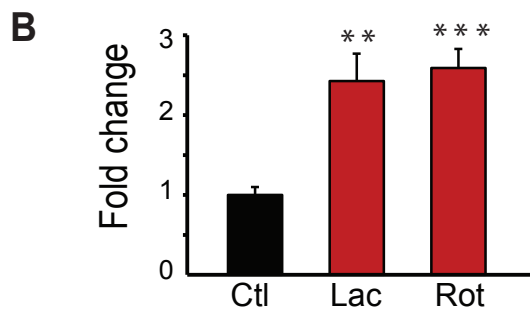
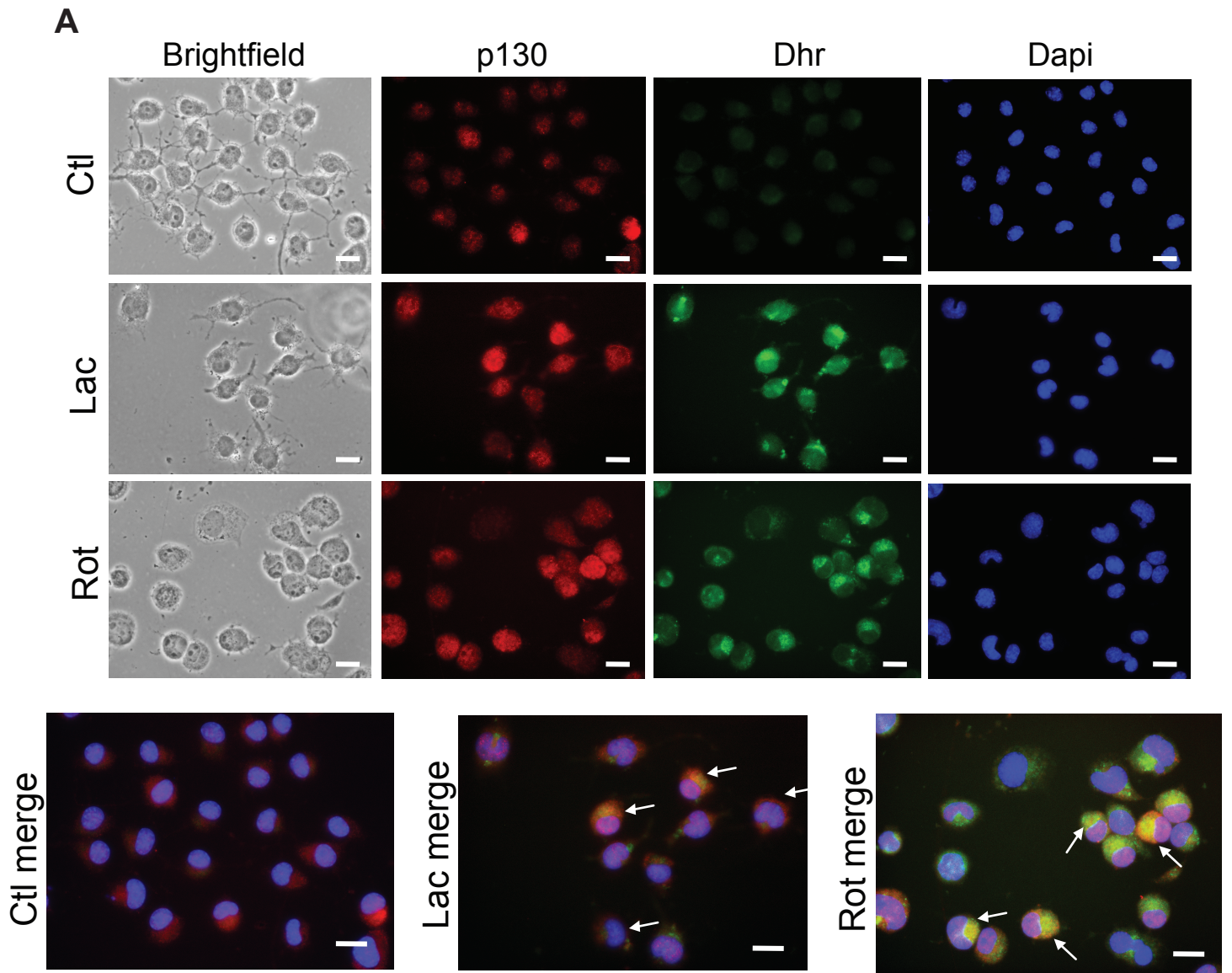


Figure 5.7. Ros increases p130 mitochondrial localization. (A) Localization of p130 visualized by immunocytochemistry for brightfield, p130 (red), ROS with dihydrorhodamine (Dhr) (green), Dapi nuclear staining (blue) and merge in untreated control (Ctl) and after 6h treatment with lactate (Lac) or rotenone (Rot). Scale bars = 20 μ m. Arrows indicate presence of p130 in the mitochondria (yellow/orange). (B) Quantification of ROS signal intensity with Dhr staining. (n=10-23, One way ANOVA with the Bonferroni post hoc test was used for analysis, asterisks denote significance. *** p < 0.001, ** p < 0.01 for Rot and Lac, respectively compared to Ctl). All data are mean \pm SD.

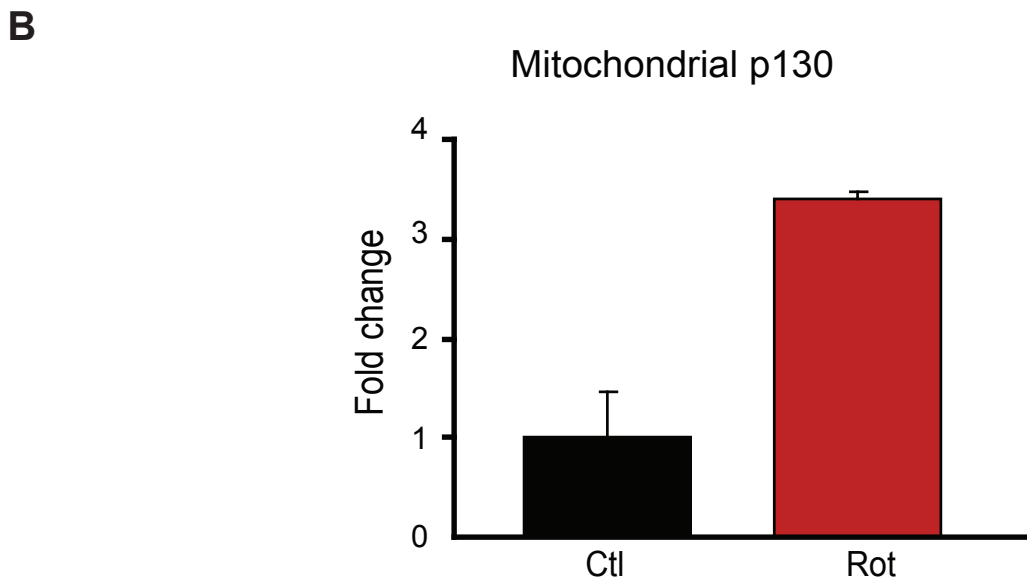
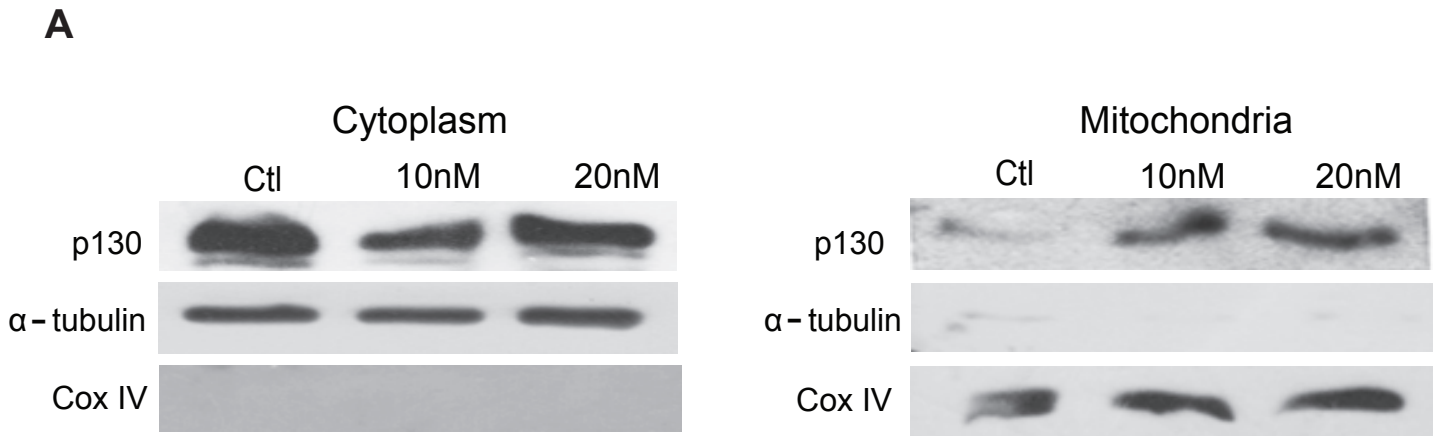


Figure 5.8. Increase in mitochondrial p130 levels with rotenone stress. (A) Representative Western blot for p130, α -tubulin and Cox IV of cytoplasmic and mitochondrial fractions of cells untreated (Ctl) and treated with 10 nM and 20 nM of rotenone for 6 hours. (B) Enumeration of p130 in mitochondrial fractions at 6 hours with 10nM rotenone (Rot) treatment (n=2).

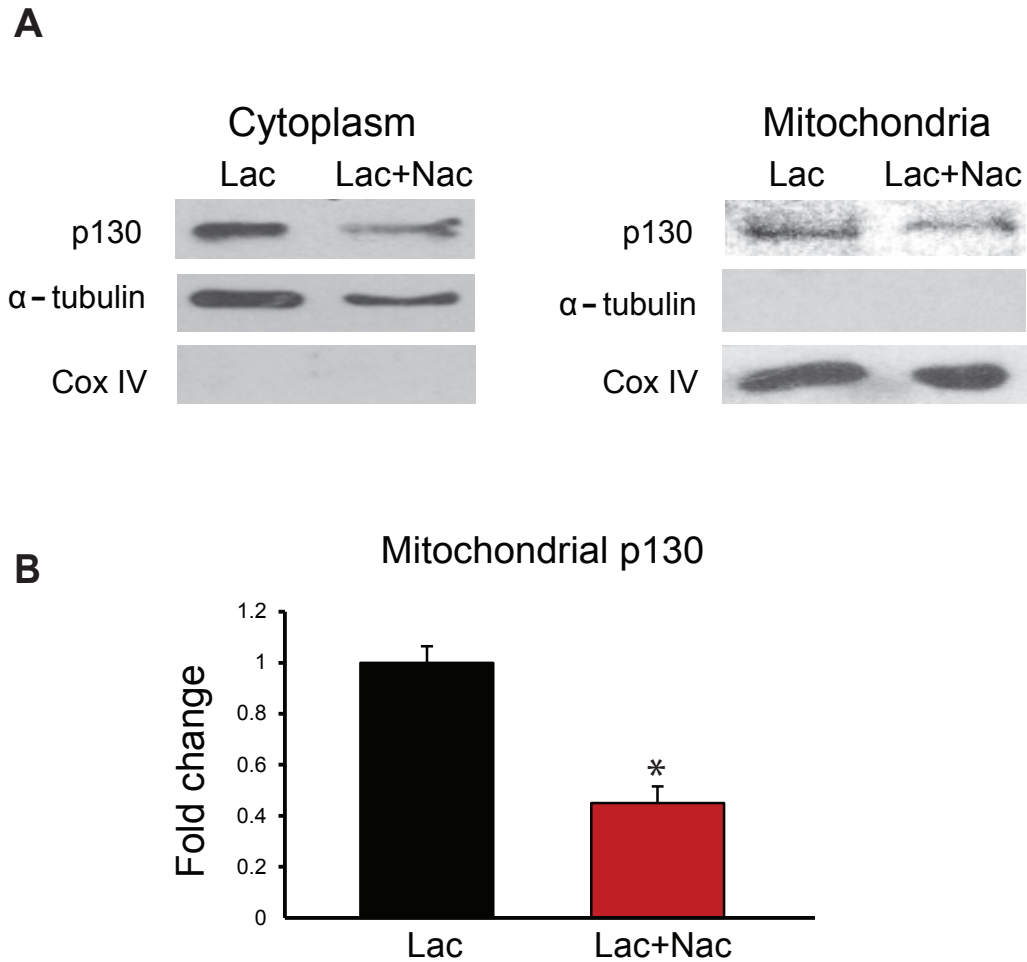


Figure 5.9. p130 mitochondrial localization decreases with Nac treatment. (A) Representative Western blot for p130, β -actin and Cox IV of mitochondrial and cytoplasmic fractions of neurons treated with lactate (Lac) in the absence or presence of Nac (Lac+Nac). **(B)** Enumeration of p130 in mitochondrial fractions in lactate treated neurons (Lac) in the absence or presence of Nac (Lac+Nac). (n=3, Student's T test was used for analysis, asterisks denote significance. * $p < 0.05$). All data are mean \pm SD.

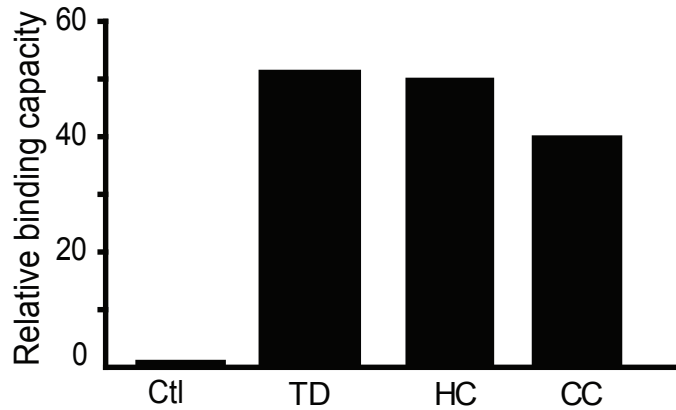


Figure 5.10. p130 binding capacity on mitochondrial D-Loop promoter in vitro and in vivo using quantitative ChIP analysis. Representative graph of binding intensity for p130 to mitochondrial D-Loop promoter in proliferating Neuro2A cells (Ctl), terminally differentiated (TD), hippocampal cortex tissue (HC) and cerebral cortex tissue (CC). Binding efficiencies normalized to non binding proliferating Neuro2A (n=1 for all samples).

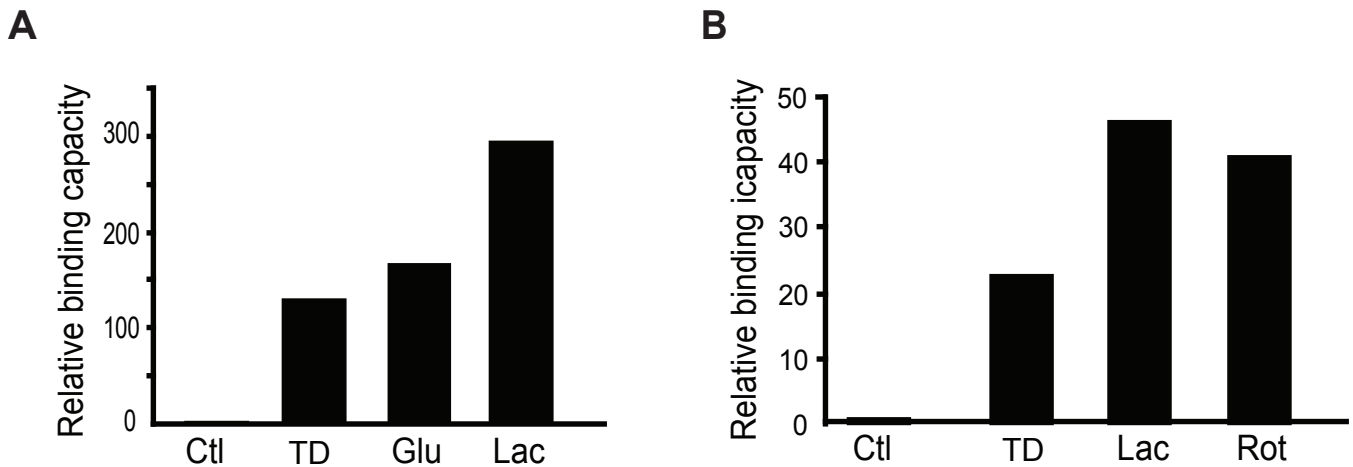


Figure 5.11. Increased p130 interaction on mitochondrial DNA with stress. (A) Representative graph of binding capacity by qChIP for p130 to mitochondrial D-Loop promoter in proliferating Neuro2A cells (Ctl), terminally differentiated (TD) and during stress inducing glucose (Glu) or lactate (Lac) treatment for 24 hours. (B) Representative graph of binding capacity by qChIP for p130 to mitochondrial D-Loop promoter in proliferating Neuro2A cells (Ctl), terminally differentiated (TD) and during stress inducing lactate (Lac) or rotenone (Rot). Binding efficiencies normalized to non binding proliferating Neuro2A (Ctl) cells (n=1 for all treatments).

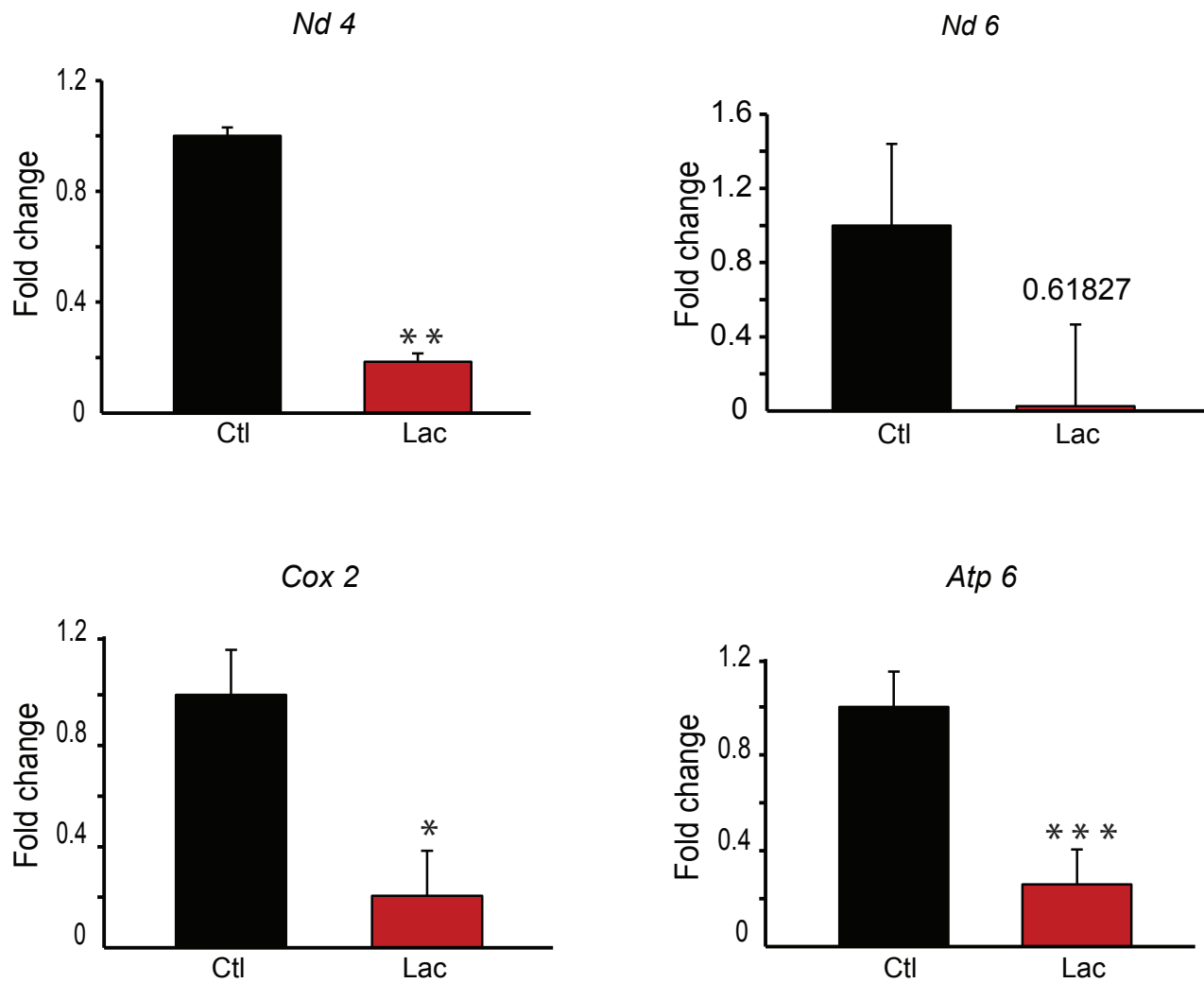
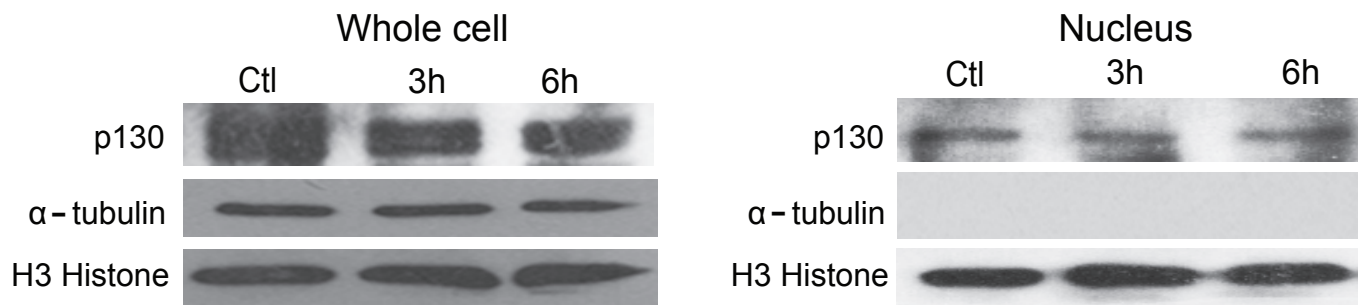


Figure 5.12: Reduced gene expression of mitochondrial encoded genes with lactate induced stress. Gene expression analysis by qPCR of untreated (Ctl) and lactate (Lac) treated neurons for mitochondrial encoded genes. *Nd4*, *Cox 2*, *Atp 6* and *Nd 6*. (n=3, Student's T test was used for analysis, asterisks denote significance. * $p < 0.05$, ** $p < 0.01$, *** $p < 0.001$). All data are mean +/- SD.

A



B

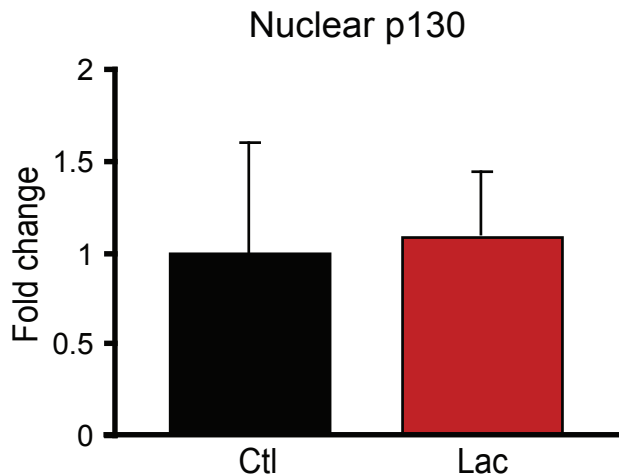


Figure 5.13. p130 protein levels remain unchanged in the nucleus of lactate stressed neurons. (A) Representative western blot for p130, α - tubulin and H3 Histone of whole cell and nuclear lysates of neurons untreated (Ctl) or treated with lactate (Lac) for 3 and 6 hours. (B) Enumeration of p130 nuclear protein expression of Ctl and Lac cells at 6h of lactate treatment. (n=3, Student's T test was used for analysis. All data are mean +/- SD)

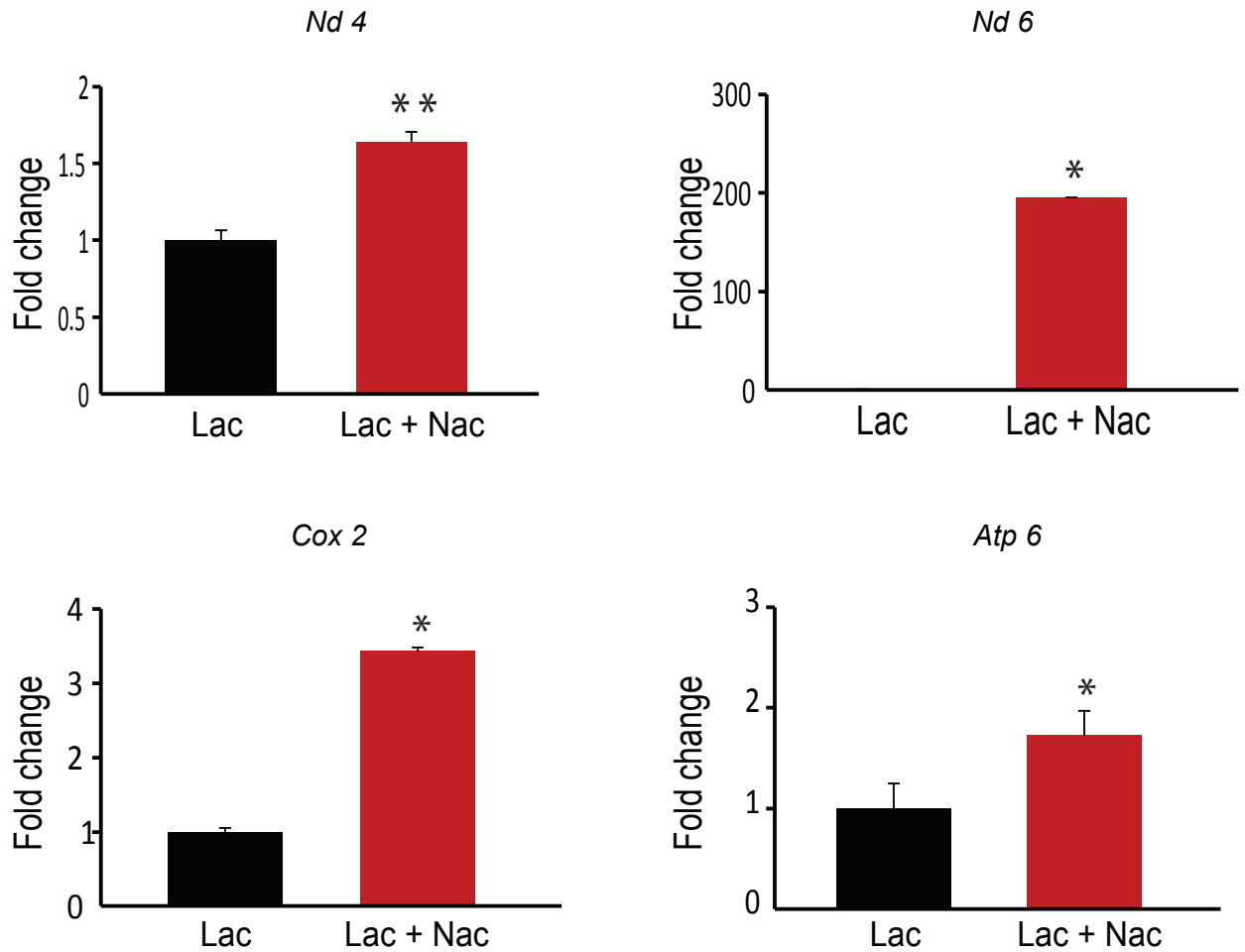


Figure 5.14. Rescue of oxidative stress increases gene expression of mitochondrial encoded OxPhos genes. Gene expression analysis by qPCR for mitochondrial encoded genes for ETC complexes, *Nd 4* (Complex I), *Cox 2* (Complex IV), *Atp 6* (Complex V) and *Nd 6* (light strand, Complex I) of neurons treated with lactate (Lac) in the absence or presence of Nac (Lac+Nac). (n=3, Student's T test was used for analysis, asterisks denote significance. * $p < 0.05$, ** $p < 0.01$). All data are mean +/- SD.

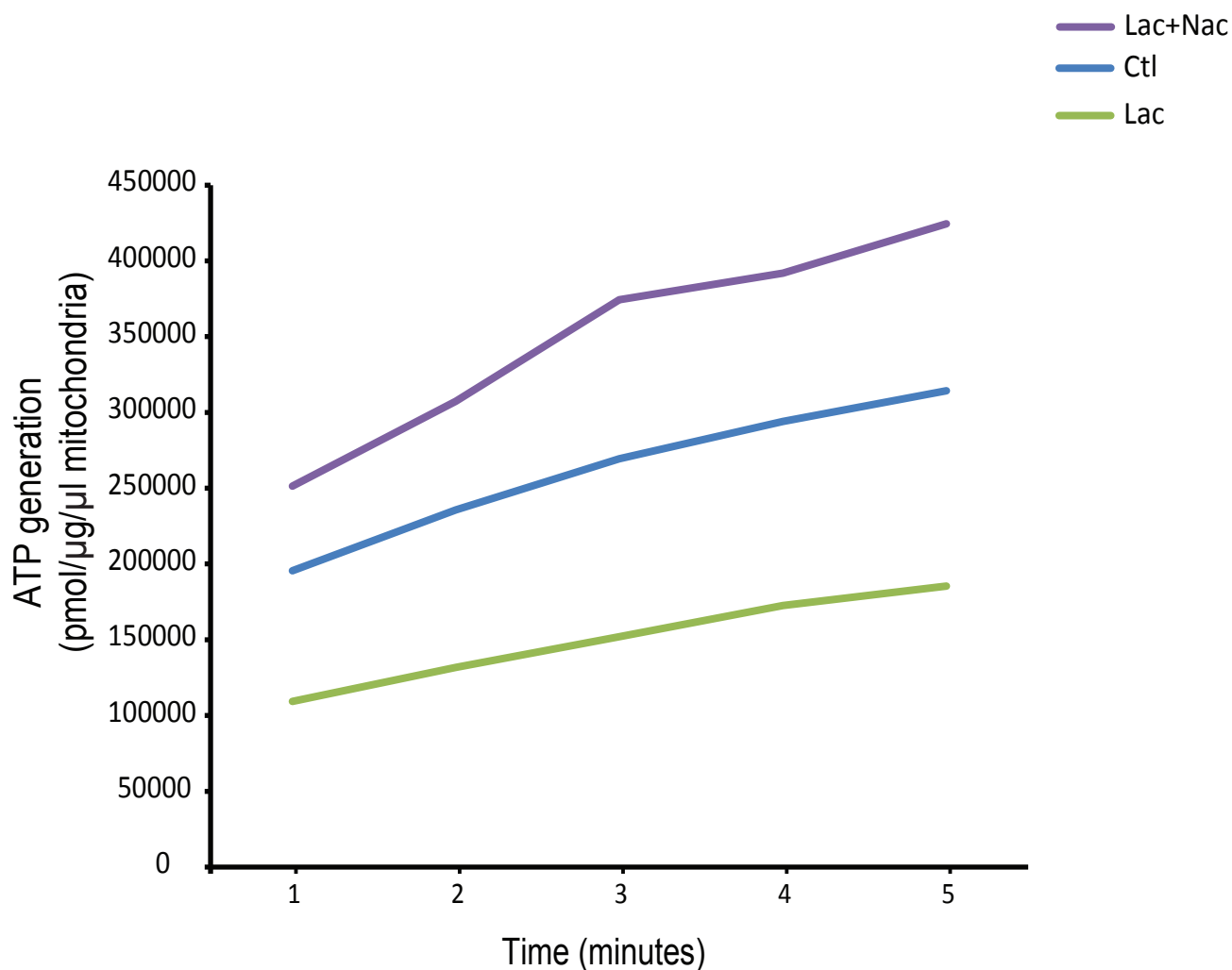


Figure 5.15. Increased ATP production with decreased mitochondrial p130 localization. Quantative graph of rate of ATP production in neurons that were untreated (Ctl), treated with lacate for 6 hours (Lac) or Lac with Nac (Lac+Nac). n=3 for all treatments.

6. DISCUSSION

The function of the Rb family member p130 has been well established as a nuclear transcriptional co-repressor that is crucial to cell survival, differentiation and regulating cell cycle progression (Litovchick et al., 2007; Takahashi et al., 2000; Bukhart and Sage., 2008; Ajioka et al., 2014; Liu et al., 2005). Although its function has been documented on a nuclear level, its role in the mitochondria has never been explored until now. Our study is the first to provide evidence that p130 might regulate oxidative metabolism in neurons by interacting at the mtDNA promoter to block gene expression. Thus, its mitochondrial function is hypothesized to provide a mechanism to reduce potential ROS generation by decreasing OxPhos. This novel defence mechanism is crucial to minimize tissue damage, as neurons are extremely susceptible to oxidative stress that is caused by the high ROS levels prevalent in the brain (Bouzier-Sore et al., 2006; Boumezbeur et al., 2010a; Sibson et al., 1998; Hyder et al., 2006; Shulman et al., 2004).

In our study we established the presence of mitochondrial p130 in vitro as well as in vivo in all brain regions assessed. This is important as prior studies have restricted the study of this co-transcriptional repressor to the nucleus and have never documented its mitochondrial presence or function. Rb has also been found in the mitochondria in both fibroblast and human lung cell lines (Hilgendorf et al., 2013). However, contrary to its anti-apoptotic role (Collard et al., 2012), Rb was instrumental in mediating direct apoptotic effects by binding the pro-apoptotic protein Bax (Hilgendorf et al., 2013). Despite its mitochondrial presence, no studies have reported the existence of any transcriptional influence on the mitochondrial promoter. Our lab has recently found that p107 which has high homology to p130, also localizes to the mitochondria, binds the mitochondrial D-Loop promoter region and regulates mitochondrial gene expression in proliferating cells (Bhattacharya et al., 2017)

Apart from p130, a number of nuclear transcription factors have also been shown to localize to the mitochondria and bind to mtDNA in vitro. Among these are the glucocorticoid receptor (Demonacos et al.; 1993), thyroid hormone 3 receptor (p43) (Casas et al., 1999; Enriquez et al., 1999), cyclic-Amp response binding element (Creb) (Cammarota et al., 1999; De Rasmio et al., 2009; Lee et al., 2005), p53 (Achanta et al., 2005; Marchenko et al., 2007; Yoshida et al., 2003; Lee et al., 2010), estrogen receptor (Chen et al., 2004; Monje et al., 2001), NFkB/ α (Cogswell et al., 2003; Johnson et al., 2011), AP-1, Ppary2 (Ogita et al., 2003), Mef2d (She et al., 2011) and Stat 3 (Gough et al., 2009; Shulga et al., 2012; Szczepanel et al., 2011; Szczepanel et al., 2012; Wegrzyn et al., 2009; Boengler et al., 2010; Carbognin et al., 2016). However, p130 is one of only four known nuclear transcription factors that can bind the mitochondrial D-Loop in vivo (**Fig. 5.10**). The others are p53, Creb, and Mef 2d, of which Mef 2d is not limited to binding to the promoter region but also to a to a consensus sequence recognition motif within Nd6. Our data obtained for qChIP evaluated binding for p130 only within the D-Loop region. ChIP analysis for the entire mitochondrial genome is required to determine if p130 binds to other regions of the mtDNA. Nonetheless, p130 is one of the few known factors that might act as a mitochondrial transcriptional repressor and potentially the only one known to have a putative role as a defence against ROS.

Our finding for the presence of p130 in the mitochondria of neural tissue is incontrovertible. We located p130 in the mitochondria of all brain regions (**Fig. 5.4 and Fig. 5.3**) and in primary astrocytes and neurons (**Fig. 5.4**), as well as terminally differentiated Neuro2A cells (**Fig. 5.2**). Although p130 interaction with mtDNA is associated with repression of mitochondria gene expression, further experiments are required to confirm direct control of gene expression. The use of transient transfection assays with a luciferase reporter containing a minimum promoter and D-loop sequences would be useful to assess

promoter activity. Also, the behaviour of mitochondrial gene expression of p130 KD and over-expressing neurons with lactate and glucose would help confirm p130 mediated regulation of transcription.

We also provide an insight into the functional role of p130 in ROS control by down regulating OxPhos in terminally differentiated neurons. Studies have shown that ROS levels are increased in conditions of nutrient stress in both high and low glucose and with lactate (Russell et al., 2002; Shi and Liu., 2006; Sepehr & Mohseni., 2010; Yates et al., 1990). In our study we found that nutrient treatment produced high ROS levels (**Fig. 5.7**). Indeed we found during nutrient stress increased mitochondrial p130 localization (**Fig. 5.5 and Fig. 5.6**) concomitant with reduced mitochondrial gene expression (**Fig. 5.12**). We believe this is an attempt of the cell to reduce its OxPhos output so as to control ROS production. Moreover, as studies have shown that neurons can take up lactate much faster than glucose (Barros L.F., 2013; Pritchard et al., 1991; Newman et al., 2011), our results suggest that the amount of p130 in the mitochondria is coupled to the amount of ROS generated. In line with this, we found an increase in p130 mitochondrial levels in merely 3 hours of lactate treatment as opposed to the 24 hours of treatment required for glucose treated neurons (**Fig. 5.5 and Fig. 5.6**).

We confirmed the importance of p130 function to ROS generation by treatment of cells with rotenone (**Fig. 5.8**) and ROS inhibitor Nac (**Fig. 5.9 and Fig. 5.14**). Rotenone results in the inhibition of CoQ, which leads to the electron build up and ROS generation from Complex I (Liu et al., 2002). Importantly, lactate treated neurons with the addition of ROS inhibitor Nac showed a rescue of the p130 stress response (**Fig. 5.9**). Not only was p130 protein localization in the mitochondria decreased in lactate treated neurons with Nac (**Fig. 5.9**), but there was also a rescue of mitochondrial encoded gene expression across every ETC

complex (**Fig. 5.14**). This is highly indicative of a role for p130 in ROS defence, its response gauged to increased or decreased levels of mitochondrial ROS generation.

Paradoxically; despite the presence of high levels of ROS, hypo metabolism is a hallmark of neurological conditions ranging from depression to schizophrenia and neurodegenerative diseases (Chih and Roberts., 2003; Kraig et al., 1987; Macauley et al., 2015; Nedergaard et al., 1991; Siesjo et al., 1985; Allen et al., 2014; Yang et al., 2015). Our results showcase that hypo metabolism is assisted by reduced mitochondrial gene expression leading to a reduction in OxPhos under conditions of increasing ROS. Thus, hypometabolism is not merely a consequence of high ROS levels negatively affecting the cell's ability to generate ATP in the ETC. Rather it is a mechanism to ward off further potential ROS generation. In vivo, we assessed p130 binding in the hippocampus and cerebral cortex regions, which are maximally impacted in neurodegenerative diseases (Mann et al., 1985; Fjell et al., 2014). There was a higher degree of p130 binding to the hippocampus compared to the cerebral cortex mtDNA D-Loop promoter region (**Fig. 5.10**). Interestingly, the cerebral cortex is more prone to oxidative stress compared to the hippocampus (Pathan et al., 2015; Cardoso et al., 2010). This implies that the higher degree of p130 binding in the hippocampus might ensure a lower level of OxPhos as well as a higher ability to down regulate OxPhos under conditions of oxidative stress.

An upregulation of OxPhos is required for production of ATP. The involvement of p130 in binding to the D-Loop promoter region and decreasing mitochondrial encoded OxPhos genes would result in a decline in the capacity of the cell for ATP production. We confirmed this by measuring the rate of ATP production in cells treated with lactate after 6 hours, which correlated with increased levels of p130 in the mitochondria (**Fig. 5.15**). As expected, the concentration of ATP in the mitochondria of lactate treated cells was lower than the concentration of untreated controls. Importantly, the rate of ATP generation was also

significantly slower in lactate treated neurons than in untreated controls. This corresponds to the increased mitochondrial p130 localization and reduced mitochondrial gene expression. Moreover, ATP production with lactate when neurons were also treated with Nac was dramatically increased (**Fig. 5.15**), in line with the decreased p130 mitochondrial localization (**Fig. 5.9**) and increased gene expression (**Fig. 5.14**). This provided a stronger indication that the rate of ATP production declines with increased localization of p130 in the mitochondria. Further experiments using p130 KD cells are required to confirm that p130 mitochondrial localization controls ATP formation, as mitochondrial gene expression would be expected to be dysregulated in these cells.

At a nuclear level, p130 has been reported to be essential in preventing apoptosis. Studies have shown that decreased p130 binding to nuclear promoters induces apoptosis by increasing the transcription of apoptotic inducing genes such as B-myb (Liu et al., 2001; Iyirhiaro et al., 2014). However, we noted that while mitochondrial levels of p130 increased, its levels in the nucleus remained more or less constant during our oxidative stress tests (**Fig. 5.13**). This suggests that the neurons treated in our study were not stressed to a point of apoptosis. It also implies that the potential effects on mitochondrial D-Loop binding and reduced gene expression are purely mitochondrial and not a consequence of nuclear gene expression changes due to p130 levels and activity on the nuclear promoters. One study to confirm the non nuclear function of p130 in regulating ROS generation would be to assess if the expression of nuclear encoded mitochondrial genes remains unaltered during ROS generation. Another study might assess if the expression levels of various p130 nuclear targeted genes such as Plk1, Dhfr and cyclin A remain unaffected during ROS generation (Stengel et al., 2009). Alternatively, generation of p130 plasmids tagged with the mitochondrial tag Acta (Kim et al., 2004) and a nuclear localization sequence tag (Giraud et al., 2014), could further track p130 subcellular localization during periods of induced ROS.

We also found that p130 might have a metabolic role during the process of neural differentiation. It plays an important role throughout neuronal specification, differentiation and maturation. The Balb/c J strain of p130 genetically deleted mice that are embryonically lethal displayed several developmental deficiencies associated with the nervous system (LeCouter et al; 1998b). This included impaired differentiation of motor neurons and decreased formation of sensory neurons. Moreover, in the developing neural tube, the basement membrane was not formed by the neural epithelium. A study by Jori et al (2001), also demonstrated the importance of p130 for neuronal specification of neural crest stem cells and neuroblastoma progenitors (Jori et al.; 2001). In particular, the study noted that p130 overexpression in neuroblastoma cell lines resulted in increased neuronal differentiation. Moreover, the expression levels of p130 were found to increase during the neuronal differentiation process and then decrease towards the end of terminal differentiation (Jori et al., 2001). We verified p130 nuclear localization and protein levels in undifferentiated Neuro2A cells at G0 of the cell cycle and during differentiation into neurons (**Fig. 5.2**). However, the increase in p130 was unexpectedly apparent in the mitochondria. The p130 mitochondrial expression at day 1 of differentiation (**Fig. 5.2**) reflects a potential switch to increased glycolysis over OxPhos for energy at early phases of differentiation. In agreement, Agostini et al (2016), have shown that glycolysis is necessary for initial stages of differentiation in neural progenitors with the metabolic state shifting to OxPhos in the differentiated state (Agostini et al, 2016). Thus, p130 might be required to reduce mitochondrial gene expression leading to decreased OxPhos potential. In the terminally differentiated neurons the level of p130 in the mitochondria is low, which corresponds to the augmented mitochondrial gene expression and increased OxPhos activity (Agostini et al, 2016). Intriguingly, our lab recently found that family member p107 regulated adipogenic stem cell fate by altering metabolism of adipocyte progenitors from glycolytic to oxidative

states, thus adding credence to our model (Porras et al, 2017). Further experiments to chart the importance of p130 and metabolism to the differentiation process are required to fully appreciate its potential impact.

Despite these important findings, three important issues remain unresolved. First, what is the upstream ROS sensing mechanism by which p130 is obliged to enter the mitochondria? We believe that a clue to this is the increase in AMPK activity during ROS generation (Hardie 2011; Emerling et al., 2009; Mungai et al., 2011). Interestingly, under conditions of oxidative stress, AMPK has been shown to cause activation of Foxo3a (Greer et al., 2007), which is known to be a direct transcriptional activator of p130 (Kops et al., 2002). Further experiments to demonstrate this potential interaction would be to assess the level of p130 mRNA expression and to qChIP Foxo3a on the p130 gene promoter after ROS stimulation. Another potential upstream mechanism is a feedback control system regulated by AMPK on mTOR. In this paradigm, activation of AMPK by ROS production would cause inhibition of mTOR, which would inhibit activation of downstream targets such as Cdks that could potentially inhibit p130 by phosphorylation (Hisanaga et al., 2012; Chen et al., 2009). To assess the involvement of mTOR with p130, experiments can be carried out with the use of mTOR inhibitors such as rapamycin to find the effect of p130 on OxPhos and ROS generation. Both of the proposed upstream mechanisms would not necessarily be mutually exclusive.

The second issue is to deconstruct the mechanism of how p130 gains entry into the mitochondria. A vast number of proteins are imported into the mitochondria based on an N-terminal mitochondrial localization motif. The motif is recognized by the TIM-TOM import complex, which allows import by cleaving N-terminus residues before and after entry into the mitochondrial matrix. This is known as the cleavage pathway. However, when resolved on a higher resolution 7.5% polyacrylamide gel, no truncated forms of p130 were visible (**Fig.**

5.2), indicative of an alternate mode of its entry into the mitochondria. Moreover, mitochondrial import search engines Mitofates (<http://mitf.cbrc.jp/MitoFates/cgi-bin/top.cgi>) and Target P 1.1 (<http://www.cbs.dtu.dk/services/TargetP/>) did not identify any potential mitochondrial localization sequences for p130. Future studies with p130 deletion mutants are required to find the mitochondrial localization motif and/or potential post translational modifications that are necessary for its mitochondrial import.

Thirdly, as p130 is a co transcriptional factor its binding partner in the mitochondria is yet to be determined. There have been no reports of a mitochondrial presence for its binding partner E2f4. However, Tfam (Dairaghi et al, 1995; Ramachandran et al, 2016), mTERF (Asin Cayuela et al, 2004) and Tfb1/2m are bona fide mitochondrial transcription factors that are required for mitochondrial gene transcription. The RNA polymerase POLRMT is also essential for providing the polymerase activity associated with transcription. p130 could act as a co-repressor by binding to and inhibiting either of these factors and thus repressing gene expression. Co-immunoprecipitation experiments are required to test the possibility of an interaction between p130 and these factors.

A study by Previl et al noted a significant increase in p130 cytoplasmic levels in the brains of patients with Alzheimer's disease (Previl et al, 2007). From our study, we hypothesize that the increase in cytoplasmic p130 in AD is due to accumulating levels of p130 in the mitochondria. In this case the high levels of ROS in AD would initiate mechanisms to reduce its generation. Thus, obtaining tissue samples from the brains of individuals affected by AD or other neurodegenerative diseases would deepen our insight into the potential mitochondrial involvement of p130 in the progression of these diseases.

Our study does not only fill the gap of knowledge on the function of p130 beyond that of cell cycle regulation. It provides a potential mechanism that could be crucial to the development of several therapeutic strategies to combat the problem of ROS production in

7. ILLUSTRATIONS

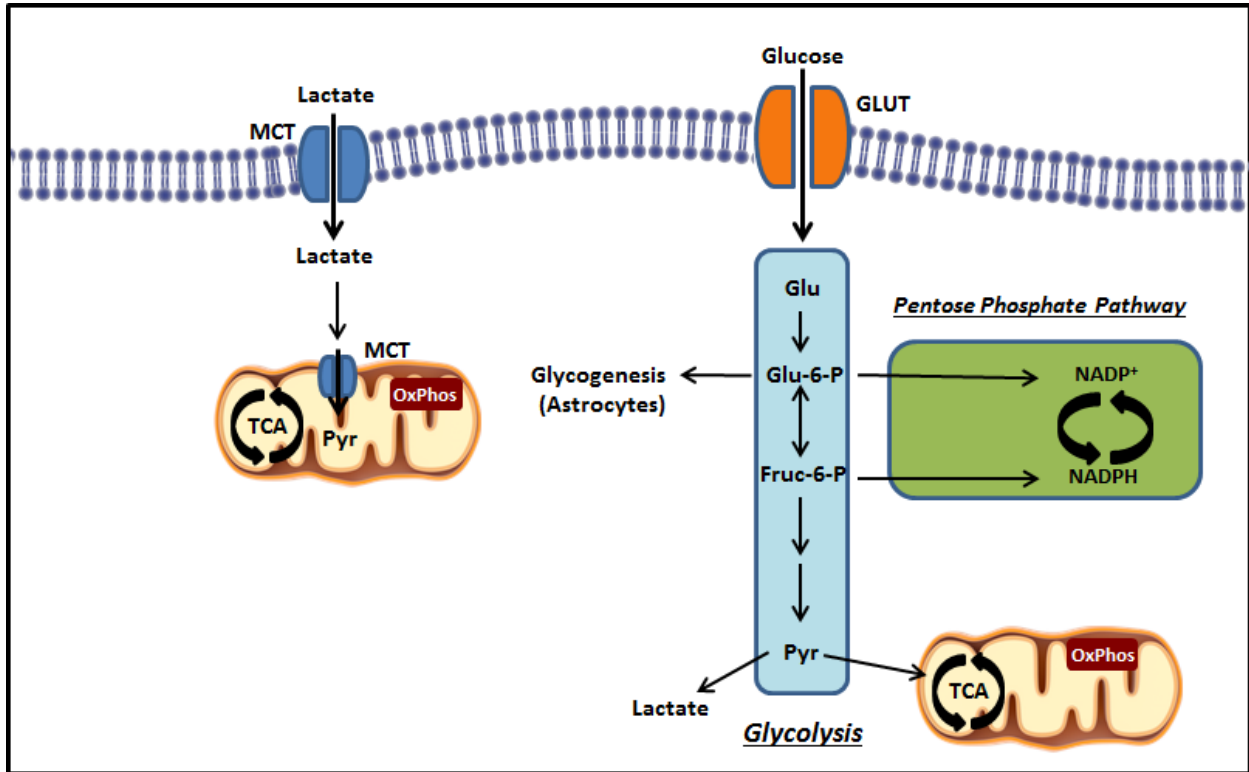


Figure 1.1 A schematic diagram illustrating nutrient shuttling in neurons. Neurons can utilize pyruvate from glucose via glycolysis or from lactate. Alternatively, under conditions of high oxidative stress, the pentose phosphate pathway (PPP) is activated to produce reducing equivalents such as NADPH. Excess glucose can also be converted to glycogen in astrocytes from Glu-6-P. (Glu, glucose; Pyr, pyruvate; GLUT, glucose transporter; MCT, monocarboxylate transporter; OxPhos, Oxidative Phosphorylation; TCA, tricarboxylic acid; Glu-6-P, Glucose-6-phosphate; Fruc-6-P, Fructose-6-phosphate) (Adapted from Mergenthaler et al., 2013).

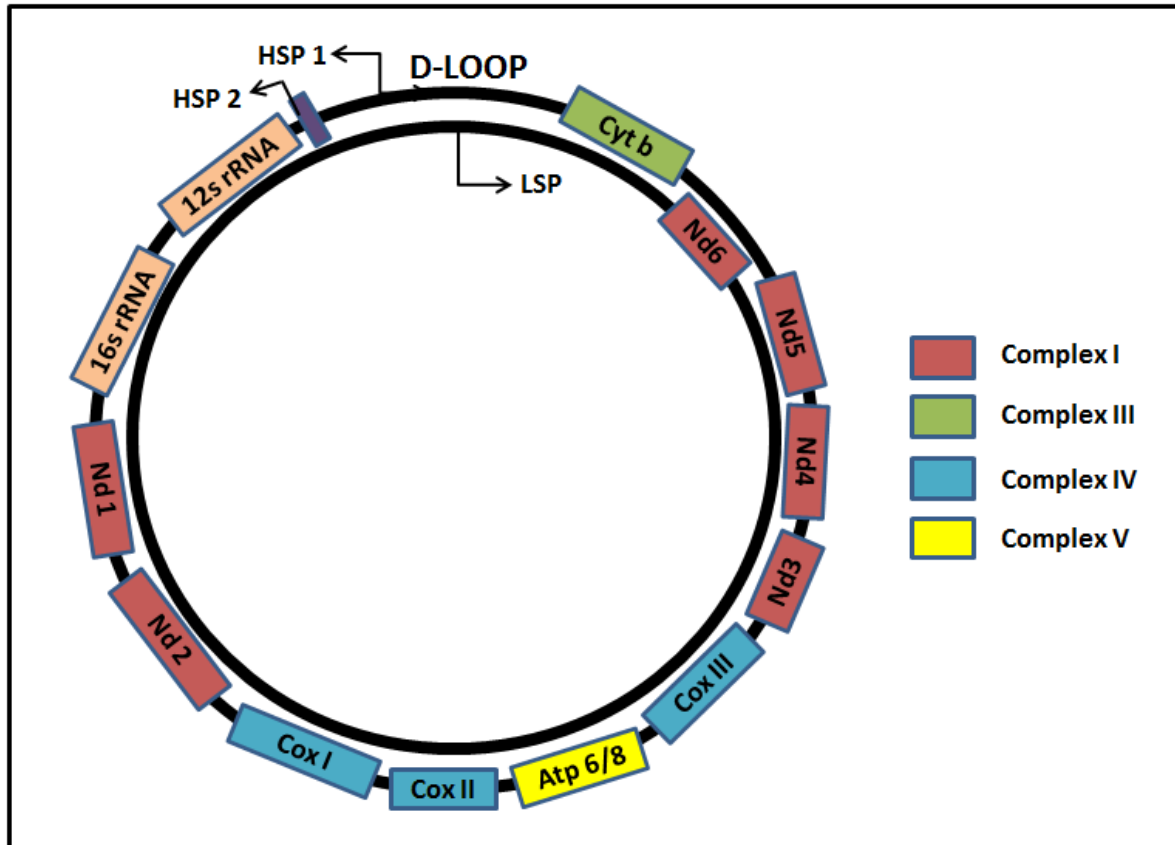


Figure 1.2 The mammalian mitochondrial genome. The double stranded mitochondrial DNA showing the 13 genes encoding subunits of ETC complexes involved in OxPhos and rRNAs. (Adapted from Uhler and Falkenberg, 2015)

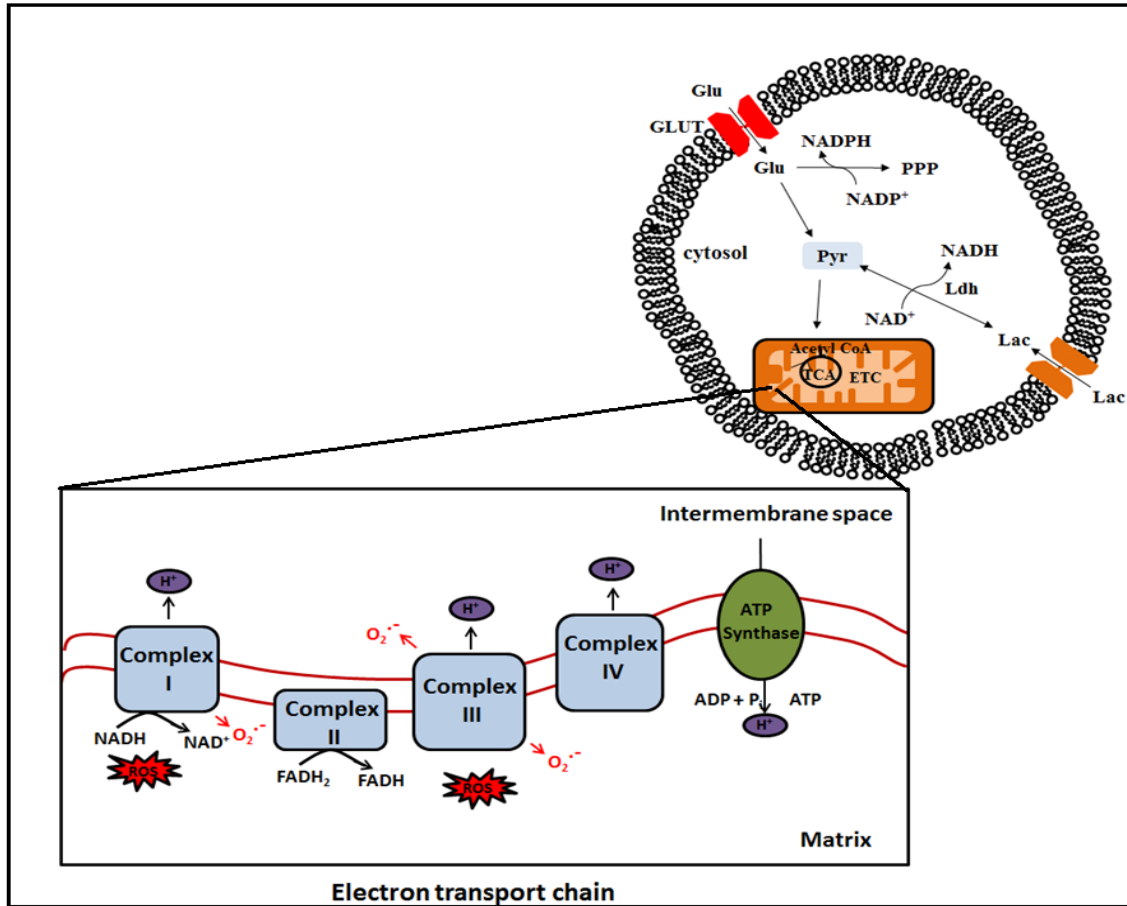


Figure 1.3 Mitochondrial oxidative phosphorylation. Pyruvate from glycolysis or lactate is ultimately used to produce reducing agents NADH and FADH₂ that transfer their electrons along the ETC complexes during the process of OxPhos to produce ATP. As electrons move across complexes protons are pumped into the inter membrane space generating a proton gradient that is used by Complex V to form ATP. ROS is produced at Complex I and Complex III as a by-product of ATP formation. (Glu, glucose; Pyr, pyruvate; GLUT, glucose transporter; Ldh, lactate dehydrogenase; Lac, lactate; ETC, electron transport chain; TCA, tricarboxylic acid; ROS, reactive oxygen species). (Adapted from Mergenthaler et al., 2013).

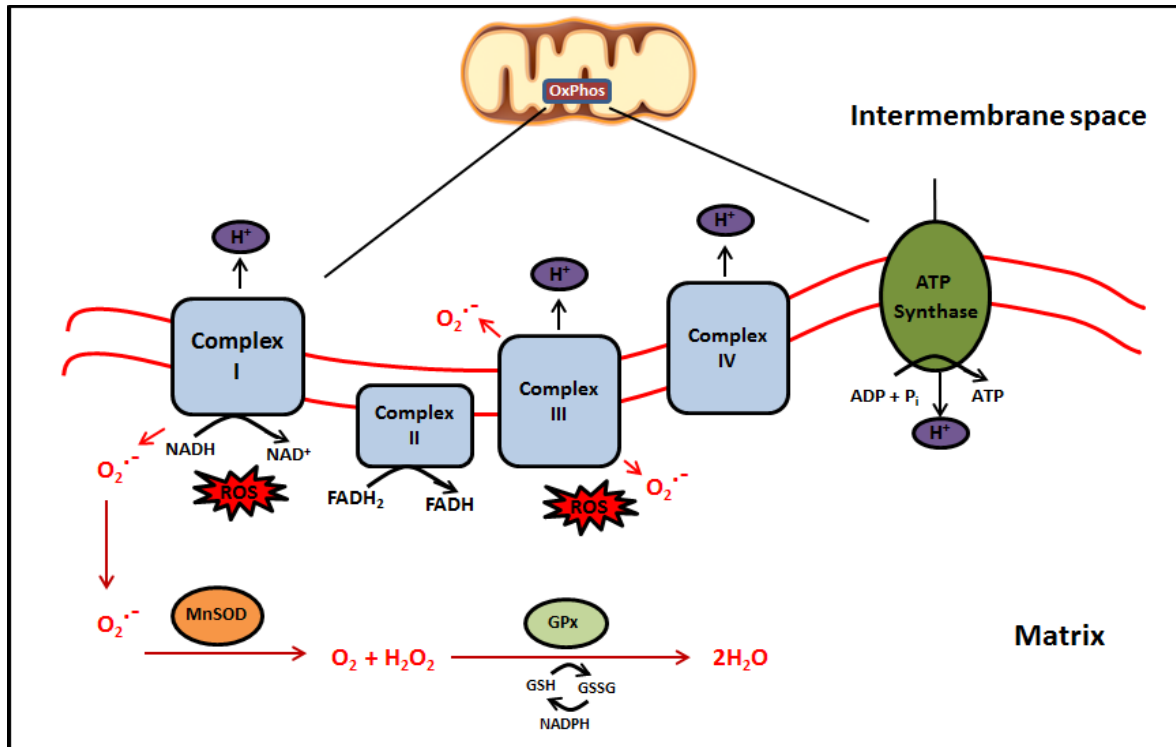


Figure 1.4 Mitochondrial ROS defence mechanisms. ROS generated from Complex I or Complex III can be neutralized through antioxidant defence mechanisms mediated by SOD and GSH. MnSOD converts superoxide radicals to hydrogen peroxide. GSH then converts this hydrogen peroxide to water in a reaction catalyzed by GPx. ROS generated from Complex III can also be released into the intermembrane space. (SOD, superoxide dismutases; MnSOD, manganese containing superoxide dismutase; ROS, reactive oxygen species; GPx, glutathione peroxidase). (Adapted from Mergenthaler et al., 2013)

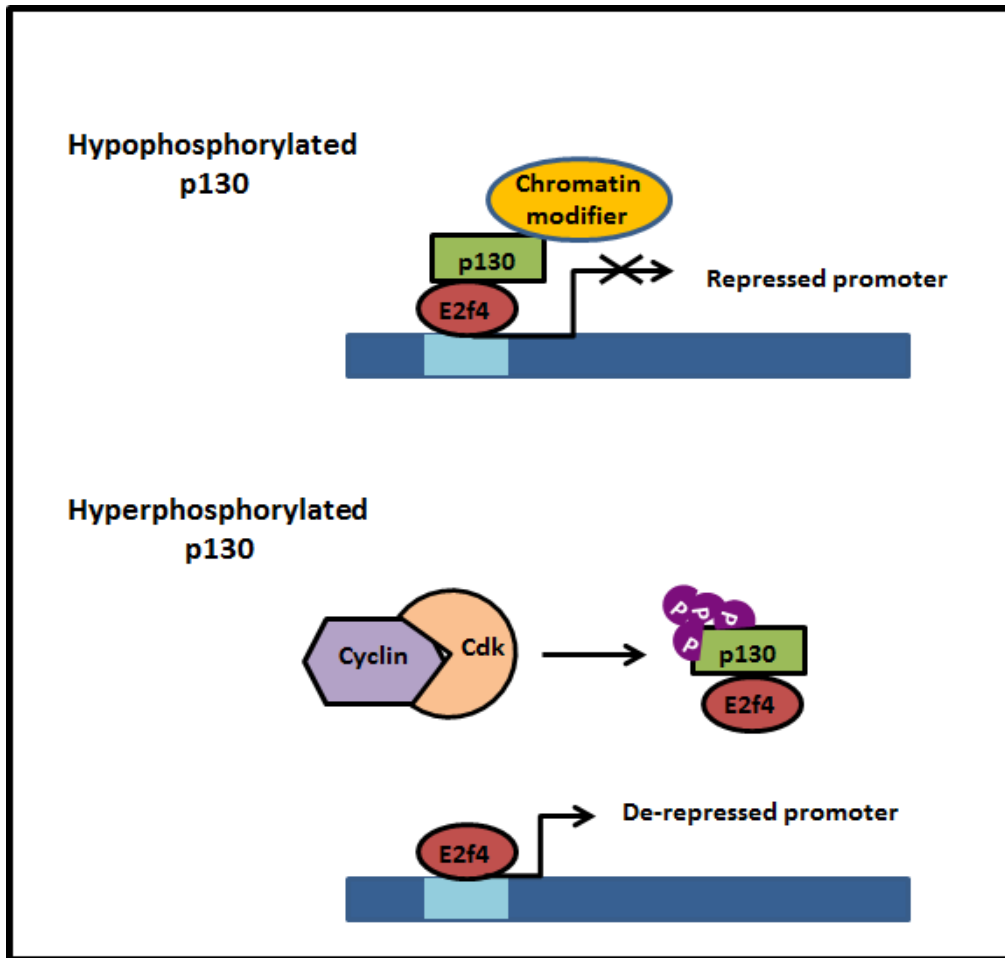


Figure 1.5 Role of p130 as a nuclear transcriptional co-repressor. In its hypophosphorylated state, p130 acts as a co-repressor by binding to E2f4 with the help of chromatin modifiers such as HDAC, thus preventing gene expression. However, when phosphorylated by cyclin/cdks, hyperphosphorylated p130 is unable to bind to E2f4, allowing it to activate gene expression. (Cdk, cyclin dependent kinase). (Adapted from Rayman et al., 2002)

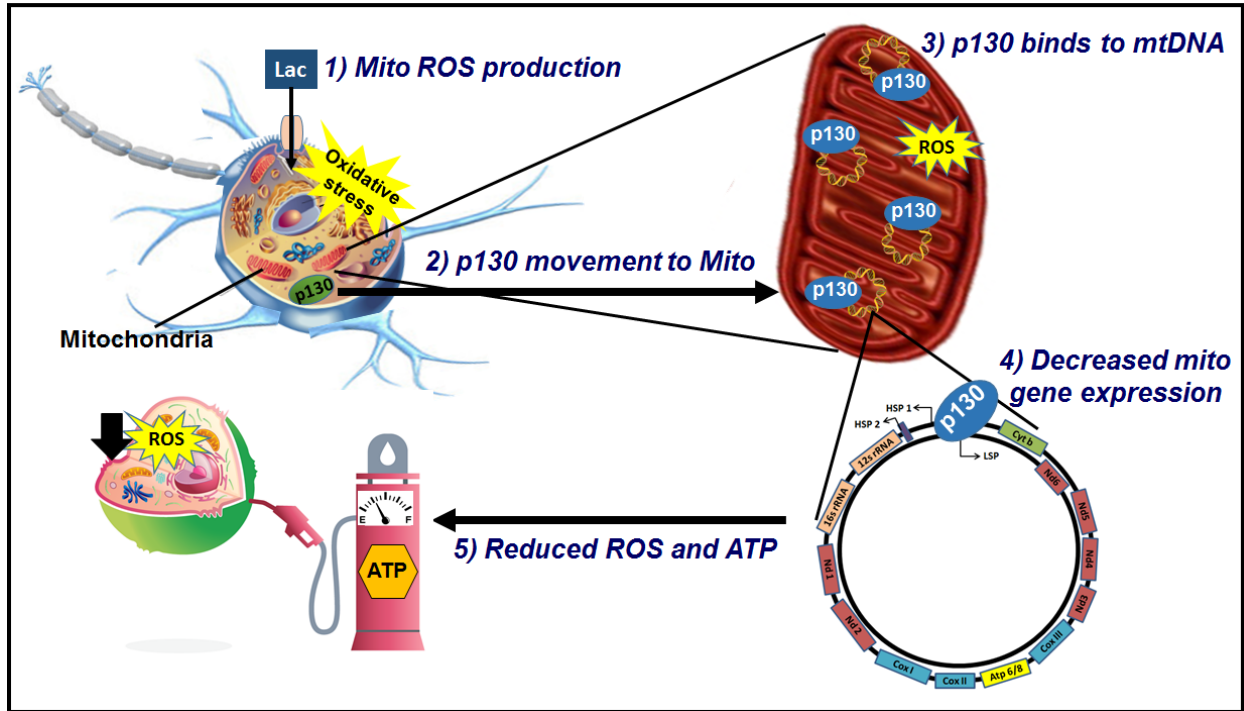


Figure 6.1 Summary figure. High nutrient conditions (Lac) result in oxidative stress due to excess ROS production. High ROS causes p130 to translocate to the mitochondria (Mito) where it binds to the mitochondrial DNA (mtDNA). By binding to the D-Loop promoter region of the mtDNA, p130 functions to represses gene expression of OxPhos encoded genes. This leads to reduced ATP production and ultimately decreased ROS generation in the mitochondria (Scimè et al., unpublished).

8. REFERENCES

1. Acín-Pérez, R., Bayona-Bafaluy, M. P., Fernández-Silva, P., Moreno-Loshuertos, R., Pérez-Martos, A., Bruno, C., ... & Enríquez, J. A. (2004). Respiratory complex III is required to maintain complex I in mammalian mitochondria. *Molecular cell*, *13*(6), 805-815.
2. Achanta, G., Sasaki, R., Feng, L., Carew, J. S., Lu, W., Pelicano, H., ... & Huang, P. (2005). Novel role of p53 in maintaining mitochondrial genetic stability through interaction with DNA Pol γ . *The EMBO journal*, *24*(19), 3482-3492.
3. Agostini, M., Romeo, F., Inoue, S., Niklison-Chirou, M. V., Elia, A. J., Dinsdale, D., ... & Melino, G. (2016). Metabolic reprogramming during neuronal differentiation. *Cell death and differentiation*, *23*(9), 1502.
4. Ajioka I. (2014) Coordination of proliferation and neuronal differentiation by the retinoblastoma protein family. *Develop. Growth Differ.* *56*, 324–334.
5. Al-Kafaji, G., Sabry, M. A., & Bakhiet, M. (2016). Increased expression of mitochondrial DNA-encoded genes in human renal mesangial cells in response to high glucose-induced reactive oxygen species. *Molecular medicine reports*, *13*(2), 1774-1780.
6. Allen, S. P., Rajan, S., Duffy, L., Mortiboys, H., Higginbottom, A., Grierson, A. J., & Shaw, P. J. (2014). Superoxide dismutase 1 mutation in a cellular model of amyotrophic lateral sclerosis shifts energy generation from oxidative phosphorylation to glycolysis. *Neurobiology of aging*, *35*(6), 1499-1509.
7. Almeida, A., Moncada, S., & Bolaños, J. P. (2004). Nitric oxide switches on glycolysis through the AMP protein kinase and 6-phosphofructo-2-kinase pathway. *Nature cell biology*, *6*(1), 45.
8. Alves, C. J., Dariolli, R., Jorge, F. M. D. H., Monteiro, M. R., Maximino, J. R., Martins, R. S., ... & Chadi, G. (2015). Gene expression profiling for human iPSC-derived motor neurons from sporadic ALS patients reveals a strong association between mitochondrial functions and neurodegeneration. *Frontiers in cellular neuroscience*, *9*, 289.
9. Anderson, S., Bankier, A. T., Barrell, B. G., De Bruijn, M. H., Coulson, A. R., Drouin, J., ... & Schreier, P. H. (1981). Sequence and organization of the human mitochondrial genome. *Nature*, *290*(5806), 457-465.
10. Andrusiak, M. G., McClellan, K. A., Dugal-Tessier, D., Julian, L. M., Rodrigues, S. P., Park, D. S., ... & Slack, R. S. (2011). Rb/E2F regulates expression of neogenin during neuronal migration. *Molecular and cellular biology*, *31*(2), 238-247.
11. Asin-Cayuela, J., Helm, M., & Attardi, G. (2004). A monomer-to-trimer transition of the human mitochondrial transcription termination factor (mTERF) is associated with a loss of in vitro activity. *Journal of Biological Chemistry*, *279*(15), 15670-15677.
12. Attwell B., Laughlin S.B. (2001). An energy budget for signalling in the grey matter of the brain. *J. Cereb Blood Flow Metab.* *21*: 1133-1145.

13. Aubert A., Pellerin L., Magistretti P.J., Costalat R. (2007). A coherent neurobiological framework for functional neuroimaging provided by a model integrating compartmentalized energy metabolism. *PNAS*, 104: 4188-4193.
14. Boengler, K., Hilfiker-Kleiner, D., Heusch, G., & Schulz, R. (2010). Inhibition of permeability transition pore opening by mitochondrial STAT3 and its role in myocardial ischemia/reperfusion. *Basic research in cardiology*, 105(6), 771-785.
15. Barros, L. F. (2013). Metabolic signaling by lactate in the brain. *Trends in neurosciences*, 36(7), 396-404.
16. Betteridge, D. J. (2000). What is oxidative stress? *Metabolism*, 49(2), 3-8.
17. Beyer, R. E. (1992). An analysis of the role of coenzyme Q in free radical generation and as an antioxidant. *Biochemistry and Cell Biology*, 70(6), 390-403.
18. Bélanger, M., Yang, J., Petit, J. M., Laroche, T., Magistretti, P. J., & Allaman, I. (2011). Role of the glyoxalase system in astrocyte-mediated neuroprotection. *Journal of Neuroscience*, 31(50), 18338-18352.
19. Bhattacharya D., Scimè A. (2017) The role for p107 in bioenergetic switching of myogenic stem cells. Unpublished.
20. Bolaños, J. P., Almeida, A., & Moncada, S. (2010). Glycolysis: a bioenergetic or a survival pathway?. *Trends in biochemical sciences*, 35(3), 145-149.
21. Bonawitz, N. D., Clayton, D. A., & Shadel, G. S. (2006). Initiation and beyond: multiple functions of the human mitochondrial transcription machinery. *Molecular cell*, 24(6), 813-825.
22. Borgstahl, G. E., Parge, H. E., Hickey, M. J., Beyer, W. F., Hallewell, R. A., & Tainer, J. A. (1992). The structure of human mitochondrial manganese superoxide dismutase reveals a novel tetrameric interface of two 4-helix bundles. *Cell*, 71(1), 107-118.
23. Boumezbeur, F., Petersen, K. F., Cline, G. W., Mason, G. F., Behar, K. L., Shulman, G. I., & Rothman, D. L. (2010). The contribution of blood lactate to brain energy metabolism in humans measured by dynamic ¹³C nuclear magnetic resonance spectroscopy. *Journal of Neuroscience*, 30(42), 13983-13991.
24. Bouzier-Sore, A. K., Voisin, P., Bouchaud, V., Bezancon, E., Franconi, J. M., & Pellerin, L. (2006). Competition between glucose and lactate as oxidative energy substrates in both neurons and astrocytes: a comparative NMR study. *European Journal of Neuroscience*, 24(6), 1687-1694.
25. Bouzier-Sore, A. K., Voisin, P., Canioni, P., Magistretti, P. J., & Pellerin, L. (2003). Lactate is a preferential oxidative energy substrate over glucose for neurons in culture. *Journal of Cerebral Blood Flow & Metabolism*, 23(11), 1298-1306.
26. Boyer, P. D. (1997). The ATP synthase—a splendid molecular machine. *Annual review of biochemistry*, 66(1), 717-749.
27. Burke, J. R., Deshong, A. J., Pelton, J. G., & Rubin, S. M. (2010). Phosphorylation-induced conformational changes in the retinoblastoma protein inhibit E2F transactivation domain binding. *Journal of Biological Chemistry*, 285(21), 16286-16293.

28. Burkhardt, D. L., & Sage, J. (2008). Cellular mechanisms of tumour suppression by the retinoblastoma gene. *Nature reviews. Cancer*, 8(9), 671.
29. Cadenas, E., & Davies, K. J. (2000). Mitochondrial free radical generation, oxidative stress, and aging. *Free Radical Biology and Medicine*, 29(3), 222-230.
30. Cammarota, M., Paratcha, G., Bevilacqua, L. R., Stein, D., Levi, M., Lopez, M., ... & Medina, J. H. (1999). Cyclic AMP-Responsive Element Binding Protein in Brain Mitochondria. *Journal of neurochemistry*, 72(6), 2272-2277.
31. Candas, D., & Li, J. J. (2014). MnSOD in oxidative stress response-potential regulation via mitochondrial protein influx. *Antioxidants & redox signaling*, 20(10), 1599-1617.
32. Carbognin, E., Betto, R. M., Soriano, M. E., Smith, A. G., & Martello, G. (2016). Stat3 promotes mitochondrial transcription and oxidative respiration during maintenance and induction of naive pluripotency. *The EMBO journal*, e201592629.
33. Cardoso, S., Santos, M. S., Seça, R., & Moreira, P. I. (2010). Cortical and hippocampal mitochondria bioenergetics and oxidative status during hyperglycemia and/or insulin-induced hypoglycemia. *Biochimica et Biophysica Acta (BBA)-Molecular Basis of Disease*, 1802(11), 942-951.
34. Casas, F., Rochard, P., Rodier, A., Cassar-Malek, I., Marchal-Victorion, S., Wiesner, R. J., ... & Wrutniak, C. (1999). A variant form of the nuclear triiodothyronine receptor c-ErbA α 1 plays a direct role in regulation of mitochondrial RNA synthesis. *Molecular and cellular biology*, 19(12), 7913-7924.
35. Chellappan, S. P., Hiebert, S., Mudryj, M., Horowitz, J. M., & Nevins, J. R. (1991). The E2F transcription factor is a cellular target for the RB protein. *Cell*, 65(6), 1053-1061.
36. Chance, B., & Hollunger, G. (1961). The interaction of energy and electron transfer reactions in mitochondria I. General properties and nature of the products of succinate-linked reduction of pyridine nucleotide. *Journal of Biological Chemistry*, 236(5), 1534-1543.
37. Chandrasekaran, K., Hatanpää, K., Brady, D. R., Stoll, J., & Rapoport, S. I. (1998). Downregulation of oxidative phosphorylation in Alzheimer disease: loss of cytochrome oxidase subunit mRNA in the hippocampus and entorhinal cortex. *Brain research*, 796(1), 13-19.
38. Chen, J. Q., Eshete, M., Alworth, W. L., & Yager, J. D. (2004). Binding of MCF-7 cell mitochondrial proteins and recombinant human estrogen receptors α and β to human mitochondrial dna estrogen response elements. *Journal of cellular biochemistry*, 93(2), 358-373.
39. Chih, C. P., & Roberts Jr, E. L. (2003). Energy substrates for neurons during neural activity: a critical review of the astrocyte-neuron lactate shuttle hypothesis. *Journal of Cerebral Blood Flow & Metabolism*, 23(11), 1263-1281.
40. Chouchani, E. T., Pell, V. R., Gaude, E., Aksentijević, D., Sundier, S. Y., Robb, E. L., ... & Eyassu, F. (2014). Ischaemic accumulation of succinate controls reperfusion injury through mitochondrial ROS. *Nature*, 515(7527), 431.

41. Cicero, C. E., Mostile, G., Vasta, R., Rapisarda, V., Santo Signorelli, S., Ferrante, M., ... & Nicoletti, A. (2017). Metals and neurodegenerative diseases. A systematic review. *Environmental Research*, *159*, 82-94
42. Cobrinik, D., Whyte, P., Peeper, D. S., Jacks, T., & Weinberg, R. A. (1993). Cell cycle-specific association of E2F with the p130 E1A-binding protein. *Genes & Development*, *7*(12a), 2392-2404.
43. Cogswell, P. C., Kashatus, D. F., Keifer, J. A., Guttridge, D. C., Reuther, J. Y., Bristow, C., ... & Baldwin, A. S. (2003). Nf-kb and ikb α are found in the mitochondria evidence for regulation of mitochondrial gene expression by nf-kb. *Journal of Biological Chemistry*, *278*(5), 2963-2968.
44. Collard, T. J., Urban, B. C., Patsos, H. A., Hague, A., Townsend, P. A., Paraskeva, C., & Williams, A. C. (2012). The retinoblastoma protein (Rb) as an anti-apoptotic factor: expression of Rb is required for the anti-apoptotic function of BAG-1 protein in colorectal tumour cells. *Cell death & disease*, *3*(10), e408.
45. Dairaghi, D. J., Shadel, G. S., & Clayton, D. A. (1995). Addition of a 29 residue carboxyl-terminal tail converts a simple HMG box-containing protein into a transcriptional activator. *Journal of molecular biology*, *249*(1), 11-28.
46. de la Monte, S. M., & Wands, J. R. (2006). Molecular indices of oxidative stress and mitochondrial dysfunction occur early and often progress with severity of Alzheimer's disease. *Journal of Alzheimer's Disease*, *9*(2), 167-181.
47. de Leon, M. J., Ferris, S. H., George, A. E., Reisberg, B., Christman, D. R., Kricheff, I. I., & Wolf, A. P. (1983). Computed tomography and positron emission transaxial tomography evaluations of normal aging and Alzheimer's disease. *Journal of Cerebral Blood Flow & Metabolism*, *3*(3), 391-394.
48. Demonacos, C., Tsawdaroglou, N. C., Djordjevic-Markovic, R., Papalopoulou, M., Galanopoulos, V., Papadogeorgaki, S., & Sekeris, C. E. (1993). Import of the glucocorticoid receptor into rat liver mitochondria in vivo and in vitro. *The Journal of steroid biochemistry and molecular biology*, *46*(3), 401-413.
49. De Rasmio, D., Signorile, A., Roca, E., & Papa, S. (2009). cAMP response element-binding protein (CREB) is imported into mitochondria and promotes protein synthesis. *The FEBS journal*, *276*(16), 4325-4333.
50. Dick, F. A., & Rubin, S. M. (2013). Molecular mechanisms underlying RB protein function. *Nature reviews Molecular cell biology*, *14*(5), 297-306.
51. DiCaprio, R. A., & Fournier, C. R. (1988). Neural control of ventilation in the shore crab, *Carcinus maenas*. *Journal of Comparative Physiology A: Neuroethology, Sensory, Neural, and Behavioral Physiology*, *162*(3), 375-388.
52. Dienel, G. A., & Hertz, L. (2001). Glucose and lactate metabolism during brain activation. *Journal of neuroscience research*, *66*(5), 824-838.
53. Duttaroy, A., Paul, A., Kundu, M., & Belton, A. (2003). A Sod2 null mutation confers severely reduced adult life span in *Drosophila*. *Genetics*, *165*(4), 2295-2299.

54. Dyer, M. A., Martins, R., da Silva Filho, M., Muniz, J. A. P., Silveira, L. C. L., Cepko, C. L., & Finlay, B. L. (2009). Developmental sources of conservation and variation in the evolution of the primate eye. *Proceedings of the National Academy of Sciences*, *106*(22), 8963-8968.
55. Dyson, N., Buchkovich, K., Whyte, P., & Harlow, E. (1989). The cellular 107K protein that binds to adenovirus E1A also associates with the large T antigens of SV40 and JC virus. *Cell*, *58*(2), 249-255.
56. Edmondson, D. E., Binda, C., Wang, J., Upadhyay, A. K., & Mattevi, A. (2009). Molecular and mechanistic properties of the membrane-bound mitochondrial monoamine oxidases. *Biochemistry*, *48*(20), 4220-4230.
57. Efeyan, A., Comb, W. C., & Sabatini, D. M. (2015). Nutrient-sensing mechanisms and pathways. *Nature*, *517*(7534), 302-310.
58. Emerling, B. M., Weinberg, F., Snyder, C., Burgess, Z., Mutlu, G. M., Violette, B., ... & Chandel, N. S. (2009). Hypoxic activation of AMPK is dependent on mitochondrial ROS but independent of an increase in AMP/ATP ratio. *Free Radical Biology and Medicine*, *46*(10), 1386-1391.
59. Enríquez, J. A., Fernández-Silva, P., Garrido-Pérez, N., López-Pérez, M. J., Pérez-Martos, A., & Montoya, J. (1999). Direct regulation of mitochondrial RNA synthesis by thyroid hormone. *Molecular and cellular biology*, *19*(1), 657-670.
60. Erlichman, J. S., Hewitt, A., Damon, T. L., Hart, M., Kurasz, J., Li, A., & Leiter, J. C. (2008). Inhibition of monocarboxylate transporter 2 in the retrotrapezoid nucleus in rats: a test of the astrocyte–neuron lactate-shuttle hypothesis. *Journal of Neuroscience*, *28*(19), 4888-4896.
61. Escartin C., Valette J., Lebon V., Bonvento G. (2006). Neuron-astrocyte interactions in the regulation of brain energy metabolism: a focus on NMR spectroscopy. *J Neurochem*. *99*(2):393-401.
62. Ewen, M. E., Xing, Y., Lawrence, J. B., & Livingston, D. M. (1991). Molecular cloning, chromosomal mapping, and expression of the cDNA for p107, a retinoblastoma gene product-related protein. *Cell*, *66*(6), 1155-1164.
63. Fisher, R. P., Lisowsky, T., Parisi, M. A., & Clayton, D. A. (1992). DNA wrapping and bending by a mitochondrial high mobility group-like transcriptional activator protein. *Journal of Biological Chemistry*, *267*(5), 3358-3367.
64. Fisher, R. P., Parisi, M. A., & Clayton, D. A. (1989). Flexible recognition of rapidly evolving promoter sequences by mitochondrial transcription factor 1. *Genes & development*, *3*(12b), 2202-2217.
65. Fjell, A. M., McEvoy, L., Holland, D., Dale, A. M., Walhovd, K. B., & Alzheimer's Disease Neuroimaging Initiative. (2014). What is normal in normal aging? Effects of aging, amyloid and Alzheimer's disease on the cerebral cortex and the hippocampus. *Progress in neurobiology*, *117*, 20-40.

66. Foster, N. L., Chase, T. N., Fedio, P., Patronas, N. J., Brooks, R. A., & Di Chiro, G. (1983). Alzheimer's disease Focal cortical changes shown by positron emission tomography. *Neurology*, *33*(8), 961-961.
67. Fridovich, I. (1995). Superoxide radical and superoxide dismutases. *Annual review of biochemistry*, *64*(1), 97-112.
68. Friedland, R. P., Budinger, T. F., Ganz, E., Yano, Y., Mathis, C. A., Koss, B., ... & Derenzo, S. E. (1983). Regional Cerebral Metabolic Alterations in Dementia of the Alzheimer Type: Positron Emission Tomography with [1818] Fluorodeoxyglucose. *Journal of computer assisted tomography*, *7*(4), 590-598.
69. Ferguson, K. L., McClellan, K. A., Vanderluit, J. L., McIntosh, W.C., Schuurmans, C., Polleux, F. & Slack, R. S. (2005). A cell autonomous requirement for the cell cycle regulatory protein, Rb, in neuronal migration. *EMBO J.* *24*:4381–4391.
70. Ghanem, N., Andrusiak, M. G., Svoboda, D., Al Lafi, S. M., Julian, L. M., McClellan, K. A., ... & Park, D. S. (2012). The Rb/E2F pathway modulates neurogenesis through direct regulation of the Dlx1/Dlx2 bigene cluster. *Journal of Neuroscience*, *32*(24), 8219-8230.
71. Gibson, G. E., Sheu, K. F., & Blass, J. P. (1998). Abnormalities of mitochondrial enzymes in Alzheimer disease. *Journal of neural transmission*, *105*(8), 855-870.
72. Giraud, G., Stadhouders, R., Conidi, A., Dekkers, D. H., Huylebroeck, D., Demmers, J. A., ... & Grosveld, F. G. (2014). NLS-tagging: an alternative strategy to tag nuclear proteins. *Nucleic acids research*, *42*(21), e163-e163.
73. Gough, D. J., Corlett, A., Schlessinger, K., Wegrzyn, J., Larner, A. C., & Levy, D. E. (2009). Mitochondrial STAT3 supports Ras-dependent oncogenic transformation. *Science*, *324*(5935),
74. Greer, E. L., Oskoui, P. R., Banko, M. R., Maniar, J. M., Gygi, M. P., Gygi, S. P., & Brunet, A. (2007). The energy sensor AMP-activated protein kinase directly regulates the mammalian FOXO3 transcription factor. *Journal of Biological Chemistry*, *282*(41), 30107-30119.
75. Grzybowska-Szatkowska, L., Ślaska, B., Rzymowska, J., Brzozowska, A., & Floriańczyk, B. (2014). Novel mitochondrial mutations in the ATP6 and ATP8 genes in patients with breast cancer. *Molecular medicine reports*, *10*(4), 1772-1778.
76. Halliwell, B. (2006). Oxidative stress and neurodegeneration: where are we now?. *Journal of neurochemistry*, *97*(6), 1634-1658.
77. Haas, R. H., Nasirian, F., Nakano, K., Ward, D., Pay, M., Hill, R., & Shults, C. W. (1995). Low platelet mitochondrial complex I and complex II/III activity in early untreated Parkinson's disease. *Annals of neurology*, *37*(6), 714-722.
78. Hardie, D. G. (2011). Energy sensing by the AMP-activated protein kinase and its effects on muscle metabolism. *Proceedings of the Nutrition Society*, *70*(1), 92-99.
79. Harlow, E. D., Whyte, P. E. T. E. R., Franza, B. R., & Schley, C. A. R. O. L. (1986). Association of adenovirus early-region 1A proteins with cellular polypeptides. *Molecular and cellular biology*, *6*(5), 1579-1589.

80. Hashimoto, T., & Brooks, G. A. (2008). Mitochondrial lactate oxidation complex and an adaptive role for lactate production. *Medicine & Science in Sports & Exercise*, 40(3), 486-494.
81. Hatanpää, K., Brady, D. R., Stoll, J., Rapoport, S. I., & Chandrasekaran, K. (1996). Neuronal activity and early neurofibrillary tangles in Alzheimer's disease. *Annals of neurology*, 40(3), 411-420.
82. Hertz, L., & Chen, Y. (2017). Glycogenolysis, an astrocyte-specific reaction, is essential for both astrocytic and neuronal activities involved in learning. *Neuroscience*.
83. Hertz L, Peng L., Dienel G.A. (2007). Energy metabolism in astrocytes: high rate of d metabolism and spatiotemporal dependence on glycolysis/glycogenolysis. *J Cereb Blood Flow Metab.* 27(2):219-49.
84. Herrero-Mendez, A., Almeida, A., Fernández, E., Maestre, C., Moncada, S., & Bolaños, J. P. (2009). The bioenergetic and antioxidant status of neurons is controlled by continuous degradation of a key glycolytic enzyme by APC/C-Cdh1. *Nature cell biology*, 11(6), 747.
85. Hiebert, S. W., Chellappan, S. P., Horowitz, J. M., & Nevins, J. R. (1992). The interaction of RB with E2F coincides with an inhibition of the transcriptional activity of E2F. *Genes & development*, 6(2), 177-185.
86. Hilgendorf, K. I., Leshchiner, E. S., Nedelcu, S., Maynard, M. A., Calo, E., Ianari, A., ... & Lees, J. A. (2013). The retinoblastoma protein induces apoptosis directly at the mitochondria. *Genes & development*, 27(9), 1003-1015.
87. Hisanaga, S. I., & Asada, A. (2012). Cdk5-induced neuronal cell death: The activation of the conventional Rb-E2F G1 pathway in post-mitotic neurons. *Cell Cycle*, 11(11), 2049-2049.
88. Hinkle, P. C., Butow, R. A., Racker, E., & Chance, B. (1967). Partial Resolution of the Enzymes Catalyzing Oxidative Phosphorylation XV. Reverse electron transfer in the flavin-cytochrome b region of the respiratory chain of beef heart submitochondrial particles. *Journal of Biological Chemistry*, 242(22), 5169-5173.
89. Hong, W. K., Han, E. H., Kim, D. G., Ahn, J. Y., Park, J. S., & Han, B. G. (2007). Amyloid- β -peptide reduces the expression level of mitochondrial cytochrome oxidase subunits. *Neurochemical research*, 32(9), 1483-1488.
90. Horowitz, M. P., & Greenamyre, J. T. (2010). Mitochondrial iron metabolism and its role in neurodegeneration. *Journal of Alzheimer's disease*, 20(S2), 551-568.
91. Hroudová, J., Singh, N., & Fišar, Z. (2014). Mitochondrial dysfunctions in neurodegenerative diseases: relevance to Alzheimer's disease. *BioMed research international*, 2014.
92. Hung, Y. P., Albeck, J. G., Tantama, M., & Yellen, G. (2011). Imaging cytosolic NADH-NAD⁺ redox state with a genetically encoded fluorescent biosensor. *Cell metabolism*, 14(4), 545-554.

93. Hyder, F., Patel, A. B., Gjedde, A., Rothman, D. L., Behar, K. L., & Shulman, R. G. (2006). Neuronal–glial glucose oxidation and glutamatergic–GABAergic function. *Journal of Cerebral Blood Flow & Metabolism*, *26*(7), 865-877.
94. Islam, M. T. (2017). Oxidative stress and mitochondrial dysfunction-linked neurodegenerative disorders. *Neurological Research*, *39*(1), 73-82.
95. Iyirhiaro, G. O., Zhang, Y., Estey, C., O'hare, M. J., Safarpour, F., Parsanejad, M., ... & Slack, R. S. (2014). Regulation of ischemic neuronal death by E2F4-p130 protein complexes. *Journal of Biological Chemistry*, *289*(26), 18202-18213.
96. Itoh, Y., Esaki, T., Shimoji, K., Cook, M., Law, M. J., Kaufman, E., & Sokoloff, L. (2003). Dichloroacetate effects on glucose and lactate oxidation by neurons and astroglia in vitro and on glucose utilization by brain in vivo. *Proceedings of the National Academy of Sciences*, *100*(8), 4879-4884.
97. Jori F.P., Galderisi, U., Piegari, E., Peluso, G., Cipalloro, M., Cascino, A., Giordano, A., & Melone, M. A. (2001). RB2/p130 ectopic gene expression in neuroblastoma stem cells: evidence of cell-fate restriction and induction of differentiation. *Biochemical Journal*, *360*(3), 569-577.
98. Johnson, R. F., Witzel, I. I., & Perkins, N. D. (2011). p53-dependent regulation of mitochondrial energy production by the RelA subunit of NF-κB. *Cancer research*, *71*(16), 5588-5597.
99. Kalgutkar, A. S., Dalvie, D. K., Castagnoli, N., & Taylor, T. J. (2001). Interactions of nitrogen-containing xenobiotics with monoamine oxidase (MAO) isozymes A and B: SAR studies on MAO substrates and inhibitors. *Chemical research in toxicology*, *14*(9), 1139-1162.
100. Keeney, P. D., Xie, J., Capaldi, R. A., & Bennett, J. P. (2006). Parkinson's disease brain mitochondrial complex I has oxidatively damaged subunits and is functionally impaired and misassembled. *Journal of Neuroscience*, *26*(19), 5256-5264.
101. Kioka, H., Kato, H., Fujikawa, M., Tsukamoto, O., Suzuki, T., Imamura, H., ... & Takafuji, K. (2014). Evaluation of intramitochondrial ATP levels identifies G0/G1 switch gene 2 as a positive regulator of oxidative phosphorylation. *Proceedings of the National Academy of Sciences*, *111*(1), 273-278.
102. Kirchner, H., Gutierrez, J. A., Solenberg, P. J., Pfluger, P. T., Czyzyk, T. A., Willency, J. A., ... & Heiman, M. L. (2009). GOAT links dietary lipids with the endocrine control of energy balance. *Nature medicine*, *15*(7), 741-745.
103. Kim, P. K., Annis, M. G., Dlugosz, P. J., Leber, B., & Andrews, D. W. (2004). During apoptosis bcl-2 changes membrane topology at both the endoplasmic reticulum and mitochondria. *Molecular cell*, *14*(4), 523-529.
104. Kish, S. J., Bergeron, C., Rajput, A., Dozic, S., Mastrogiacomo, F., Chang, L. J., ... & Nobrega, J. N. (1992). Brain cytochrome oxidase in Alzheimer's disease. *Journal of neurochemistry*, *59*(2), 776-779.

105. Kops, G. J., Medema, R. H., Glassford, J., Essers, M. A., Dijkers, P. F., Coffey, P. J., ... & Burgering, B. M. (2002). Control of cell cycle exit and entry by protein kinase B-regulated forkhead transcription factors. *Molecular and cellular biology*, 22(7), 2025-2036.
106. Kraig, R. P., Petito, C. K., Plum, F., & Pulsinelli, W. A. (1987). Hydrogen ions kill brain at concentrations reached in ischemia. *Journal of Cerebral Blood Flow & Metabolism*, 7(4), 379-386.
107. Kudin, A. P., Debska-Vielhaber, G., & Kunz, W. S. (2005). Characterization of superoxide production sites in isolated rat brain and skeletal muscle mitochondria. *Biomedicine & pharmacotherapy*, 59(4), 163-168.
108. Kudin, A. P., Malinska, D., & Kunz, W. S. (2008). Sites of generation of reactive oxygen species in homogenates of brain tissue determined with the use of respiratory substrates and inhibitors. *Biochimica et Biophysica Acta (BBA)-Bioenergetics*, 1777(7), 689-695.
109. Lam, T. K. (2010). Neuronal regulation of homeostasis by nutrient sensing. *Nature medicine*, 16(4), 392-395.
110. Lash, L. H. (2006). Mitochondrial glutathione transport: physiological, pathological and toxicological implications. *Chemico-biological interactions*, 163(1), 54-67.
111. Lebon, V., Petersen, K. F., Cline, G. W., Shen, J., Mason, G. F., Dufour, S., ... & Rothman, D. L. (2002). Astroglial contribution to brain energy metabolism in humans revealed by ¹³C nuclear magnetic resonance spectroscopy: elucidation of the dominant pathway for neurotransmitter glutamate repletion and measurement of astrocytic oxidative metabolism. *Journal of Neuroscience*, 22(5), 1523-1531.
112. LeCouter, J. E., Kablar, B., Whyte, P. F., Ying, C., & Rudnicki, M. A. (1998). Strain-dependent embryonic lethality in mice lacking the retinoblastoma-related p130 gene. *Development*, 125(23), 4669-4679.
113. Lee, J., Kim, C. H., Simon, D. K., Aminova, L. R., Andreyev, A. Y., Kushnareva, Y. E., ... & Ferrante, R. J. (2005). Mitochondrial cyclic AMP response element-binding protein (CREB) mediates mitochondrial gene expression and neuronal survival. *Journal of Biological Chemistry*, 280(49), 40398-40401.
114. Lee, H. J., Chattopadhyay, S., Yoon, W. H., Bahk, J. Y., Kim, T. H., Kang, H. S., & Lee, K. (2010). Overexpression of hepatocyte nuclear factor-3 α induces apoptosis through the upregulation and accumulation of cytoplasmic p53 in prostate cancer cells. *The Prostate*, 70(4), 353-361.
115. Lee, H. P., Pancholi, N., Esposito, L., Previll, L. A., Wang, X., Zhu, X., ... & Lee, H. G. (2012). Early induction of oxidative stress in mouse model of Alzheimer disease with reduced mitochondrial superoxide dismutase activity. *PloS one*, 7(1), e28033.
116. Lee, Y., Morrison, B. M., Li, Y., Lengacher, S., Farah, M. H., Hoffman, P. N., ... & Pellerin, L. (2012). Oligodendroglia metabolically support axons and contribute to neurodegeneration. *Nature*, 487(7408), 443-448.
117. Li, N., Ragheb, K., Lawler, G., Sturgis, J., Rajwa, B., Melendez, J. A., & Robinson, J. P. (2003). Mitochondrial complex I inhibitor rotenone induces apoptosis through enhancing

- mitochondrial reactive oxygen species production. *Journal of Biological Chemistry*, 278(10), 8516-8525.
118. Liemburg-Apers, D. C., Willems, P. H., Koopman, W. J., & Grefte, S. (2015). Interactions between mitochondrial reactive oxygen species and cellular glucose metabolism. *Archives of toxicology*, 89(8), 1209-1226.
119. Liu, D. X., & Greene, L. A. (2001). Neuronal apoptosis at the G1/S cell cycle checkpoint. *Cell and tissue research*, 305(2), 217-228.
120. Liu, Y., Fiskum, G., & Schubert, D. (2002). Generation of reactive oxygen species by the mitochondrial electron transport chain. *Journal of neurochemistry*, 80(5), 780-787.
121. Liu, D. X., Nath, N., Chellappan, S. P., & Greene, L. A. (2005). Regulation of neuron survival and death by p130 and associated chromatin modifiers. *Genes & development*, 19(6), 719-732.
122. Liu, S., Reilly, S. M., & Lee, C. H. (2013). Transcriptional repression of mitochondrial function in aging: a novel role for the silencing mediator of retinoid and thyroid hormone receptors co-repressor. *Antioxidants & redox signaling*, 19(3), 299-309.
123. Litovchick, L., Sadasivam, S., Florens, L., Zhu, X., Swanson, S. K., Velmurugan, S., ... & DeCaprio, J. A. (2007). Evolutionarily conserved multisubunit RBL2/p130 and E2F4 protein complex represses human cell cycle-dependent genes in quiescence. *Molecular cell*, 26(4), 539-551.
124. Lovatt D., Sonnewald U., Waagepetersen H.S., Schousboe A., He W., Lin J.H., Han X., Takano T., Wang S., Sim F.J., Goldman S.A., Nedergaard M. (2007). The transcriptome and metabolic gene signature of protoplasmic astrocytes in the adult murine cortex. *J Neurosci*. 27(45):12255-66.
125. Macauley, S. L., Stanley, M., Caesar, E. E., Yamada, S. A., Raichle, M. E., Perez, R., ... & Holtzman, D. M. (2015). Hyperglycemia modulates extracellular amyloid- β concentrations and neuronal activity in vivo. *The Journal of clinical investigation*, 125(6), 2463-2467.
126. Magistretti, P. J. (2008). *Brain energy metabolism* (No. LNDC-CHAPTER-2010-001, pp. 271-293). Academic Press.
127. Magistretti, P. J. (2009). Role of glutamate in neuron-glia metabolic coupling. *The American journal of clinical nutrition*, 90(3), 875S-880S.
128. Magistretti, P. J., & Chatton, J. Y. (2005). Relationship between L-glutamate-regulated intracellular Na⁺ dynamics and ATP hydrolysis in astrocytes. *Journal of neural transmission*, 112(1), 77-85.
129. Manczak, M., Park, B. S., Jung, Y., & Reddy, P. H. (2004). Differential expression of oxidative phosphorylation genes in patients with Alzheimer's disease. *Neuromolecular medicine*, 5(2), 147-162.
130. Manczak, M., Anekonda, T. S., Henson, E., Park, B. S., Quinn, J., & Reddy, P. H. (2006). Mitochondria are a direct site of A β accumulation in Alzheimer's disease neurons:

- implications for free radical generation and oxidative damage in disease progression. *Human molecular genetics*, 15(9), 1437-1449.
131. Marchenko, N. D., Wolff, S., Erster, S., Becker, K., & Moll, U. M. (2007). Monoubiquitylation promotes mitochondrial p53 translocation. *The EMBO journal*, 26(4), 923-934.
132. McClellan, K. A., Ruzhynsky, V. A., Douda, D. N., et al. (2007). Unique requirement for Rb/E2F3 in neuronal migration: evidence for cell cycle-independent functions. *Mol. Cell Biol.* 27:4825–4843.
133. Meister, A. (1974). 22. Glutathione Synthesis. *The enzymes*, 10, 671-697.
134. Mergenthaler, P., Lindauer, U., Dienel, G. A., & Meisel, A. (2013). Sugar for the brain: the role of glucose in physiological and pathological brain function. *Trends in neurosciences*, 36(10), 587-597.
135. Monje, P., & Boland, R. (2001). Subcellular distribution of native estrogen receptor α and β isoforms in rabbit uterus and ovary. *Journal of cellular biochemistry*, 82(3), 467-479.
136. Moreira P.I., Cardoso S.M., Santos M.S., Oliveira C.R. (2006). The key role of mitochondria in Alzheimer's disease. *J. Alzheimer's Dis.* 9:101–110.
137. Moreira, P. I., Nunomura, A., Nakamura, M., Takeda, A., Shenk, J. C., Aliev, G., ... & Perry, G. (2008). Nucleic acid oxidation in Alzheimer disease. *Free Radical Biology and Medicine*, 44(8), 1493-1505.
138. Mungai, P. T., Waypa, G. B., Jairaman, A., Prakriya, M., Dokic, D., Ball, M. K., & Schumacker, P. T. (2011). Hypoxia triggers AMPK activation through reactive oxygen species-mediated activation of calcium release-activated calcium channels. *Molecular and cellular biology*, 31(17), 3531-3545.
139. Nedergaard, M., Kraig, R. P., Tanabe, J., & Pulsinelli, W. A. (1991). Dynamics of interstitial and intracellular pH in evolving brain infarct. *American Journal of Physiology-Regulatory, Integrative and Comparative Physiology*, 260(3), R581-R588.
140. Nehlig, A. (2004). Brain uptake and metabolism of ketone bodies in animal models. *Prostaglandins, leukotrienes and essential fatty acids*, 70(3), 265-275.
141. Newman, L. A., Korol, D. L., & Gold, P. E. (2011). Lactate produced by glycogenolysis in astrocytes regulates memory processing. *PloS one*, 6(12), e28427.
142. Nunomura, A., Perry, G., Aliev, G., Hirai, K., Takeda, A., Balraj, E. K., ... & Chiba, S. (2001). Oxidative damage is the earliest event in Alzheimer disease. *Journal of Neuropathology & Experimental Neurology*, 60(8), 759-767.
143. Ogita, K., Fujinami, Y., Kitano, M., & Yoneda, Y. (2003). Transcription factor activator protein-1 expressed by kainate treatment can bind to the non-coding region of mitochondrial genome in murine hippocampus. *Journal of neuroscience research*, 73(6), 794-802.
144. Okado-Matsumoto, A., & Fridovich, I. (2001). Subcellular distribution of superoxide dismutases (SOD) in rat liver Cu, Zn-SOD in mitochondria. *Journal of Biological Chemistry*, 276(42), 38388-38393.

145. Oshikawa, M., Okada, K., Nakajima, K. & Ajioka, I. (2013). Cortical excitatory neurons become protected from cell division during neurogenesis in an Rb family-dependent manner. *Development* 140:2310–2320.
146. Pathan, K. H., Gajare, K. A., & Deshmukh, A. A. (2015). Ultrastructural study reveals that mouse hippocampal neurons are more protected than the cerebrocortical neurons from age related cytological alterations. *Cell Science and Report. MOJ Cell Sci Rep*, 2(5), 00039.
147. Parisi, M., & Clayton, D. A. (1991). Similarity of human mitochondrial transcription factor 1 to high mobility group proteins. *Science*, 252(5008), 965.
148. Parker, W. D., Filley, C. M., & Parks, J. K. (1990). Cytochrome oxidase deficiency in Alzheimer's disease. *Neurology*, 40(8), 1302-1302.
149. Pellerin, L., Bouzier-Sore, A. K., Aubert, A., Serres, S., Merle, M., Costalat, R., & Magistretti, P. J. (2007). Activity-dependent regulation of energy metabolism by astrocytes: an update. *Glia*, 55(12), 1251-1262.
150. Porras, D. P., Abbaszadeh, M., Bhattacharya, D., D'Souza, N. C., Edjiu, N. R., Perry, C. G., & Scimè, A. (2017). p107 Determines a Metabolic Checkpoint Required for Adipocyte Lineage Fates. *STEM CELLS*, 35(5), 1378-1391.
151. Previll, L. A., Crosby, M. E., Castellani, R. J., Bowser, R., Perry, G., Smith, M. A., & Zhu, X. (2007). Increased expression of p130 in Alzheimer disease. *Neurochemical research*, 32(4-5), 639-644.
152. Prichard, J., Rothman, D., Novotny, E., Petroff, O., Kuwabara, T., Avison, M., ... & Shulman, R. (1991). Lactate rise detected by 1H NMR in human visual cortex during physiologic stimulation. *Proceedings of the National Academy of Sciences*, 88(13), 5829-5831.
153. Ramachandran, A., Basu, U., Sultana, S., Nandakumar, D., & Patel, S. S. (2016). Human mitochondrial transcription factors TFAM and TFB2M work synergistically in promoter melting during transcription initiation. *Nucleic Acids Research*, gkw1157.
154. Ravindranath, S. D., & Fridovich, I. (1975). Isolation and characterization of a manganese-containing superoxide dismutase from yeast. *Journal of Biological Chemistry*, 250(15), 6107-6112.
155. Rayman, J. B., Takahashi, Y., Indjeian, V. B., Dannenberg, J. H., Catchpole, S., Watson, R. J., ... & Dynlacht, B. D. (2002). E2F mediates cell cycle-dependent transcriptional repression in vivo by recruitment of an HDAC1/mSin3B corepressor complex. *Genes & development*, 16(8), 933-947.
156. Russell, J. W., Golovoy, D., Vincent, A. M., Mahendru, P. I. A., Olzmann, J. A., Mentzer, A., & Feldman, E. L. (2002). High glucose-induced oxidative stress and mitochondrial dysfunction in neurons. *The FASEB Journal*, 16(13), 1738-1748.
157. Ruzsiewicz, J., & Albrecht, J. (2015). Changes in the mitochondrial antioxidant systems in neurodegenerative diseases and acute brain disorders. *Neurochemistry international*, 88, 66-72.

158. Scarpulla, R. C. (2008). Transcriptional paradigms in mammalian mitochondrial biogenesis and function. *Physiological reviews*, 88(2), 611-638.
159. Sepehr, A., & Mohseni, S. (2010). Lactate damages primary hippocampal neurons in vitro. *Cell biology international*, 34(1), 61-65.
160. Shi, H., & Liu, K. J. (2006). Effects of glucose concentration on redox status in rat primary cortical neurons under hypoxia. *Neuroscience letters*, 410(1), 57-61.
161. Shadel, G. S. (2008). Expression and maintenance of mitochondrial DNA: new insights into human disease pathology. *The American journal of pathology*, 172(6), 1445-1456.
162. Sharma, L. K., Lu, J., & Bai, Y. (2009). Mitochondrial respiratory complex I: structure, function and implication in human diseases. *Current medicinal chemistry*, 16(10), 1266-1277.
163. She, H., Yang, Q., Shepherd, K., Smith, Y., Miller, G., Testa, C., & Mao, Z. (2011). Direct regulation of complex I by mitochondrial MEF2D is disrupted in a mouse model of Parkinson disease and in human patients. *The Journal of clinical investigation*, 121(3), 930.
164. Shimohama, H. Tanino, N. Kawakami et al., "Activation of NADPH oxidase in Alzheimer's disease brains," *Biochemical and Biophysical Research Communications*, vol. 273, no. 1, pp. 5-9, 2000.
165. Shinde, S., & Pasupathy, K. (2006). Respiratory-chain enzyme activities in isolated mitochondria of lymphocytes from patients with Parkinson's disease: preliminary study. *Neurology India*, 54(4), 390.
166. Shulman R.G., Rothman D.L., Behar K.L., Hyder f., (2004). Energetic basis of brain activity: implications for neuroimaging. *Trends Neurosci.* 27: 489-495.
167. Shulga, N., & Pastorino, J. G. (2012). GRIM-19-mediated translocation of STAT3 to mitochondria is necessary for TNF-induced necroptosis. *J Cell Sci*, 125(12), 2995-3003.
168. Sibson, N. R., Shen, J., Mason, G. F., Rothman, D. L., Behar, K. L., & Shulman, R. G. (1998). Functional Energy Metabolism: In vivo ¹³C-NMR Spectroscopy Evidence for Coupling of Cerebral Glucose Consumption and Glutamatergic Neuronal Activity. *Developmental neuroscience*, 20(4-5), 321-330.
169. Siesjö, B. K., Bendek, G., Koide, T., Westerberg, E., & Wieloch, T. (1985). Influence of acidosis on lipid peroxidation in brain tissues in vitro. *Journal of Cerebral Blood Flow & Metabolism*, 5(2), 253-258.
170. Simonian, N. A., & Hyman, B. T. (1994). Functional alterations in Alzheimer's disease: selective loss of mitochondrial-encoded cytochrome oxidase mRNA in the hippocampal formation. *Journal of Neuropathology & Experimental Neurology*, 53(5), 508-512.
171. Smith, E. J., Leone, G., DeGregori, J., Jakoi, L., & Nevins, J. R. (1996). The accumulation of an E2F-p130 transcriptional repressor distinguishes a G0 cell state from a G1 cell state. *Molecular and Cellular Biology*, 16(12), 6965-6976.
172. Sokoloff L. (1999). Energetics of functional activation in neural tissues. *Neurochem Res.* 24: 321-329.

173. Stengel, K. R., Thangavel, C., Solomon, D. A., Angus, S. P., Zheng, Y., & Knudsen, E. S. (2009). Retinoblastoma/p107/p130 Pocket Proteins protein dynamics and interactions with target gene promoters. *Journal of Biological Chemistry*, 284(29), 19265-19271.
174. Stocchi, F., & Olanow, C. W. (2003). Neuroprotection in Parkinson's disease: clinical trials. *Annals of neurology*, 53(S3).
175. Su, B., Wang, X., Nunomura, A., Moreira, P. I., Lee, H. G., Perry, G., ... & Zhu, X. (2008). Oxidative stress signaling in Alzheimer's disease. *Current Alzheimer Research*, 5(6), 525-532.
176. Suzuki, A., Stern, S. A., Bozdagi, O., Huntley, G. W., Walker, R. H., Magistretti, P. J., & Alberini, C. M. (2011). Astrocyte-neuron lactate transport is required for long-term memory formation. *Cell*, 144(5), 810-823.
177. Svoboda, D. S., Paquin, A., Park, D. S. & Slack, R. S. (2013). Pocket proteins pRb and p107 are required for cortical lamination independent of apoptosis. *Dev. Biol.* 384:101–113.
178. Szczepanek, K., Chen, Q., Larner, A. C., & Lesnefsky, E. J. (2012). Cytoprotection by the modulation of mitochondrial electron transport chain: the emerging role of mitochondrial STAT3. *Mitochondrion*, 12(2), 180-189.
179. Szczepanek, K., Chen, Q., Derecka, M., Salloum, F. N., Zhang, Q., Szelag, M., ... & Larner, A. C. (2011). Mitochondrial-targeted Signal transducer and activator of transcription 3 (STAT3) protects against ischemia-induced changes in the electron transport chain and the generation of reactive oxygen species. *Journal of Biological Chemistry*, 286(34), 29610-29620.
180. Takahashi, Y., Rayman, J. B., & Dynlacht, B. D. (2000). Analysis of promoter binding by the E2F and pRB families in vivo: distinct E2F proteins mediate activation and repression. *Genes & development*, 14(7), 804-816.
181. Takeshige, K., & Minakami, S. (1979). NADH-and NADPH-dependent formation of superoxide anions by bovine heart submitochondrial particles and NADH-ubiquinone reductase preparation. *Biochemical Journal*, 180(1), 129-135.
182. Topper, J. N., & Clayton, D. A. (1989). Identification of transcriptional regulatory elements in human mitochondrial DNA by linker substitution analysis. *Molecular and cellular biology*, 9(3), 1200-1211.
183. Trifunovic, A. (2006). Mitochondrial DNA and ageing. *Biochimica et Biophysica Acta (BBA)-Bioenergetics*, 1757(5), 611-617.
184. Uhler, J. P., & Falkenberg, M. (2015). Primer removal during mammalian mitochondrial DNA replication. *DNA repair*, 34, 28-38.
185. Van Hall, G., Størmstad, M., Rasmussen, P., Jans, Ø., Zaar, M., Gam, C., ... & Nielsen, H. B. (2009). Blood lactate is an important energy source for the human brain. *Journal of Cerebral Blood Flow & Metabolism*, 29(6), 1121-1129.
186. Voets, A. M., Lindsey, P. J., Vanherle, S. J., Timmer, E. D., Esseling, J. J., Koopman, W. J., ... & de Coo, I. F. M. (2012). Patient-derived fibroblasts indicate oxidative stress status

- and may justify antioxidant therapy in OXPHOS disorders. *Biochimica et Biophysica Acta (BBA)-Bioenergetics*, 1817(11), 1971-1978.
187. Wegrzyn, J., Potla, R., Chwae, Y. J., Sepuri, N. B., Zhang, Q., Koeck, T., ... & Moh, A. (2009). Function of mitochondrial Stat3 in cellular respiration. *Science*, 323(5915), 793-797.
188. Weisiger, R. A., & Fridovich, I. (1973). Mitochondrial superoxide dismutase site of synthesis and intramitochondrial localization. *Journal of Biological Chemistry*, 248(13), 4793-4796.
189. Yang, J., Ruchti, E., Petit, J. M., Jourdain, P., Grenningloh, G., Allaman, I., & Magistretti, P. J. (2014). Lactate promotes plasticity gene expression by potentiating NMDA signaling in neurons. *Proceedings of the National Academy of Sciences*, 111(33), 12228-12233.
190. Yang, S. H., Li, W., Sumien, N., Forster, M., Simpkins, J. W., & Liu, R. (2015). Alternative mitochondrial electron transfer for the treatment of neurodegenerative diseases and cancers: methylene blue connects the dots. *Progress in neurobiology*.
191. Yates, C. M., Butterworth, J., Tennant, M. C., & Gordon, A. (1990). Enzyme Activities in Relation to pH and Lactate in Postmortem Brain in Alzheimer-Type and Other Dementias. *Journal of neurochemistry*, 55(5), 1624-1630.
192. Yoshida, Y., Izumi, H., Torigoe, T., Ishiguchi, H., Itoh, H., Kang, D., & Kohno, K. (2003). P53 physically interacts with mitochondrial transcription factor A and differentially regulates binding to damaged DNA. *Cancer research*, 63(13), 3729-3734.
193. Zielke, R. H., Zielke, C. L., & Baab, P. J. (2009). Direct measurement of oxidative metabolism in the living brain by microdialysis: a review. *Journal of neurochemistry*, 109(s1), 24-29.
194. Zhang, J., Gray, J., Wu, L., Leone, G., Rowan, S., Cepko, C. L., ... & Dyer, M. A. (2004). Rb regulates proliferation and rod photoreceptor development in the mouse retina. *Nature genetics*, 36(4), 351.
195. Zhou, Q., Liu, C., Liu, W., Zhang, H., Zhang, R., Liu, J., ... & Chen, L. (2014). Rotenone induction of hydrogen peroxide inhibits mTOR-mediated S6K1 and 4E-BP1/eIF4E pathways, leading to neuronal apoptosis. *Toxicological sciences*, kfu211.